2014-01-01

Long-term Deformation in the Southern Río Grande Rift as Inferred from Topographic and Uplifted Terraces

Linda K. Armour
University of Texas at El Paso, pterodactyl3@juno.com

LONG-TERM DEFORMATION IN THE SOUTHERN RÍO GRANDE RIFT AS INFERRED FROM TOPOGRAPHY AND UPLIFTED TERRACES

LINDA KAY ARMOUR

Department of Geological Sciences

APPROVED:

Richard P. Langford, Ph.D., Chair

Thomas E. Gill, Ph.D.

Richard S. Jarvis, Ph.D.

Terry L. Pavlis, Ph.D.

Robert C. Trentham, D.G.S.

Benjamin C. Flores, Ph.D.
Dean of the Graduate School

Dedication

to Glen and Alma Armour who made this possible
and
Marcia and Glenda who tolerated years of Mom's night classes

LONG-TERM DEFORMATION IN THE SOUTHERN RÍO GRANDE RIFT AS INFERRED FROM TOPOGRAPHY AND UPLIFTED TERRACES

by

LINDA KAY ARMOUR, BA, BS, MS

DISSERTATION

Presented to the Faculty of the Graduate School of

The University of Texas at El Paso

in Partial Fulfillment

of the Requirements

for the Degree of

DOCTOR OF PHILOSOPHY

Department of Geological Sciences

THE UNIVERSITY OF TEXAS AT EL PASO

August 2014

ACKNOWLEDGMENTS

Thank yous are extended to:

Richard Langford for recommending the topic, assisting with field work, assistance with the computer maps. Without his direction, I would still be writing.

Tom Gill for serving as sounding board, alerting me to upcoming deadlines, and for being the final set of "fresh eyes" to do proof read the work..

Terry Pavlis and Richard Jarvis for proof-reading and alerting me to areas that needed clarification.

Robert C. Trentham for serving on a second of my graduate committies. In spite of being 300 miles away, he had major input in the content. Without Dr. Trentham' help while I worked toward the BS and MS, I would not have had the background to attempt this effort..

Carlos Montana for last minute help with the gravity data relating to the Sacramento, San Andres, and Guadalupe Mountains.

Franklin State Park and the Bowen Ranch gave permission to access the areas of interest.

Robert F. Lindsay for directing me to the terraces near Guadalupe Peak.

Stephanie Ray who was my field assistant. Scheduling made her more a proof reader and a questioner who forced me to think through what I was writing.

James W. Granath agreed to be one of my referees, and H. Jay Melosh clarified sections of his quoted effort. Their structural and geomorphology classes taken nearly 35 years ago provided me with a good foundation in geology. Both have answered innumerable questions in the intervening years.

Daughter Marcia taught me how to use Excel's graphing capabilities, answered statistical questions, then proofread the final drafts.

Daughter Glenda took care of my home in Midland, looked for books and whatever else was at "the wrong house". They tolerated my early geology and leveling classes when they were in grade school and would really rather have had me paying attention to their wishes.

Marcia Beth Couch, Robin O'Connor, and Michael Sorensen, consistently served as sounding boards and generally offered general technical support.

And maybe I should thank my friends in Midland who asked every time I was in town "When will you finish and come home?"

ABSTRACT

This study examines Basin and Range topography relating tectonic processes to topographic features. The observation that the terraces along either side of the Franklin Mountains were deformed and uplifted is a reflection of tectonic uplift. The uplift represents long-term deformation of the range. This led to the question of what shapes the deformation and does it represent differential subsidence into the Rio Grande Rift or true uplift. A more regional study of the Sacramento, San Andres, and Guadalupe Mountains follows. Two papers form this dissertation.

The Río Grande Rift and the Franklin Mountains, in particular, are the subject of the second chapter. The indication for tectonic uplift is the terraces along the flanks of the Franklin Mountains mimicking the curve along the crest of the range.

In light of the results from the Franklin Mountains, Chapter three examines the Sacramento, San Andres, and Guadalupe Mountains. Location data were converted to UTM Zone 13 measurements then long-wavelength elevation changes were modeled by use of transects drawn from digital elevation models (DEM) at 15 minute intervals between the Pecos River of eastern New Mexico across to Arizona on the west. A 2ndorder polynomial was fit across the transects then a map was constructed based on the polynomials. The three modeled ranges are among those that show uplift above the smoothed surface. Furthermore, the ranges all exhibit arcuate crests implying a similar origin. A gravity map between 31˚ N, -104˚ W and 35˚ N, -110˚ W was multiplied by the inverse of elevation to emphasize the correlation between elevation and subsidence into the rift basins.

TABLE OF CONTENTS

CHAPTER 1: INTRODUCTION

This study examines the Basin and Range province topography and relates it to local tectonism. The Franklin Mountains are flanked by terraces that have been deformed. Their uplift represents long-term deformation of the range. This led to the question of what was the shape of the deformation, and whether it represented differential subsidence or true uplift. The study expanded to a more regional study that included the Sacramento and Guadalupe Mountains and then to the Basin and Range as a whole. Two papers, comprising Chapters 2 and 3 resulted from this research.

The Chapter 2 investigates the Río Grande Rift and the Franklin Mountains. Terraces were mapped using a high resolution GPS to determine the elevations of the highest terraces underlain by basin-floor sediment. Uplift of the Franklin Mountains was demonstrated by a topographic profile of terraces that on the east and west flanks mimicking the crest of the range is indication of tectonic uplift.

Chapter 3 compares the Guadalupe, San Andres, and Sacramento Mountains in light of the results from the Franklin Mountains. First, a gravity map that combines gravity with topography was created. Digital elevation models (DEM) were profiled at 15 minute intervals between latitude 31 and 35, between longitudes 104 and 110 west. A second degree polynomial was fit to the transcripts and a smoothed surface was constructed. This was related to the uplift history of the ranges and to the evidence of tectonic uplift versus differential subsidence was discussed.

CHAPTER 2: LONG-TERM DEFORMATION IN THE SOUTHERN RÍO GRANDE RIFT AS INFERRED FROM TOPOGRAPHY AND UPLIFTED TERRACES

ABSTRACT: The long-term deformation of the Franklin Mountains in the Río Grande Rift was estimated by measuring the elevation of Late Pliocene terraces that line the footwalls of the range-front faults. In most extensional terrains, alluvial fans and bajadas cover faults and terraces thus making documentation of long term uplift difficult. However, rapid aggradation of the basin floors by extensive playa lakes and floodplain deposits of the Río Grande river buried the irregular mountain front fans creating the low-gradient surface. Subsequent faulting deformed and uplifted the low-gradient surface, revealing the long-term deformation of the mountains.

The uplifted terraces are exposed along both sides of the Franklin Mountains and along the east side of the Sierra Robledo in south central New Mexico. In the Franklin Mountains, the terraces lie 130 m above a younger surface, indicating that this is the minimum amount of uplift. The profile of the anticline parallels the profile of the range crest of the mountains. Three important conclusions can be drawn from uplift of the terraces. First, the observation that the terraces parallel the range crest implies that the topography of the mountains is tectonic in origin and that there was a low relief surface prior to deformation. Second, the east side terraces are higher than the west side terraces, showing rotation of the mountains during deformation, and providing an estimate of the percentage of deformation recorded by the terraces at about five percent of the total rotation. Third, the open arch correlates points to differential slip on the fault plane as a factor in the uplift.

Two models for causing the differential slip associated with apparent uplift are 1) differential subsidence that results in the denudation of the horst blocks that are subsiding less rapidly and 2) true uplift, related to flexural deformation along with the fault plane and mid-crustal flow rotate the Franklin Mountains block.

INTRODUCTION

This paper documents and discusses the uplift of Pliocene terraces surrounding the Franklin Mountains within the southern Río Grande Rift, in far west Texas and south central New Mexico and reveals the shape of long-term extensional uplift of the terraces. The terraces along the slopes of the mountains are composed of the Fort Hancock and the Camp Rice Formations, part of the Santa Fe Group; deposition of these formations took place between 20 and 2 Ma (Gile and others, 1981; Collins and Raney, 1991)

REGIONAL SETTING

The Franklin Mountains extend from the City of El Paso, Texas on the south end into southern New Mexico (Figure 2.1). The range trends north-south and exposes Precambrian granite and metavolcanic rocks overlain by Paleozoic strata. Uplift of the mountains tilted the strata so the mountains presently dip westward at angles 40 to 80 degrees (Harbour, 1972).

The Franklin Mountains are an uplift associated with the Río Grande Rift. There are nine basins and 16 sub-basins within the Río Grande Rift (Mack and others, 1997) (Figure 2.1, Figure 2.2, and Figure 2.3). The majority of the basins of the Río Grande

Rift are half grabens that alternate orientation along the rift (Mack and Seager, 1990). Chapin and Cather (1994) propose accommodation zones as the links between the west-tilted and east-tilted basins. Figure 2.1 shows the accommodation zones that lie along the small circles of an Euler Pole in eastern Utah (Chapen and Cather, 1994).

The Tularosa and Hueco Basins combine to form a basin nearly 300 km (Figure 2.1). The Mesilla Basin is approximately 35 km wide by 100 km long. The Mesilla Basin, on the west side of the Franklin Mountains, is distinguished from the Los Muertos Basin in Mexico by a "poorly defined ground-water divide" (Hawley and Lozinsky, 1992). Mack and others (1997) also consider the Mimbres Basin west of the Mesilla Basin to be part of the Río Grande Rift. The total width of the Mimbres, Mesilla, and Orogrande Basins spans approximately 100 km.

Beginning in the Miocene, the Río Grande carried sediment from the mountains of Colorado and northern New Mexico modifying the landscape in ways important to this study. The southern part of the rift was the depositional center of this extended axial stream system and pre-existing topography was largely buried under rapidly aggrading fluvial and lacustrine sediments.

The first evidence of the Rio Grande in the southern rift near the Franklin Mountains has been dated at five Ma by using paleomagnetic reversals and dating of volcanic rocks interbedded within the sediments (Mack and others, 1998). Fluvial deposition shifted to the east side of the Franklin Mountains by two million years ago when the ancestral Rio Grande spilled through Fillmore Pass between the Organ and Franklin Mountains (Hawley and others, 1969). By the early Quaternary (2 Ma), the ancestral Rio Grande had spilled through Fillmore Pass between the Organ and

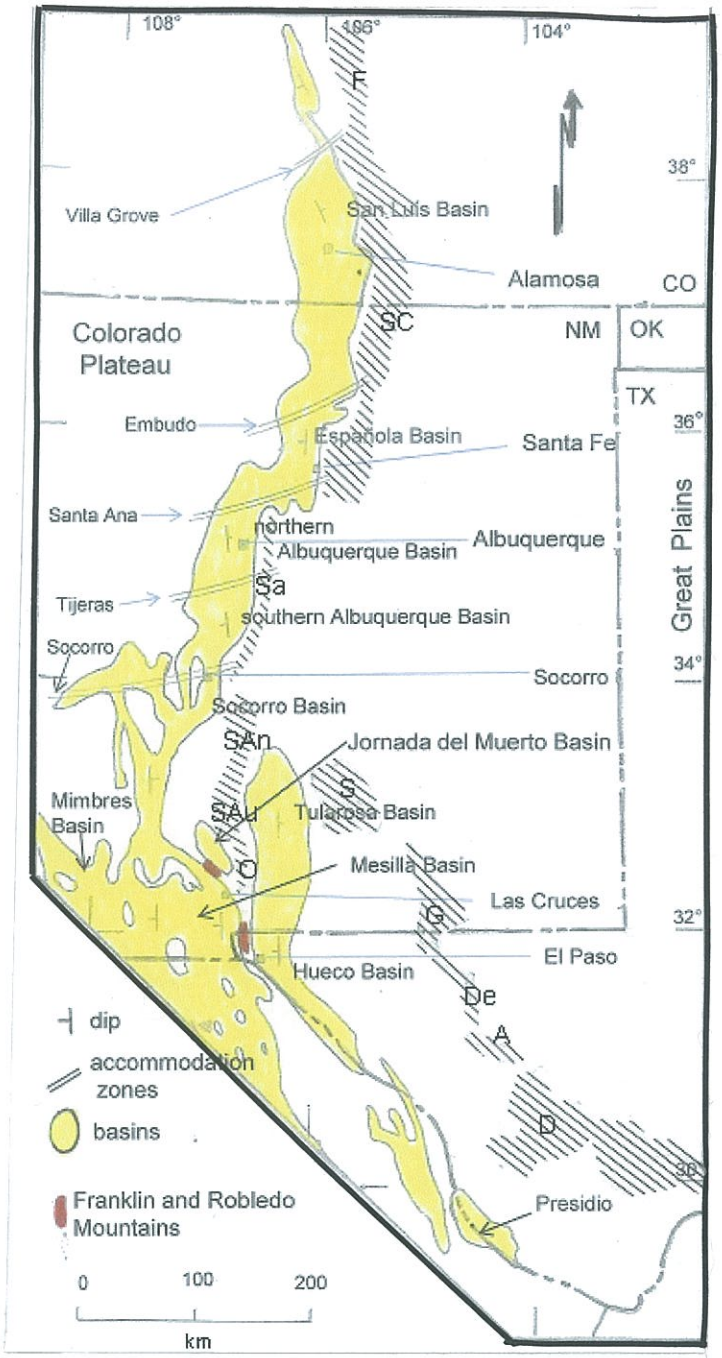

Figure 2.1 Index map (modified from Keller and Cather, 1994) of the Río Grande Rift with accommodation zones(adapted from Chapin and Cather, 1994) shown as parallel lines and traditional dip symbols displayed in the asymmetric grabens. The two areas of interest are in black. Basin bounding mountains (adapted from Armstrong and others, 2013) are: D-Davis, A-Apache, De-Delaware, G-Guadalupe, S-Sacramento, O-Organ, SAu-San Augustine, SAn-San Andres, Sa-Sandia, SC-Sangre de Cristo, F-Front Range.

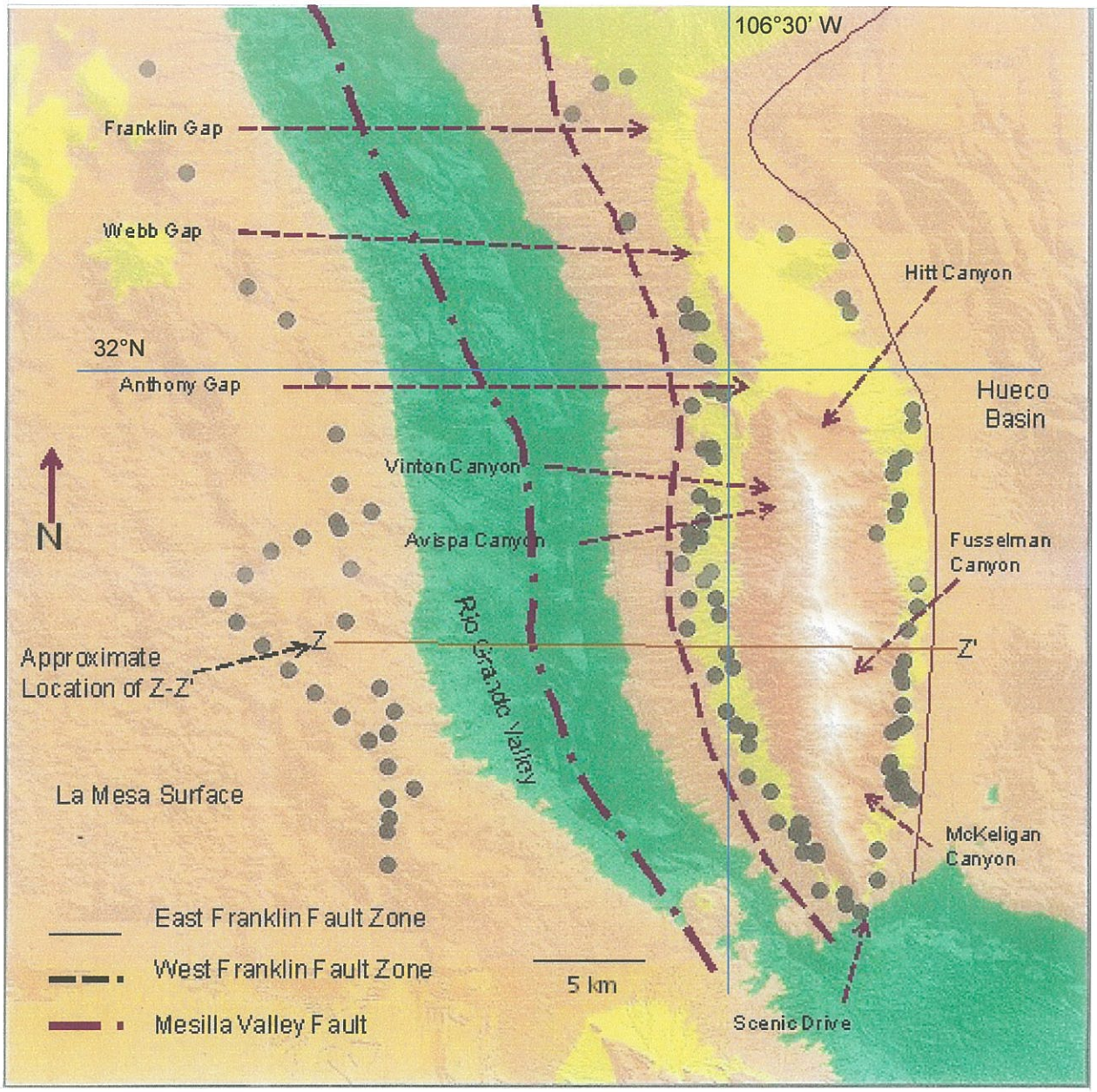

Figure 2.2. Map showing the collected points with relation to mountain. Not all points were used-higher points were replaced with lower points to avoid the influence of the alluvial fans.

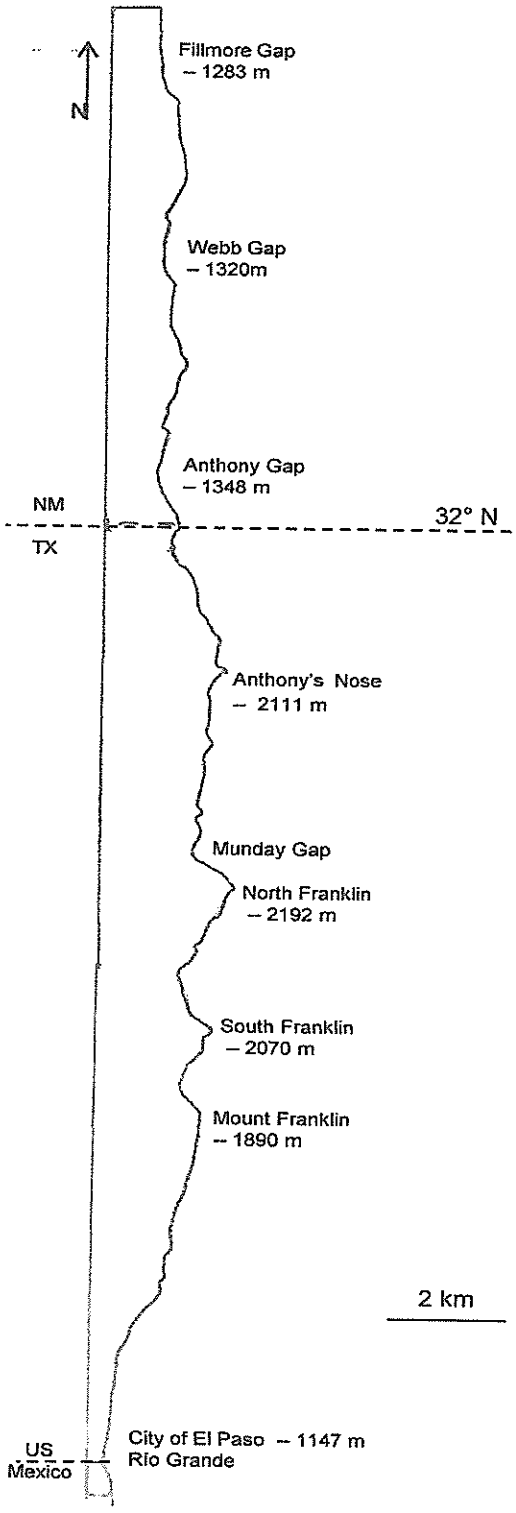

Figure 2.3. Cross-section showing the general location and elevations of the major peaks and gaps in the Franklin Mountains.

Franklin Mountains and was filling the Hueco Basin with river sediments (Hawley and others, 1969).

Deposition on the basin floors ended about 700,000 years ago (Vanderhill 1986; Mack and others, 1993; Hawley and others, 1969; Mack and others 1998; Lucas and others 1999; Gile 2007). The 640,000 year old Lava Creek Ash B is found in the oldest sediments inset into the top of the valley in Selden Canyon and El Paso Narrows, demonstrating that initial Mesilla Valley down-cutting occurred before 650,000 years ago (Izett and Wilcox, 1982; Seager and others 1984; Gile and others 1981 and 1995). The final depositional surface forms the lower La Mesa surface (Gile and others, 1981), a broad flat slope that dips southward at approximately 0.001 meter per kilometer.

FRANKLIN MOUNTAINS and EAST FRANKLIN FAULT ZONE

The Franklin Mountains are separated from the Hueco Basin to the east by the East Franklin Fault Zone. On the west, a complex of faults known as the West Franklin Fault Zone and the Mesilla Valley Fault separate the range from the Mesilla Basin (Lovejoy, 1971), (Figure 2.2). The range is cross-cut by several northwest and west trending normal faults (Lovejoy, 1975; Collins and Raney, 1991). None of these faults offsets the range-bounding faults so their movement must have ceased prior to the deposition of covering basin fill (Scharman, 2006).

The Hueco Basin (Figure 2.1) is more than 170 km long and 50 km wide, approaching three km deep near the east side of the Franklin Mountains (Collins and Raney, 1997; Averill and Miller, 2013). Numerous Quaternary faults cut the surface of

the Hueco Basin (Collins and Raney, 1994), (Figure 2.4). The fill is a combination of alluvium and Fort Hancock Formation sediments dating from 20 Ma (Gile and others, 1981; Collins and Raney, 1991) covered initially by Camp Rice Formation. Since 700,000 years ago, the basin has been weakly eroded and covered by alluvium and sand dunes.

Ramberg and others (1978) show en echelon faulting along the east side of the Franklin-Organ-St. Augustine-San Andres chain. Their data do not contain sufficient detail to distinguish small fault segments. They estimated 9.6 m of Holocene to late Quaternary slip based on a fault scarp 35 m long on the east side of North Franklin Mountain and about seven meters of slip near the south end of the Franklin Mountains.

The East Franklin Fault is the more active of the boundary faults. Studies near White Sands Missile Range indicate the last movements on the East Franklin-Organ Fault Zone occurred within the last 4000 to 5000 years (Seager, 1980). The date was determined by comparing soil development on the oldest unfaulted fan to the soil on the youngest faulted fan (Seager, 1983). Movement along the Artillery Range Fault section of the East Franklin Fault Zone may have blocked the ancestral Río Grande's course into the Hueco Basin (Mack and others, 2006).

A study of the East Franklin Mountain Fault Zone by McCalpin (2006) focused on a trench a few meters south of Hitt Canyon within three km south of the Texas-New Mexico state line (Figure 2.2). McCalpin found five normal faults, though there was uncertainty associated with the older faults. He was able to date three slip episodes using ^{14}C and compared them with infrared-simulated luminescence done on four fine, inorganic silt samples. The mean throw was 3.5 m although two paleoearthquakes

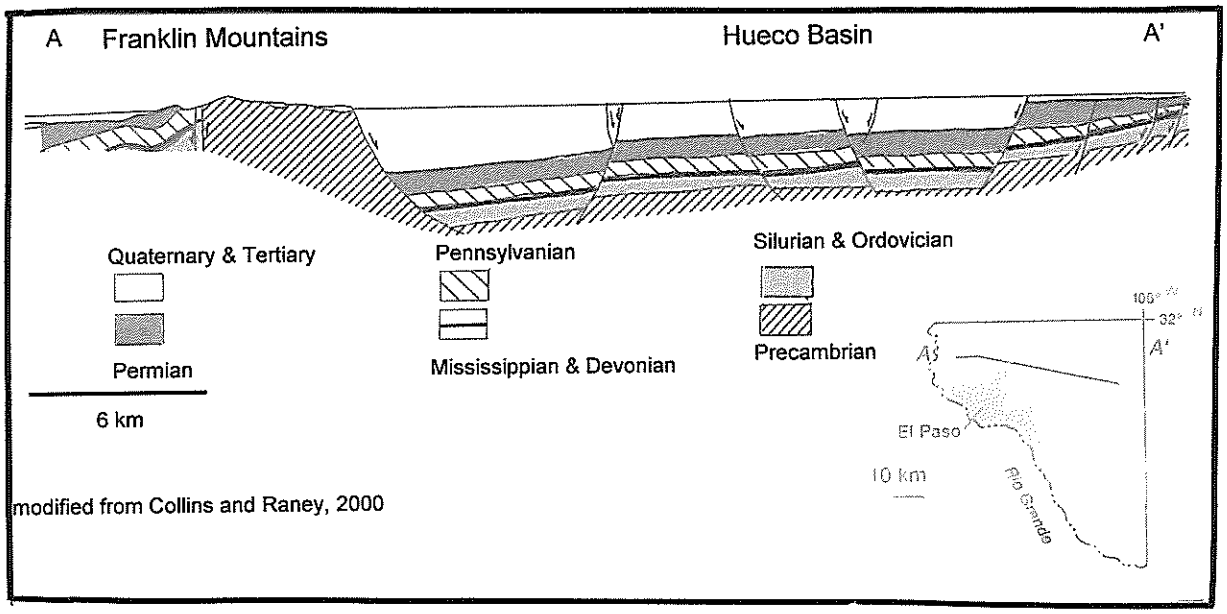

Figure 2.4. Cross-section through Munday Gap area showing two boundary faults across the Franklin Mountains plus the faults within the Hueco Basin.

exhibited displacement of about three meters. A mean slip rate of 0.175 mm/yr was estimated as a minimum slip rate from the last 16,400 years from the total displacement of 11.2 meters.

WEST BOUNDARY FAULT ZONE and MESILLA BASIN

There are differing interpretations of the West Franklin Fault Zone. Lovejoy (1975) proposed that this fault extends the entire length of the Franklin Mountains and possibly as far north as along the west side of the Organ, San Augustin, and San Andres ranges (Figure 2.1), though he believed it is partially covered by possible landslides especially along the Franklin Mountains. Harbour (1972) saw no evidence of this fault north of Avispa Canyon (Figure 2.2). There are no conspicuous offsets of the Pliocene terraces along the fault trace indicating the fault is no longer active or has a very long interval between seismic episodes.

Scharman (2006) pointed out that there are many low angle normal faults associated with the Franklin Mountains and other ranges along the Río Grande Rift. Based on the angle the low-angle faults cross bedding plains, Scharman (2006) supported Seager's (1980) hypothesis that the low-angle faults originally were high angle normal faults rotated during uplift and extension and are older than the range-bounding faults.

The Western Boundary Fault Zone cuts a major thrust fault and numerous smaller faults so this fault is strictly of Basin and Range origin and not a reactivation of previous deformations (Scharman, 2006). The fault boundaries of the Franklin Mountain structure are curved in map view; this may be due to irregularities within the

basement rocks (Harbour, 1972; Collins, 1996).

The West Franklin Fault Zone appears to be inactive because nowhere does it disrupt the terraces (Scharman, 2006). The active major fault along the western side of the Franklin Mountains is the Mesilla Valley Fault (Henry and others, 1985) (Figure 2.2). This fault is between Interstate 10, a kilometer or more west of the mountains, and the Río Grande still farther west. It may extend north to Las Cruces where it merges with similar faults between the Doña Ana and East Robledo Faults (Lovejoy, 1975). Gravity and magnetic data between the West Franklin Fault Zone and the Mesilla Valley Fault suggest there are three smaller, stair-step faults under valley fill (Imana, 2003).

SEDIMENTARY RECORD

Basin fill has buried the bedrock of all but the Franklin and Juarez Mountains (Hawley and Lozinsky, 1992). The sedimentary record of the Río Grande rift system includes Miocene strata and the Plio-Pleistocene Fort Hancock and Camp Rice Formations of the Santa Fe Group (Hawley, 1975; Mack and others, 1998), (Figure 2.5). The Fort Hancock Formation is composed of playa, lacustrine, and alluvial fan facies derived from the local mountains (Figure 2.6); the Camp Rice Formation sediments are the Río Grande gravels and alluvium derived from upstream sources (Chapin and Seager, 1975; Collins and Raney, 1991) (Figure 2.7). The Fort Hancock is evenly bedded with fine texture and in Hudspeth County, based on borehole evidence (Strain, 1969), is 1067 m deep (Strain, 1980).

Mack and Seager (1990) place the appearance of the Río Grande in the Mesilla Basin at five Ma. In the Hueco Basin, Albritton and Smith (1968) and Gustavson

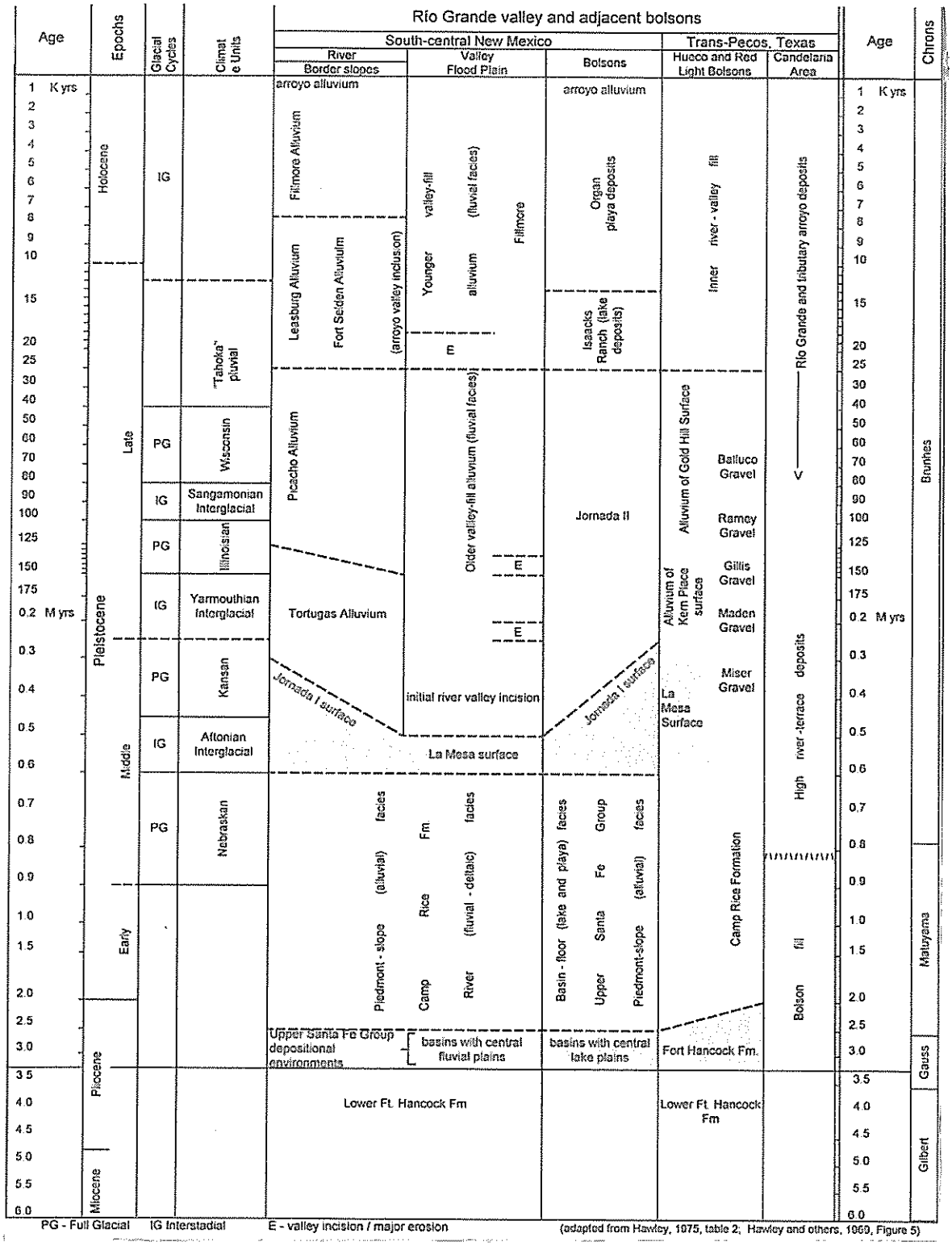

Figure 2.5. Stratigraphic column showing Quaternary deposits and events in south-central New Mexico and far western Texas.

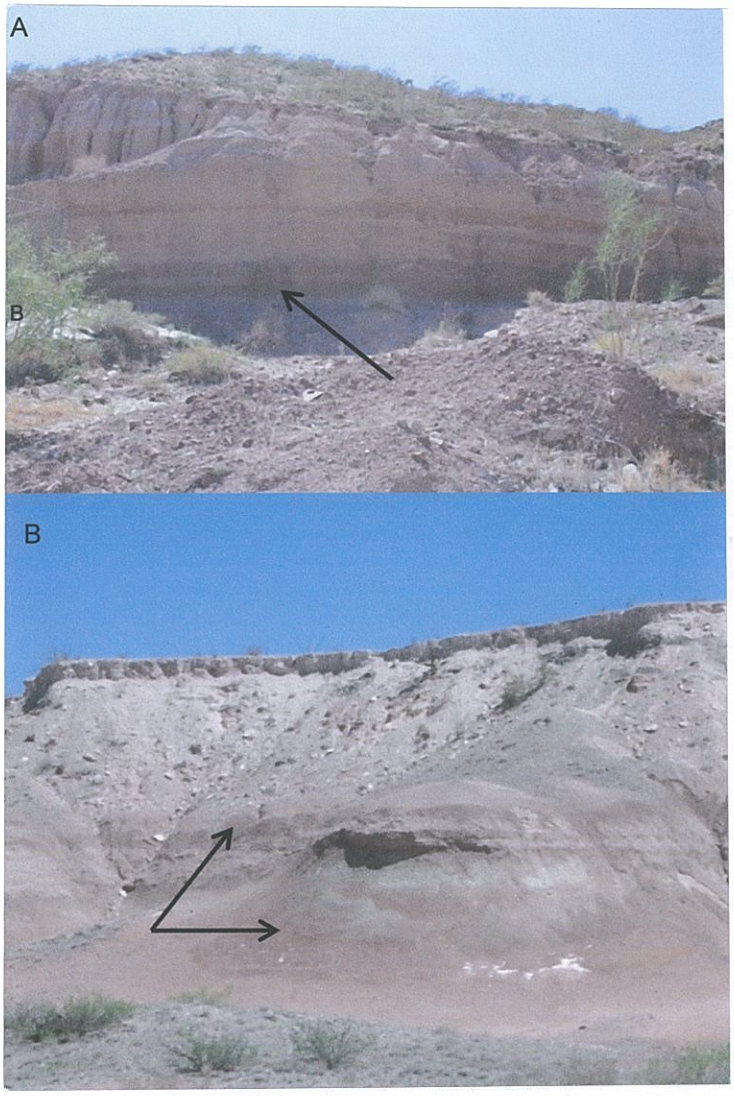

Figure 2.6A. Outcrop above Idalia Street showing playa sediments (east side, El Paso). Ordovician bedrock to right of photo.

Figure 2.6B Closer view of playa sediments at west end of Idalia Street (rod 2 m). Sand flats, mud flats, and debris flow deposits result of earthquakes or storms.

Figure 2.7. Camp Rice Formation as exposed in a road cut north of New Mexico Highway 404. Note cross-bedding (solid arrows) and soil contact (dashed arrow).

(1991), date the appearance of the Río Grande at 2.1 Ma. Along the Franklin Mountains, a series of terraces are observed that date to this inception of the Río Grande with river channel sands along the western side sand playa muds along the eastern flank atop the terraces. This constrains the highest terrace ages to between five and two Ma. These ages were determined by K/Ar dating of volcanic deposits (Chapin and Seager, 1975; Seager and others, 1984), vertebrate fauna (Strain, 1966; Metcalf, 1969) as well as studies of soil development on upper beds of the Camp Rice Formation, (Seager, 1980; Gile and others, 1981). The volcanic ashes found in the Camp Rice Formation match air-fall ashes from the Lava Creek Ash B dated at 640,000 years ago and two Ma. and Bishop ash from about 700,000 years ago (Gile and others, 1981).

Up to 150 m of Camp Rice Formation conglomerate and sandstone deposits in alluvial fans and alluvial flats are exposed in outcrops. The ancestral Río Grande left cross-beds and horizontally laminated pebbly sand/sandstone and mudstones that formed the terraces (Mack and others, 1998) (Figure 2.7).

The basins in the southern Río Grande rift were filled by rapidly aggrading fluvial and playa sediments which created broad, low gradient basin floors. For example, the La Mesa surface remains on the west side of the Río Grande (Gile and others, 1981). The aggradation during Fort Hancock and Camp Rice deposition buried the toes of the alluvial fans along the eastern flank of the Franklin Mountains, with the possible exception of the area near mouths of the two large canyons - Fusselman Canyon and McKelligon Canyon. Along most of the east flank of the mountain front, playa muds inter-tonguing with debris flows and thin alluvial fan gravels are exposed within a few

meters of bedrock (Figure 2.6A). Along the western flank of the mountain, fluvial sediments of the Camp Rice formation are intermittently exposed within a few tens of meters of the mountain front.

Intrenchment of the ancestral Río Grande system ended deposition of the Camp Rice Formation. The La Mesa Surface (middle Pleistocene) between the Río Grande valley floor and the East Portrillo and Robledo fault zones is 100 m above the current floodplain (Figure 2.8). It is approximately 780,000 year old (Mack and others, 1998). The surface is underlain by Camp Rice fluvial facies partially covered by Holocene sediments and coppice dunes. The surface sediments are gravelly strata that are resistant to erosion.

Unlike most ranges in extensional terraces, the Franklin Mountains are flanked by terraces composed of Fort Hancock and Camp Rice Formation sediments capped by thick alluvial fan gravels instead of growing together and becoming sloping bajadas. These terraces lie on the footwall of the east and west Franklin faults and were uplifted along with the footwall (Figure 2.9). Thus, these terraces record overall deformation of the range after their deposition.

Harbour (1972) first noted that terraces had been uplifted along the eastern flank of the Franklin Mountains. The only previous studies of the Franklin Terraces were those of Kottlowski (1958) and Lovejoy (1975). Lovejoy (1975) documented 105 - 120 meters of basin-downward displacement of the terraces on the west side of the Franklin Mountains and suggested that the Franklin Mountains had been tilted two degrees to the west after deposition of the alluvial terraces due to relatively greater uplift on the East Franklin Fault (Figure 2.10). This configuration exhibits a classic half-graben tilt.

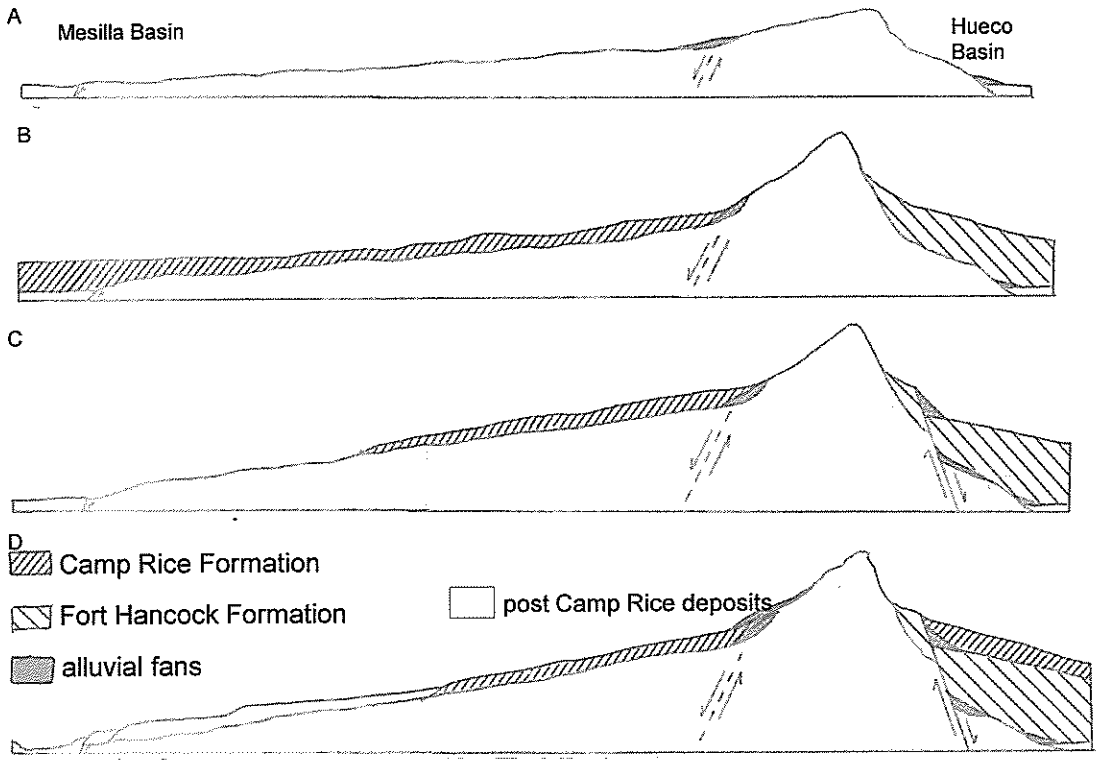

Figure 2.8. A - Schematic cross-sections of the Hueco Basin to the Río Grande Valley showing the progression that uplifted the terraces. A - the surface is eroded to previously lithified layers prior to Camp Rice deposition.
B - deposition from floods caused by warming periods probably within the Nebraskan Glacial period or early Aftonian Interglacial period on the west side of the mountain; Fort Hancock sediments were deposited on east side of the mountain.
C - later flow erodes the Camp Rice deposits shown in section B; the Fort Hancock sediments are faulted and begin developing alluvial fans along the East Franklin Fault Zone.
D - after more faulting, uplift, and additional deposition, additional deposits form the lower terraces on the west side; the eastern side sediments continue to erode with the lower area being covered by bajadas along the mountain front.

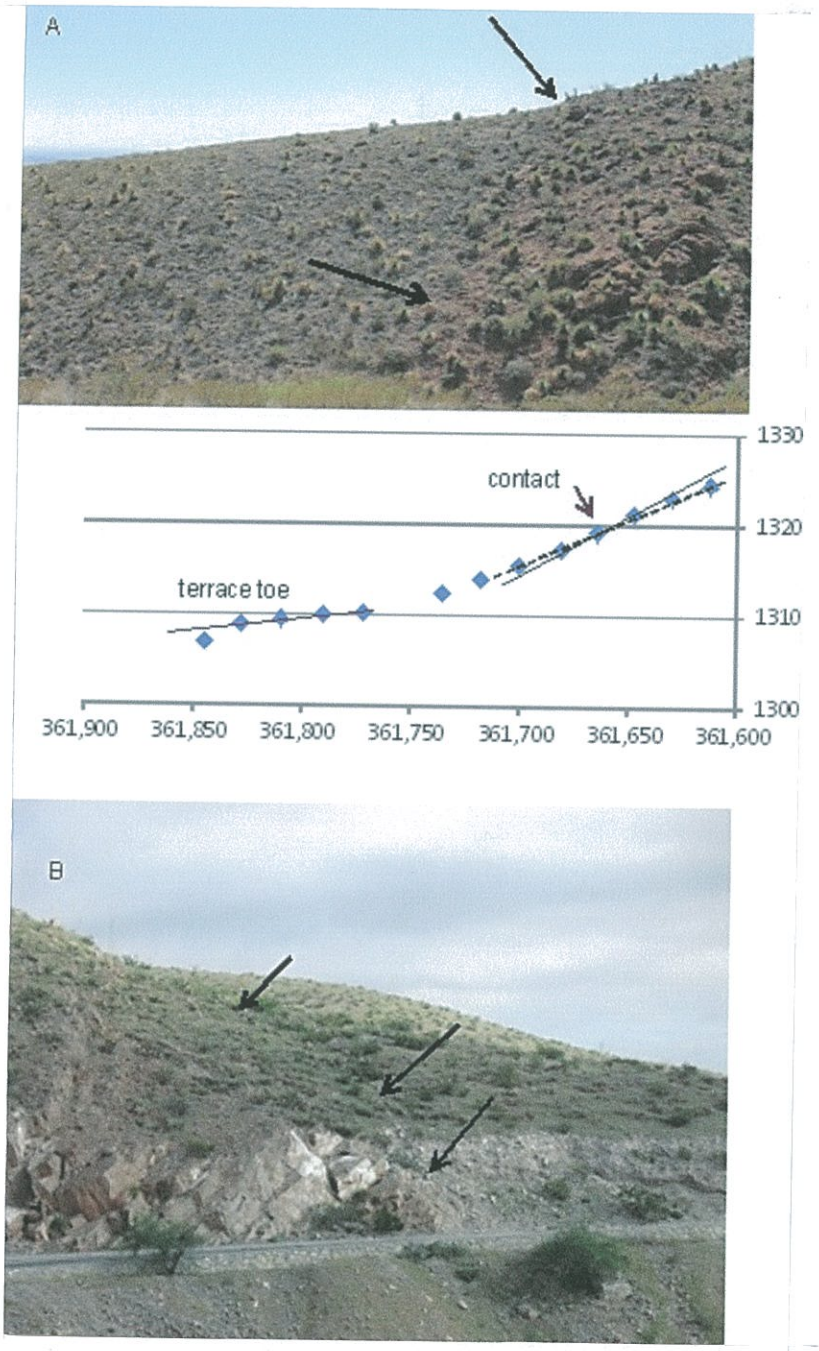

Figure 1.9. East side of the Franklin Mountains, with Fort Hancock sediments in contact with the Precambrian mountain front. The contact is not immediately obvious when underfoot because of Precambrian rhyolite pieces that rolled over the alluvium. In picture A, the difference is the slope and the general roughness of the terrain above the arrow. (Photo above El Maida Shrine Temple in El Paso) The graph shows the slope that was measured using the GPS.
Figure 9B shows the same contact as seen along Scenic Drive a few meters north of the El Paso Police Academy.

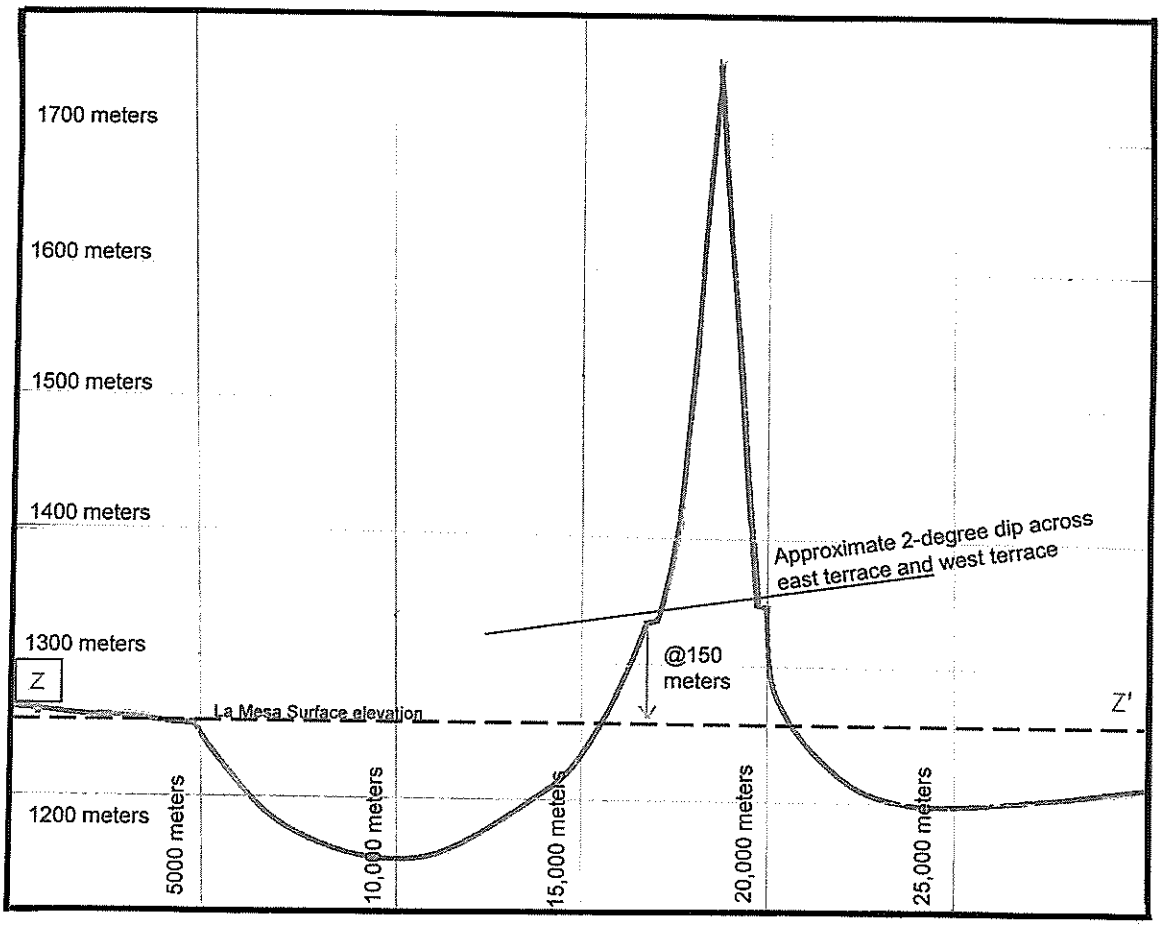

Figure 2.10. Cartoon cross-section Z-Z' with 2 x vertical exaggeration showing dip from east side of Franklin mountains to west side. Section also shows approximate 150 meter difference between west terrace and elevation of La Mesa Surface west of Río Grande.

The terraces are the remains of a relatively smooth surface that now is disrupted by arroyos formed by down-cutting to the base-level of the Río Grande.

The entrenchment of the ancestral Río Grande system ended deposition of the Camp Rice Formation (Figure 2.11). During deposition of the Camp Rice and Fort Hancock Formations, uplift of the mountain blocks began to lift parts of this low-relief surface above the aggrading basin floors, causing deposition to stop and defining the uplifted terrace surfaces that are the subject of this study. "Uplifted terrace" is an appropriate term for the terraces that are the focus of this study; it is the term also used by Harbour (1972). The uplifted terraces are the remains of the original fluvial and lacustrine surface that formed the valley floor. The younger terraces, closer to the river were formed in a more traditional fashion - parallel to the river as it flowed through its valley.

As the terraces were uplifted, aggradation continued on the footwall block by Camp Rice and Fort Hancock sediments burying the equivalent surfaces in the subsiding Hueco and Mesilla Basins, until the 700,000 years ago incision of the Río Grande Valley commenced.

ROBLEDO MOUNTAIN

The Robledo Mountain exposes Paleozoic and Eocene age rocks that are tilted 10° to 14° to the south (Figure 2.1). Down-faulted blocks on both sides of the mountain are topped with fluvial Río Grande deposits. The Camp Rice Formation on-laps the southern part of the mountain (Hawley and others, 1975; Kottlowski and Seager, 1998) as it does with the terraces observed in the Franklin Mountains. The East Robledo

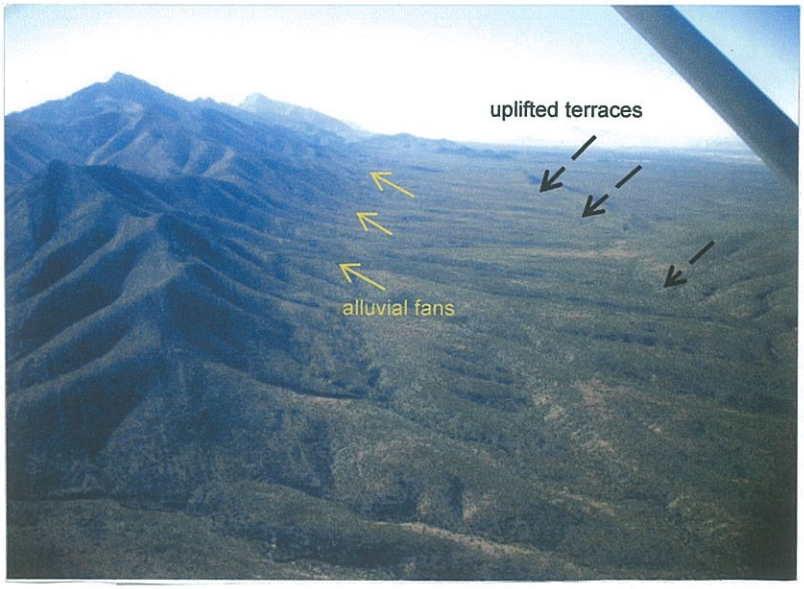

Figure 2.11. West flank of the fault zone forms a dark, eroded band separating relict alluvial fans shown with upward pointing arrows along the mountain front. The gently sloping terrace surfaces are indicated by downward pointing, dashed arrows.

Fault cuts Camp Rice fanglomerates exposing a sequence up to about 90 meters thick. Metcalf (1967) and Hawley and Kottlowski (1969) saw three episodes of valley entrenchement followed by partial backfilling of the arroyos (Figure 2.12).

The East Robledo Fault has been active since late Pliocene as is shown by the comparative thicknesses of the Camp Rice sediments on either side of the fault. The sediments on the hanging wall side of the fault are appreciably deeper than the sediments on the footwall side of the fault (Mack and Seager, 1990) indicating the movement provided more fill space than had previously been available.

METHODS

A TRIMBLE Geo Xh, 2005 Series Pocket PC was used to acquire approximately 50 GPS-located elevations from both flanks of the Franklin Mountains as well as the La Mesa Surface from the Texas/New Mexico border to nearer the international boundary. The elevation of data were generally better than 30 cm and commonly better than 15 cm. The profiles of some uplifted terraces were measured along the crest of the terrace from the alluvial fan at the head of the slope break at the toe of the terrace; a reading was taken about every 70 cm. Measurements were estimated from the USGS 7½ minute topographic maps or DEMs in areas where the terraces were inaccessible as on the firing range at Fort Bliss.

Data from the La Mesa Surface along the western side of the Río Grande Valley in New Mexico were used as a control because there is evidence for much less deformation of this younger deposition surface. South of 32° N latitude, deformation of

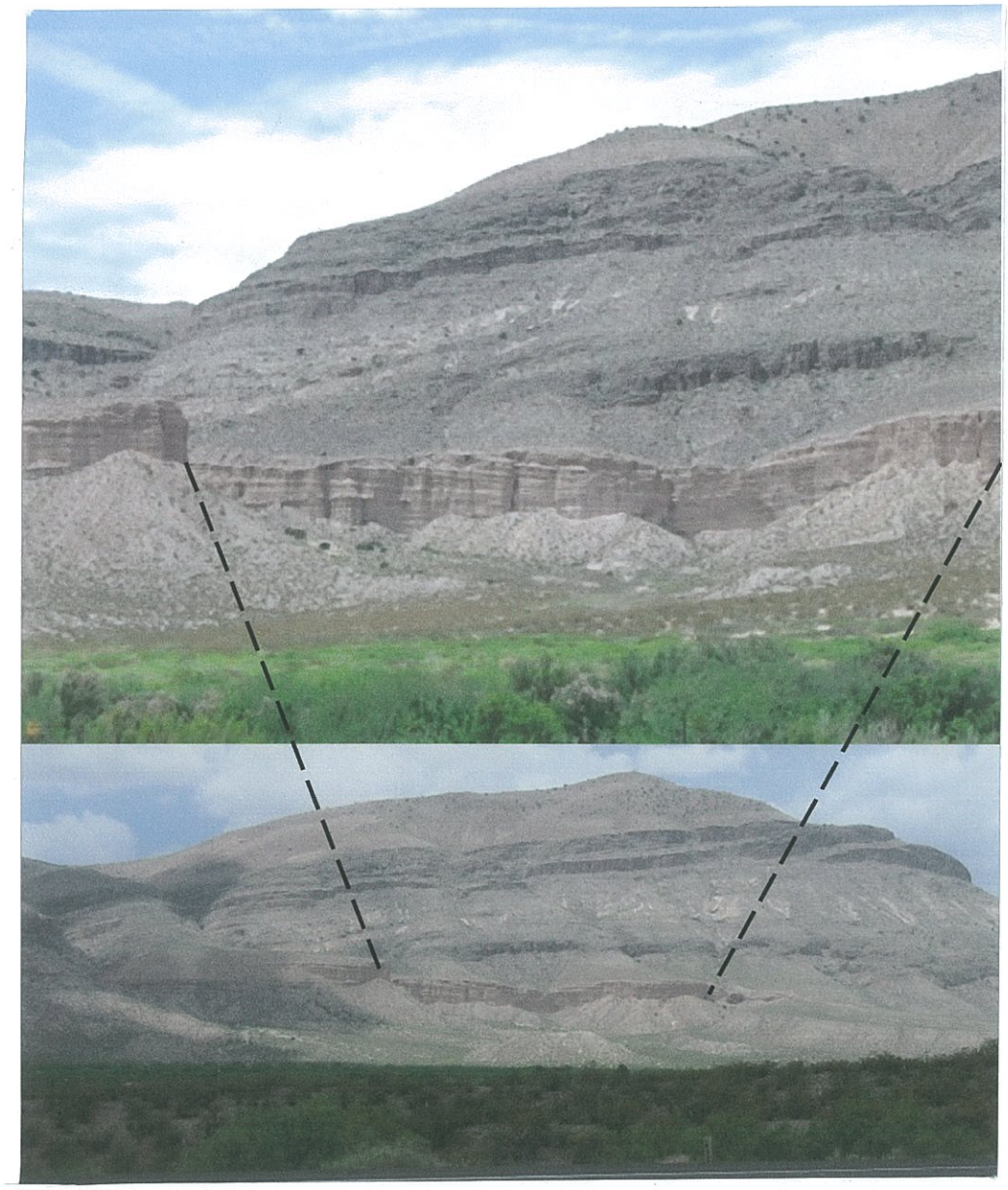

Figure 2.12. Sierra Robledo, lines bound the area of greatest interest. This 500,000-- 600,000 year old surface maintains a slope parallel to the modern stream system.

Data were exported in UTM, zone 13N projection, and plotted in a variety of orientations to allow description of the geometries of the uplifted terrace. The measurements were taken where the slope was the flattest to minimize the younger alluvial fan deposits that fell and rolled onto the terrace proper.

RESULTS

Examination of uplifted terraces along the northern end of the range provided naturally exposed outcrops (Figure 2.13). Along most of the uplifted terraces, alluvial fans continued to build over the Camp Rice Formation. In the lower part of the terrace, however, the surface of the uplifted basin floor was better preserved near the toe of the terrace. After this discovery, the data were reexamined. Slopes were checked, the points used for comparison were moved from the head of the uplifted terraces to a point near the toe of the terraces where alluvium carried from the mountains has not obviously added to the elevation. Some of the terraces previously selected were probably alluvial fans instead of uplifted terraces. The younger alluvial fan deposits can be observed in aerial view but are nearly impossible to discern from ground level (Figure 2.9).

The alluvial fans have a steeper slope than the terraces. An oblique aerial view often gives some indication of the extent to which alluvial fans prograde over the terraces (Figure 2.14). At the toe of the terrace, the surface cover can be thin desert soil with a scattering of medium to coarse gravel or a well cemented cobble to boulder o of varying thickness. The varying thickness of gravel creates noise in the interpreted terrace elevations, however, the magnitude of deformation due to uplift greatly exceeds

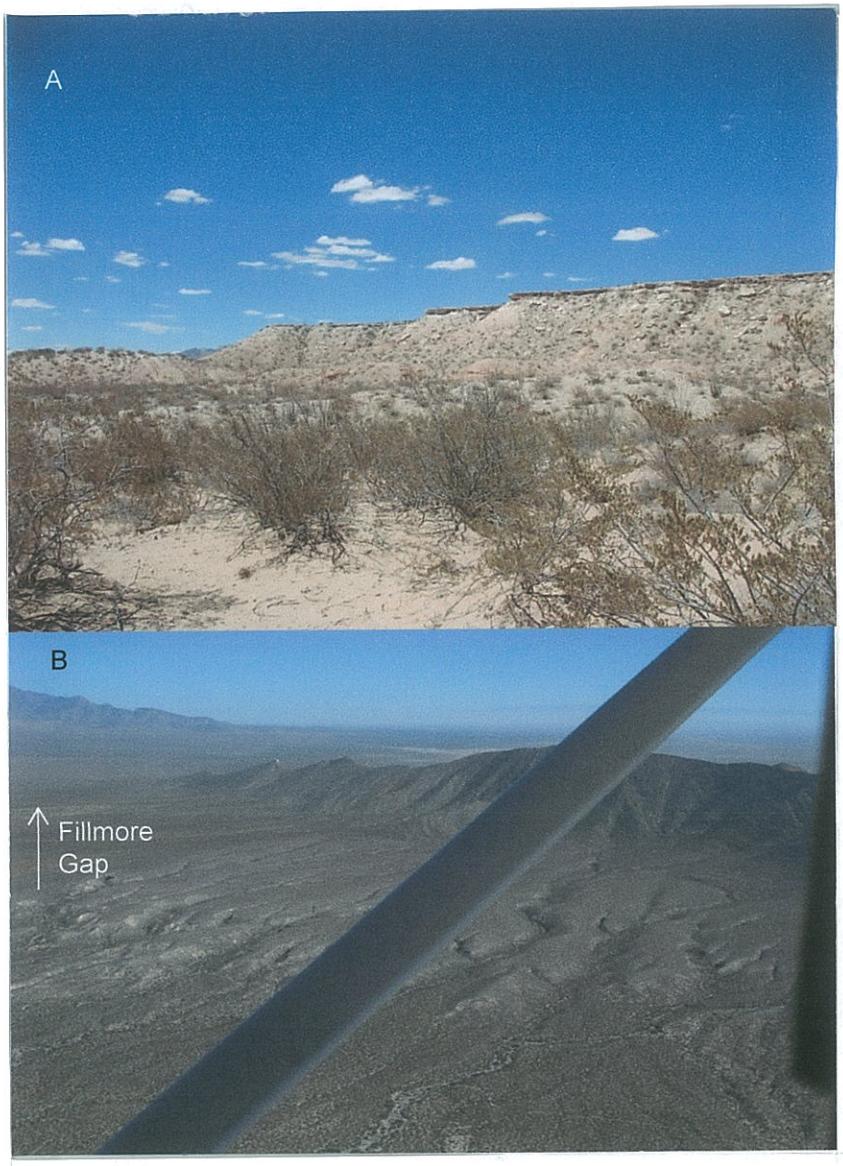

Figure 2.13A. Camp Rice sediments at Fillmore Gap as approached from the south.
Figure 2.13B Fillmore Gap from southwest - note extent of sediments

the noise resulting from fan deposition.

The uplifted terraces have been protected from erosion by a mantle of alluvial fan gravels of varying thicknesses. The structure of the terraces is revealed in exposures in the Robledo Mountains where recent erosion has dissected several terraces. The basin floor sediments, in this case fluvial sandbars, made the Camp Rice Formation, are tilted down and toward the mountain front to the west. This is inferred to result from down to the west rotation of the rising Robledo Fault Block. Alluvial fan gravels formed beds inclined to the east opposite to the basin fill and reveal a gradual progradation of an alluvial fan that grew across the rising terraces.

The terrace elevations, when plotted along the strike of the mountains, show a broad - 40 km long - asymmetrical anticlinal arch. The circles on the graph represent data points on the east side of the Franklin Mountains (Figure 2.15A and Figure 2.15B). The northern eight km of the eastern side rise 30 meters along a relatively gentle trend. From approximately 18 to 24 km, the slope Anthony's Nose (Figure 2.3), the slope changes again; it flattens to a 20 meter rise over nine kilometers. The high spot is 1364 m on the east side. East of that point, approximately 8.5 km north to approximately two kilometers from the southern end of the mountains, the slope of the terrace decreased to 39 m over 10.5 kilometers.

TERRACE MORPHOLOGY and STRATIGRAPHY

A typical uplifted terrace appears to be a relatively low gradient finger of higher topography extending from the mountains. The measured terraces are 85 to 150 m across and extend 140-350 m from the steeper alluvial fan portions. Crests of terraces

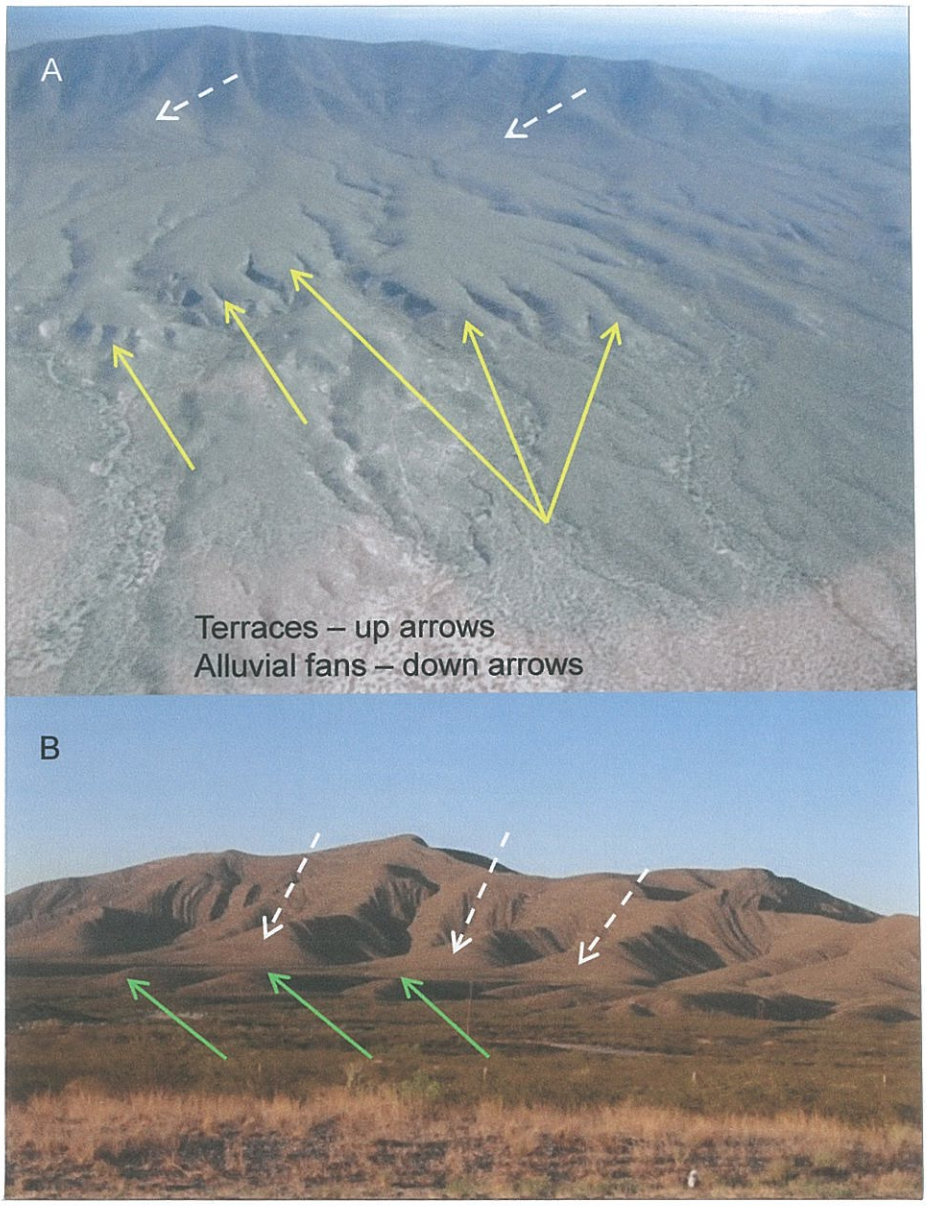

Figure 2.14A. Aerial view of the terraces west of the North Franklin Mountains. The difficulty in identifying fans vs terraces is that alluvial material is found nearly to toe of the terrace – without an arroyo or road cut, it is difficult to determine what is fan or what is terrace.

Figure 2.14B. Photo taken from New Mexico Highway 404 looking toward same area as A. Arrows pointing up highlight the terrace toes; the down arrows indicate more deeply dipping alluvial fans that bury the upper parts of the terraces against the mountain front. There is relatively little uplift along the western front of the North Franklins as compared to the central and southern parts of the range.

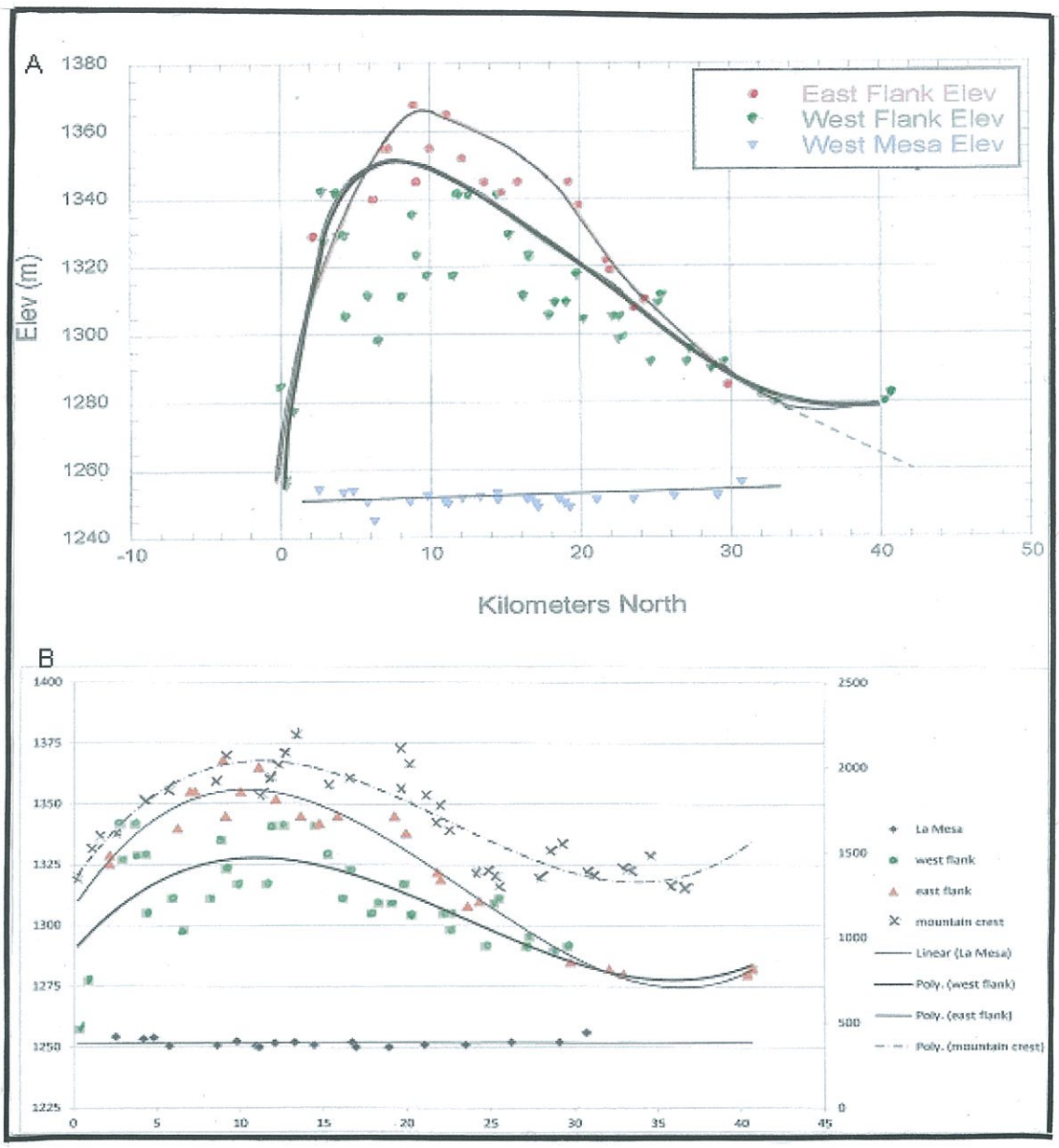

Figure 2.15. Graph A shows the La Mesa Surface - the flat line - as a control, with the west side terraces of the Franklin Mountains (square data points) and the east side points (designated with triangles). This plot is from Quantum GIS; the trend is hand-fit. The northern end of the North Franklin Mountains is buried under Camp Rice sediments so the northern end of the mountains is projected by the dashed line.

Figure 2.15B shows the same data and was plotted in Excel with the left Y axis for the same data as above as compared with the mountain peaks and passes (X points) plotted against the Y-axis on the right. The La Mesa Surface line is linear. The other three trend lines are third order polynomials.

are low gradient, with slopes of 5% to 10% from the mountain front. The flanks of the terraces are steeper, with slopes of 35% to 50%. Figure 16 illustrates the form of the terraces. Many of the larger terraces are associated with canyon mouths and arroyos that exit the canyons and are diverted along the mountain front for a short distance before continuing between the terrace remnants. This suggests that early alluvial gravel deposition in the upper terraces protected the terraces from erosion; the more exposed areas flanking the canyons have less gravel so were more vulnerable to incision.

Along their bases and flanks, the terraces merge with steeper slopes that form their margins. On the mountain side of the terraces, they commonly merge into steeper intervals (Figure 2.6A). The surfaces of these steeper intervals are littered with coarse, angular clasts from the adjacent mountain slopes; these are interpreted as relict alluvial fans, now isolated by incision of the drainages. The boundary between the alluvial fan and terrace can be difficult to identify in the field as it is marked by a gradual increase in slope angle (Figure 2.9).

The internal structure of the uplifted terraces is difficult to observe as the strata are usually covered by indurated Pleistocene or Holocene calcic soils that, except where exposed by arroyo incision, obscure the stratigraphy and structure of the terraces. Several uplifted terraces in the Robledo Mountains are incised through their length and expose both the internal structure and stratigraphy (Figure 2.7). The strata consist of fine- to medium-grained sands of the Camp Rice Formation that are dipping into the Robledo Mountains block at 2-4 degrees. This tilting is similar, but at lower angles than the overall tilt of the range. This is ascribed to tilting of the hanging wall

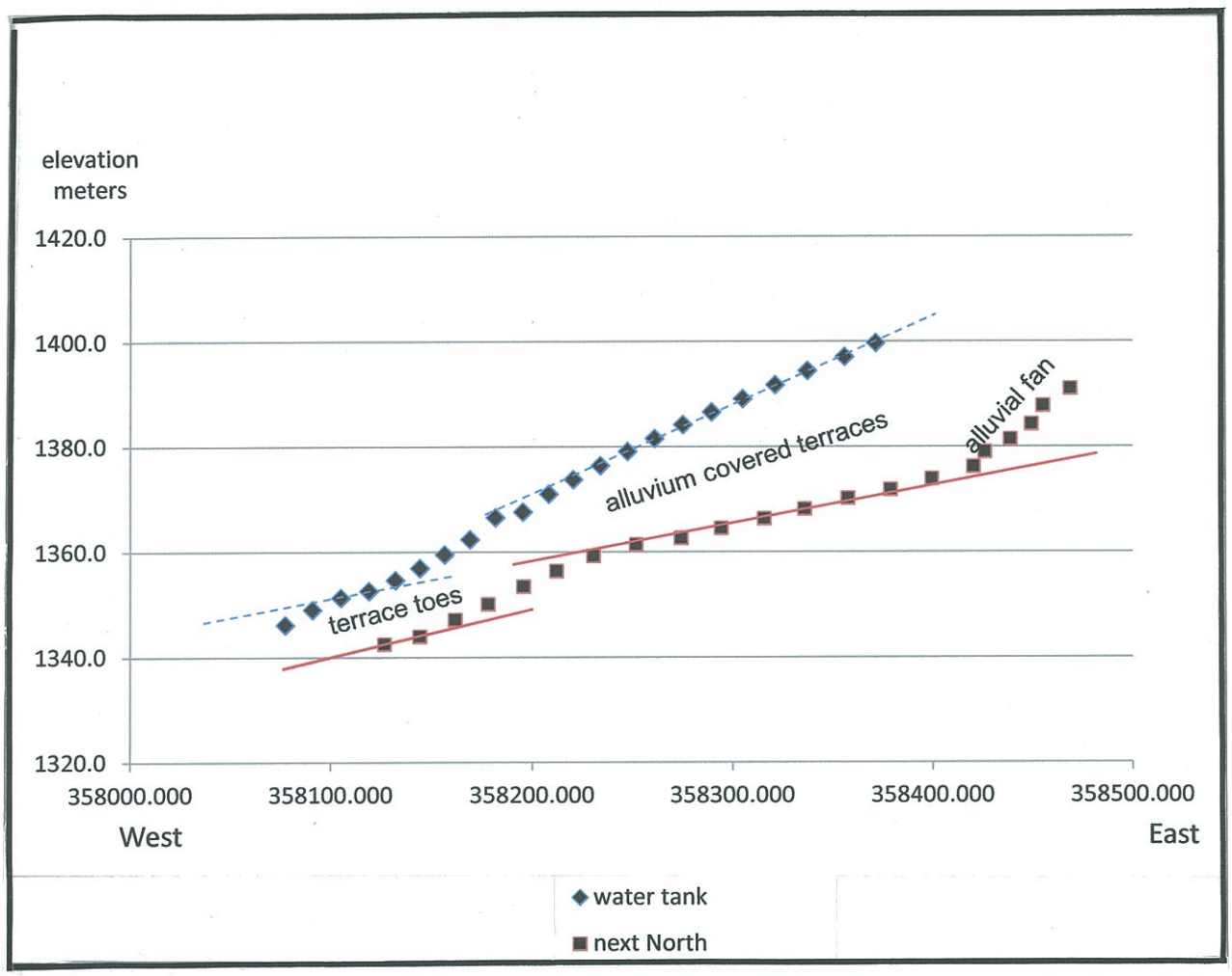

Figure 2.16. Comparison of the terrace above the water tank with the next terrace north – southern group of terraces on west side, Figure 2.2

block during extensional deformation. Similar strata are exposed along both flanks of the Franklin Mountains, but the limited exposures preclude estimates of the dip of the bedding.

In the well-exposed Robledo examples, the basin floor strata are overlain by crude layers of coarse gravel that dip basinward. These beds lap onto the basin floor sediments and are truncated at the top (Figure 2.12). They are inferred to represent the progradation of fan gravels across the sediments prior to erosion during the uplift of the hanging wall on which they sit. The terrace surface overlying these inclined strata is much flatter and appears to be an almost horizontal finger extending from the range front, similar to those in the Franklin Mountains.

The important lesson of the Robledo examples is that there are relatively thick gravels extending across the terrace and the surface that is measured today is an erosional surface that is higher by as much as 15 m than the uplifted basin floor. The data from the Franklin Mountains, described below, contains considerable noise in the form of varying elevations in adjacent terraces. This is attributed to varying thicknesses of gravels, ranging to 25 m, that bury the basin floor sediments. Early in this research, the heads of the terraces were measured as these were thought to exhibit less potential erosion, but greater noise was found within the data. Terraces were then re-measured near their toes where the gravel cover thickness was minimized. Observed thicknesses of gravels capping the uplifted terraces vary from no cover in the northern Franklin Mountains to over 15 m in the central and southern Franklin Mountains. The thickest observed gravel was in one dissected terraces in Robledo Mountain that exposed 30 m of gravel near the mountain fronts. Unexposed gravel thicknesses may reach 25 m as

this is the mean maximum variation between adjacent terrace surfaces in the Franklin Mountains (Figure 2.15).

The uplifted terraces have been deformed from an initially planar surface that filled the entire area to the west side of the incipient mountains into a broad anticlinal arch that is highest near North Franklin Peak in the central part of the range (Figure 3). The uplifted terraces on the east side of the Franklin Mountains appear to be approximately 20 m higher than the uplifted terraces on the west side of the Franklin Mountains but the eastern high points are three kilometers south of the high points on the western side of the mountain. The east side of the mountains also does not exhibit the multiple terraces that are found on the west side. The highest terraces on the east side are at 1370 m elevation, approximately 120 m above the La Mesa Surface (Figure 2.15). This represents a minimum uplift as the floors of the Hueco and Mesilla Basins are younger and the equivalent surface to that of the terraces is buried under an unknown thickness of younger sediment.

At the north end of the range, the topography is flat although still 22 m higher than the La Mesa Surface. This surface is underlain by fluvial channel sands of the Camp Rice Formation (Hawley and Kottlowski, 1969). Lava Creek B Ash in the uppermost fill of Fillmore Gap dates the uplift of the Fillmore Gap surface to post two Ma (Bachman and Mehnert, 1978). The Fillmore Gap segment, also, is not deformed as are the terraces to the south. This leads to the inference that the Fillmore Gap is a younger terrace that formed on sediment that buried the older terrace where uplift was less than uplift in the rest of the Franklin Mountains.

The La Mesa surface forms a low gradient surface with an elevation of 1253.6 m

elevation at the Santa Teresa Airport (Figure 2.15A, Figure 2.15B). The uplifted terraces on both the east and west sides of the Franklin Mountains are higher than the La Mesa surface on the west side of the present Río Grande Valley. The La Mesa Surface has not been deformed and so preserves the southerly gradient of the paleo-Río Grande. A surveyed point at the Las Cruces, New Mexico air port is 1354 meters. This is 101 m higher than the Santa Teresa Airport 50.5 km to the south.

There may be two sets of uplifted terraces on the west side. The gray line and inverted triangles show data found on the west side of the Franklin Mountains. The bold line also traces a broad, asymmetric anticline (Figure 2.15A, 2.Figure 15B). Erosion no doubt has reduced the peaks. The third order polynomial trend lines for the mountain peaks and the elevations of the terraces have similar shape. The La Mesa Surface across the bottom of the graph is best described as linear.

DISCUSSION

Previous models of deformation associated with extension tectonics have largely been oriented perpendicular to the structures. The data presented here constrains these models as it presents along-fault-strike data. The older terraces have been deformed by mountain uplift into a broad anticline that extends the length of the range. Figure 15B, right axis, shows the curve that mimics the elevations along the mountain crest. Because of this extensive deformation, the surface probably dates more closely to five million years. The uplifted terraces flanking the Franklin Mountains can be dated to between five million years when the Río Grande appeared in the Mesilla Basin, and two million years when the river flowed through Fillmore Gap at the north end of the

range (Figure 2.2, Figure 2.13). The uplifted, but generally horizontal surface flanking the northern part of the range probably dates to near the two million year date and buries the older, deformed terraces.

In contrast, the La Mesa Surface has essentially been undeformed and only weakly incised since it was deposited approximately 700,000 years ago. The only way the terraces could have risen above the La Mesa surface from their original elevations is for them to have risen along with the mountains. The terraces at the crest of the anticlines have been uplifted 110 m above the undeformed and only weakly incised La Mesa Surface. Because the La Mesa Surface is much younger than the Franklin Mountains and basin floor aggradation continued during the deformation of the range, the 100 m uplift represents a minimum uplift of the terraces.

The uplifted terrace elevations correlate with the range crest elevations, deformation by the faults may correlate with range topography thus implying a low relief surface prior to deformation on the East Franklin Fault.

This prompts the question, "What shaped the uplift of the range?" Of the various mechanisms for uplift associated with extensional deformation, only the flexural model of Brown and Phillips (1999), or the block rotation model of Melosh and Williams's (1989) and Melosh's (1990) numerical analysis model provides uplift that is associated with the magnitude of faulting observed and are supported by the data in the Franklin Mountains. These models also imply that uplift of the mountains should largely correlate with deformation along the East Franklin Fault. As the East Franklin Boundary Fault rotated the eastern side upwards, it also lifted the west side of the mountains.

Gravity maps (Marrufo, 2011) show that the gravity low indicating the deepest

part of the Hueco Basin is opposite the central and southern parts of the Franklin Mountains. This is the area where terrace uplift is greatest. Opposite the northern end of the range, the fault veers to the northeast end and becomes less of a half-graben and more of a graben, correlating with the lower topography of the range front.

The terraces along the east side of the mountain are as much as 20 m higher than the terraces on the west side (Figure 2.10, Figure 2.15A, Figure 2.15B). If the terraces were originally at nearly the same elevation; the 20 m difference across the 4000 m width of the mountain represents a 2-degree rotation of the Franklin Mountain block after terrace deformation. Lovejoy (1971) also described this difference as resulting from a 2.3-degree rotation of the Franklin Mountain block.

As described above, the Franklin Mountains form a complex tilted horst with the major boundary fault on the east flank and a broad complex of faults separating it from the Mesilla Basin to the west. The West Franklin fault zone was inactive after deposition of the uplifted terraces and does not offset the terraces (Scharman, 2006). However, faults near the modern course of the Río Grande offset the Camp Rice fluvial deposits and terraces flanking the river. Using a horizontal plane extending from the west mesa and a two degree inclination from the uplifted terraces provides a pivot-point west of the mountain front. Assuming 150 m of deposition, burying the surface in the Mesilla Basin equivalent to the terrace depositional surface results in a 300 m elevation difference and a pivot point approximately 8.6 km west of the mountains near the trace of the Mesilla Valley Fault.

The deformation of the older uplifted terraces presents an unusual opportunity to measure the long-term uplift of the extensional Franklin Mountain block. The rapid

aggradation during the Pliocene buried the mountain front and created nearly horizontal surfaces that have been deformed by long-term deformation.

Three key observations can be derived from this deformation. First, the deformation mimics range topography. This has important implications for understanding the pre-extensional topography of the region. The correlation between deformation and topography implies that excepting volcanic edifices, topography in the region has a low relief surface. This leads to the inference that topography in the southern Río Grande rift is largely tectonic and not inherited. Several authors have discussed the potential for inherited topography in the northern Río Grande rift (Chapin and Cather, 1994; May and others, 1994; Lucas and others, 1999) however this does not seem to be a factor in the El Paso area.

The second observation is where there is true uplift of the Franklin Mountains resulting from either flexure or from mid-crustal flow, in both cases, the uplift is related to extension on the East Franklin Fault.

The third observation is that the terraces show differential uplift that correlates with displacement on the East Franklin Fault. Two models can account for this observation.

Model one contains no uplift of the range, but rather exhumation of the range results from the greater subsidence of the Hueco and Mesilla Basin blocks. Model two relies on flexure and uses gravity and mid-crustal flow to explain the movements.

There are two models of uplift that appear to fit the observed motions of the Franklin Mountains. The first model for uplift of the mountains flanking the Río Grande rift is that of Roy and others (1999), who used a flexural model to show how mountains

can develop in an extensional setting. They show that ranges developed along rift settings with the steep side facing the fault zone have a gentle up-warp on the other side. Some of this up-warp may be related to isostatic unloading adjacent to the fault. Flexural uplift appears to be most apparent in areas with a single master fault and asymmetric basins (Roy and others, 1999).

Perhaps the best model to explain uplift of the Franklin Mountains is proposed by Brown and Phillips (1999). They agree that uplifts may be due to more than one mechanism. They considered that the flanks of the section of the rift including the Sacramento Mountains to extend east approximately 150 km to the Pecos River valley. The Sacramento Mountains are the only one of several mountain chains bounding the Río Grande Rift that Brown and Phillips (1999) feel fits the flexural rift flank model. The Sacramento Mountains are not complicated by earlier tectonism along the eastern side of the range, therefore, they are simple to model as a flexure.

Brown and Phillips (1999) examined several possible flexural models including Zandt and Owens's (1980) elastic plate model and broken plate models. Thermal and mechanical processes were proposed to explain the rift flank relief. They concluded that both broad thermal uplift and narrower flexure combine to create the uplift of the Sacramento Mountains.

A second model that makes sense in this area is that of Melosh and Williams (1989) and Melosh (1990) (Figure 2.17). They used a finite element model to create a flexural model in which the flow in the ductile middle crust allows deformation of the think upper crust. They include only gravity as a vertical stress though they state that extension could result from regional doming or flexure on a broader scale than crustal

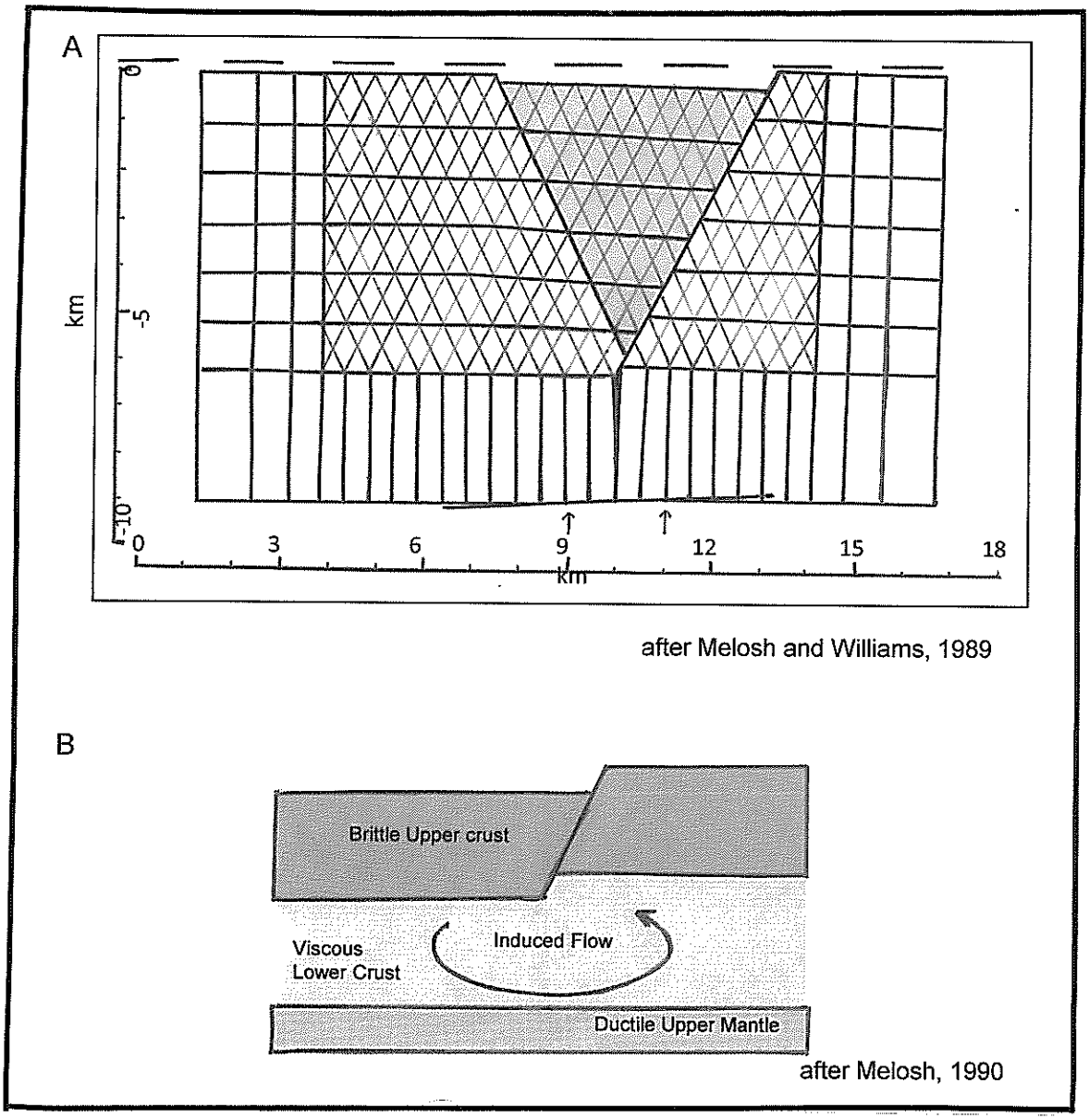

Figure 2.17A . Results from the finite element run. Note the diagonal at the base of finite element model as well as the top of the figure.

Figure 2.17B. Figure shows an enlargement of the area beneath the fault in the model run.

thicknesses or proximity to tectonic features. When the elastic upper layer is displaced horizontally with respect to a lower elastic layer, the sandwiched viscous layer is subject to simple shear (Melosh, 1990). The principle stress orientation is oriented 45 degrees to vertical. Melosh (1990) relies on the rheological structure of the crust combined with high heat flow and stresses within the crust to run the finite element analysis mode. This resulted in uplift of the footwall block through rotation of the normal fault with resulting spatial gap filled through viscous flow (Melosh, 1990)

Other models do not appear to work in the southern Río Grande area. May and others (1994) believe the flank uplift results from isostatic rebound due to tectonic unloading of the lithosphere rather than from flexure. Manning and Bartley (1994); Axen and others (1995); and Wernicke and Axen (1998) believe flexural faulting aided by isostatic forces produce rotational folding in the eastern Basin and Range. Isostatic rebound prompted by unloading is the preferred mechanism behind faulting as studied by Buck (1988); Weissel and Karner (1989); and Wernicke and Axen (1998).

CONCLUSIONS

Because the geometry of the uplifted terraces match the mountain crests, a tectonic origin is implied. This also implies a low relief surface prior to deformation.

Uplift on the eastern flank resulted in a two degree rotation of the uplifted terraces. This combined with terrace geometry implies differential slip on the East Franklin Fault Zone controls terrace deformation and resulted in asymmetric anticline into which the terraces deformed. The rotation down to the west implies a rotational point west of the range.

Anticlinal uplift of the terraces may be due to either differential subsidence or tectonic uplift of the Franklin Mountain block. Tectonic uplift can be explained by either Melosh, 1990), Melosh and Williams, 1989), or Brown and Phillips (1999).

CHAPTER 3: INFLUENCE OF EXTENSIONAL UPLIFT AND TOPOGRAPHY IN THE SOUTHERN BASIN AND RANGE / RÍO GRANDE RIFT, THE INFLUENCE OF TECTONISM ON TOPOGRAPHY

ABSTRACT

In an earlier study, long-term tectonic deformation of the Franklin Mountains was documented indicating over a hundred meters of uplift in the Late Pliocene and Pleistocene. One observation in the Franklin Mountains study was that the overall range topography mimicked the tectonic uplift that was documented in Pliocene terraces. A hypothesis from this study was that the topography of the was tectonic in origin, and the topography or the range reflected deformation of an originally low-relief surface that existed prior to Río Grande Rift deformation.

This study is a comparison to the other topographically high mountains in the area; the Guadalupe, San Andres, and Sacramento Mountains are well-studied examples that should allow for inferences about whether the observed topography is also tectonic in origin. The study applies information from other researchers about the history of deformation in the Guadalupe, the San Andres, and Sacramento Mountains. Uranium-Lead dates from other researchers of caves in the Guadalupe Mountains show that the range was near the water table 11.4 Ma; the water table was preserved in the caves and shows an uplift of at least 855 m. The Sacramento Mountains show that the low-relief mountain crest has been near the surface since the Mesozoic with little denudation of the surface and no evident pre-Rift deformation of the area.

Along with other researcher's results that show little pre-rift, deformation, the

the long-wavelength topography of the southern Rift. A surface that eliminates structural basins and erosional valleys shows that the Guadalupe Mountains and Sacramento Mountains extend well above this smooth surface, as do the other ranges in the area that have significant Holocene faulting along their escarpments.

The four range peaks stand significantly above the surface. Guadalupe Mountains stand about 325 m above the polynomial surface that describes the uneroded surface of a long wave-length surface. The Franklin Mountains are 350 m above the surface, the Sacrament Mountains rise approximately 1 km above the model surface, and the southern San Andres Mountains Salinas Peak protrudes approximately 600 m above the surface.

INTRODUCTION

This study compares uplift histories and geometries of four ranges along the eastern side of the Basin and Range Province (Figure 3.1). The ranges are within the southern extension of the Río Grande Rift where it merges into the Basin and Range Province (Chapin, 1971, 1979; Seager and Morgan, 1979). The Franklin and San Andres Mountains are part of the Mexican Highlands section of the Basin and Range; the Sacramento Section of the Basin and Range that Fenneman (1928, 1931) defined as "a belt on its [Basin and Range] eastern margin, whose mountains are in large part simple dissected cuestas", includes the Sacramento and Guadalupe Mountains. The Sacramento Section is physiographically defined as "the broad upland between the Río Grande and half-way to the Pecos Valley" (Fenneman, 1928).

Does range topography in this part of the Basin and Range/Río Grande Rift

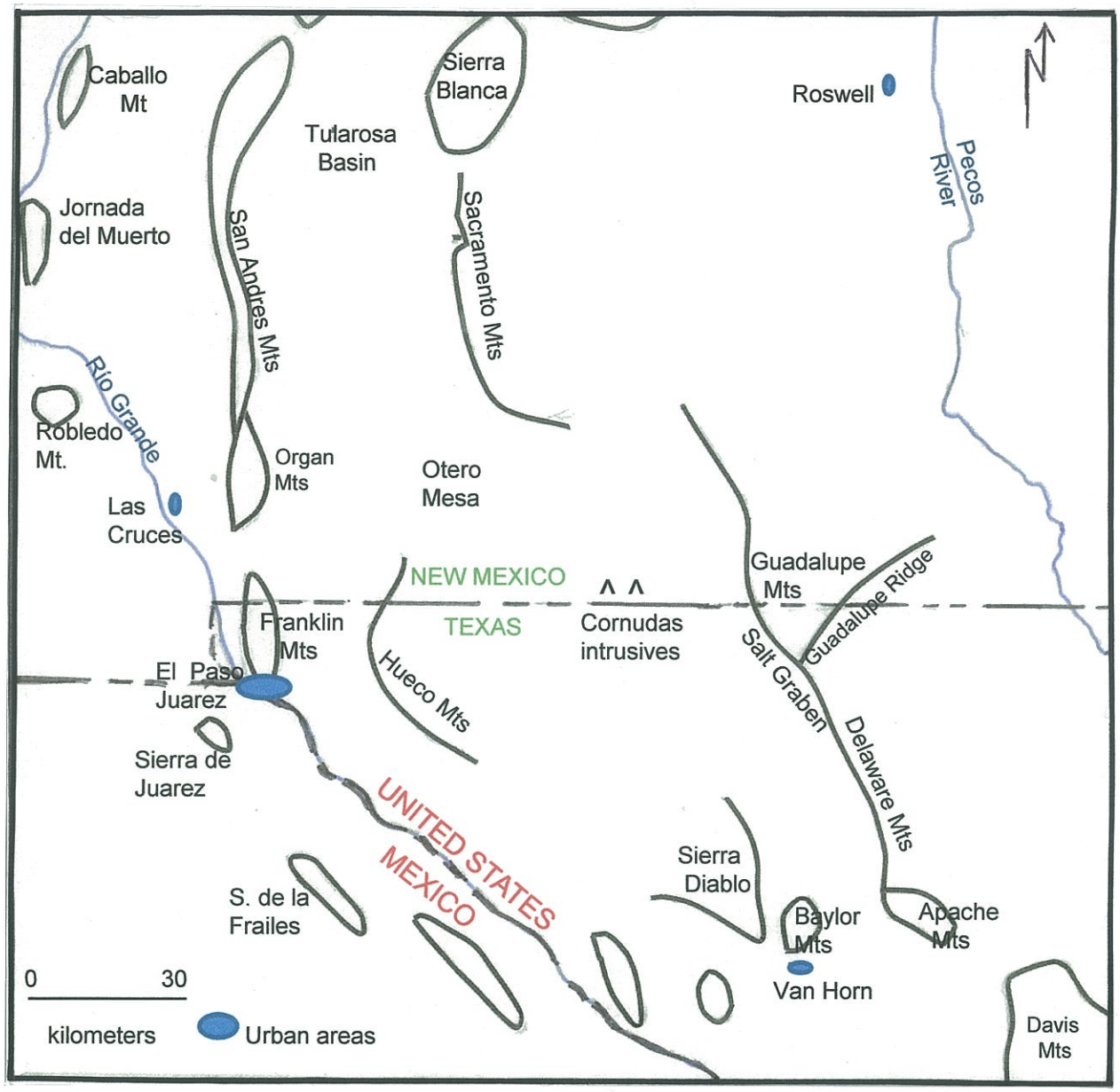

Figure 3.1 Generalized index map of Trans-Pecos Texas and south central New Mexico. The main faults associated with the Guadalupe, Sacramento, and Hueco Mountains are on the western side of the ranges. The primary bounding faults for the San Andres and Franklin Mountains are on the eastern side of the ranges. (after Hayes, 1964)

represent deformation of an older, low relief surface? Can Basin and Range long-term tectonism be used to estimate range topography? In a previous chapter, the long-term uplift of the Franklin Mountains, in the southern Río Grande Rift was inferred from uplifted Pliocene terraces. This paper will investigate these questions by comparing the mountain ranges with the results of the study of the Franklin Mountains with the nearest high relief mountains; the San Andres, Sacramento and Guadalupe Mountains.

One important result of an earlier Franklin Mountain study (Armour, 2014) was that the range topography mimicked the uplift and that the topography was largely tectonic. Terraces along the sides of the Franklin Mountains mimic the arch formed along the crest of the mountains (Figure 3.2). The long-term deformation of these terraces implied that the topography of the range is largely tectonic in origin and that prior to Late Tertiary extensional deformation, the area was a low relief plain.

Uplifting of the terraces suggests that the topography may also be an indication of uplift of other ranges in the area. More importantly, it suggests that, at least for this part of the Basin and Range, topography can be used as a crude proxy for extensional tectonism in the region. The largest uplifts in the area are those of the San Andres, Sacramento and Guadalupe uplifts. This chapter will compare range topography with evidence for the amplitude of deformation.

All of these ranges are bounded on one side by a master fault (Figure 3.1). A half graben down to the west forms the relatively gently sloping side of the Hueco Basin east of the Franklin Mountains. The Hueco Mountains east of the Hueco Basin merge by way of Otero Mesa with the Sacramento Mountains to the north. The Sacramento Mountains present a steep face to the west but the difference between Cathy Peak and

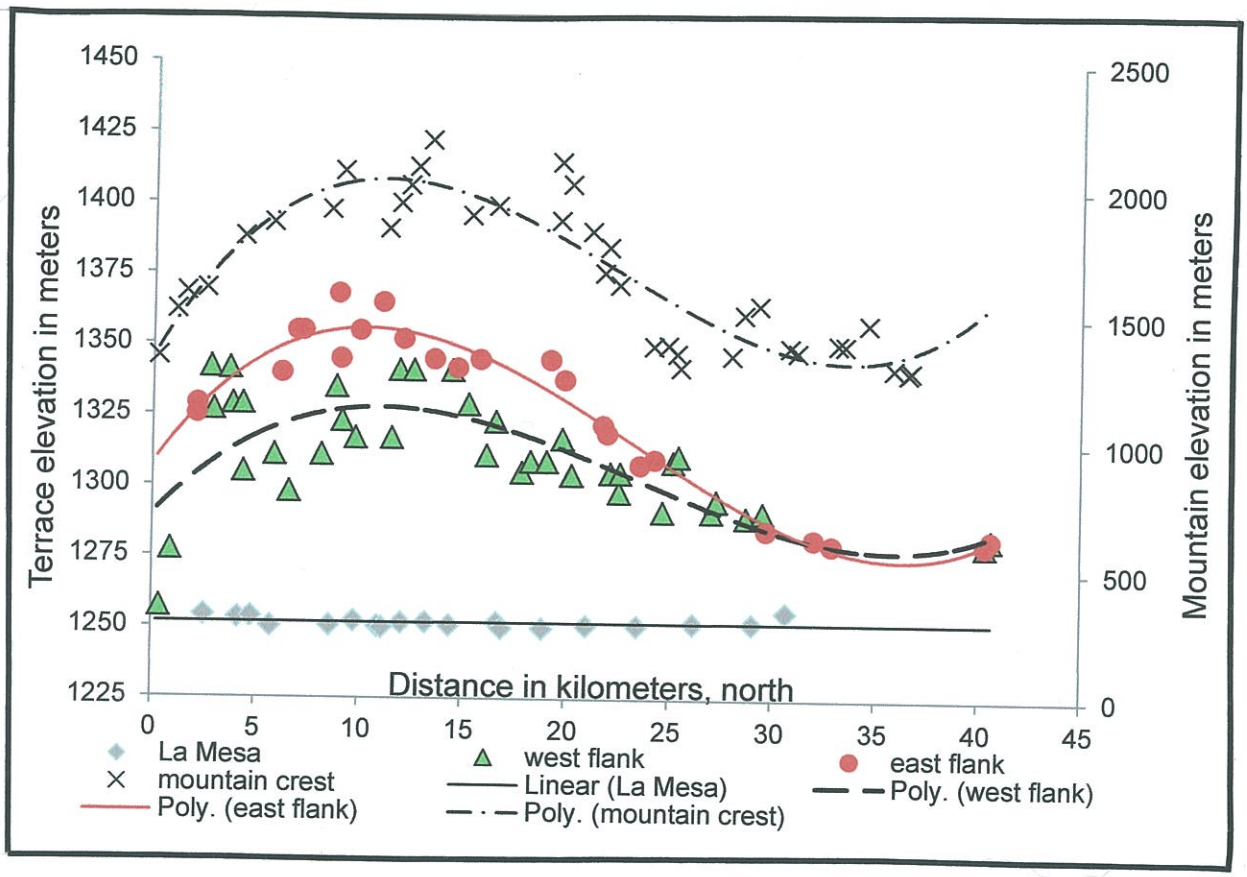

Figure 3.2 Graph showing terraces from east and west flanks of the Franklin Mountains with the trace of the mountain crest shown by Xs. The fact that the uplifts follow similar curves indicates that the mountains and terraces were uplifted together.

the Pecos River is approximately 1950 m over 170 km for an average slope of 1.15%. The main fault for the Guadalupe Mountains is on the west side of the range with the majority of the east side of the range sloping gently to the Pecos River. A myriad of small faults plus erosion has exposed the reef face on the east side to at least Walnut Canyon approximately 55 km north of the southern expression of the Guadalupe Mountains. The San Andres Mountains have their primary fault again on the east side adjacent to the Tularosa Basin; this range slopes into the Jornada del Muerto (Figure 3.1).

SACRAMENTO MOUNTAINS

The Sacramento Mountains extend from approximately 34° N to 32.5° N where they merge with the Otero Mesa. In north-south profile, the crest of the Sacramento Mountains forms a gentle arch (Pray, 1961). Yeso and Abo Formations (Permian Leonardian, 275-270 Ma) are found at Cathey Peak, the highest peak (2955 m) of the Sacramento Mountains of southern New Mexico. Cathey Peak is 1633 m above Alamogordo, New Mexico, the town for which the bounding western fault is named. Like the Franklin Mountains, the escarpment of the Sacramento Mountains is relatively abrupt with low pediments along the faulted west side and few fans at the mouths of canyons. There are a few treads and benches at formation contacts along the faulted face of the Sacramento Mountains but there are no terraces as with the Franklin Mountains. Pray's (1961) Figure 4 shows this well.

The Sacramento Mountains are part of an uplift that extends 109 km along the Alamogordo Fault and bounds the western side of the Sacramento Mountains

separating the mountains from the Tularosa Basin (Machette and Kelson, 1996). The fault extends south nearly to the Hueco Mountains where it terminates among a series of "anastomosing" (Collins and Raney, 1997) faults that continue the trend south into Trans-Pecos Texas. A pair of un-named faults that continue the trend bound the west side of the low Hueco Mountains (Collins and Raney, 1991). Farther south, relatively small faults break the surface of the Hueco Basin (Collins and Raney, 2000).

The Alamogordo Fault appears from description to be a fault zone (Pray, 1961) as are the East Franklin Fault of the Franklin Mountains and the Border Fault of the Guadalupe Mountains. The Alamogordo Fault dip is at high angle to the west with dip-slip movement; scarps to about 25 m displace alluvium and other piedmont surfaces exposing bedrock on the footwall side.

Ramberg and others (1978) attempted to model the gravity of the southern Río Grande Basin as it integrates with the Basin and Range Physiographic province. Ramberg and others (1978) had to manipulate their data in order to remove known geological features including Laramide structures, Ancestral Rockies features, and Tertiary intrusives to obtain observed elevations and known depths as shown in their Figures 3, 4, and 6 on pages 110 -112.

The high along the crest of the Sacramento Mountains is reported at approximately 32°45.5' N, 105°48' W; the city of Alamogordo is reported near, 32° 51' N, 105° 58' W (Wikipedia). The isopach maps (Raatz and others, 2002) indicate the thickest portion of the basin is west and north of Alamogordo. Based on this information, the low of the eastern side of the Tularosa Basin appears to be in the proximity of the high points of the mountains similar to Marrufo's (2011) findings

associated with the Hueco Basin and Franklin Mountains.

GUADALUPE MOUNTAINS

Beginning 64 km to the south and east of the Sacramento Mountains, the Border Fault bounds the west side of the Guadalupe, Delaware, and Apache Mountains. The Guadalupe Mountains at the northern end of the group are the highest of the trio of mountains. Guadalupe Peak is the highest elevation in Texas at 2667 m; it is topped by Permian Guadalupian age (270 - 260 Ma) formations. The uplift extends from the Sacramento Mountains south along the eastern edge of the Salt Basin to the Oligocene age Davis Mountains, a total of 240 km. The Guadalupe, Delaware, and Apache Mountains are a late-Tertiary Basin and Range feature that extends from approximately 50 km north of the 32nd parallel to 25 km south of the parallel.

The Guadalupe Mountains form a wedge-shaped feature with the southern end at El Capitan being a prominent escarpment. A few kilometers to the north is Guadalupe Peak. The western or main portion of the Guadalupe Mountains extends northwest from El Capitan and Guadalupe Peak toward the Sacramento Mountains approximately 110 km (Hill, 1996). The Northeastern Prong forms the eastern side of the wedge.

Except for the erosional topography along the southwest - northeast trend of the Permian Reef, the Guadalupe Mountain's topography dips gently toward the Pecos River and the sub-surface Delaware Basin to the east. The Guadalupe Ridge was part of a reef that surrounded the Permian age Delaware Basin. Uplift of this section of the reef suggests compaction and subsidence rather than compression. King (1948) noted

that a widespread erosional surface intersected the Guadalupe Ridge folds and other prominences, indicating that the folds probably were pre-Laramide.

Movement along the Border Fault zone between the Guadalupe Mountain and Salt Graben has been right-lateral trans-tensional (Goetz, 1985). The area between the Border Fault and the Hueco Mountains to the west of the Guadalupe Mountains is considered by some to be a younger extension of the Río Grande Rift (Keller and Peeples, 1985; Goetz, 1985). Others consider the average 500 m of Cenozoic fill in the northern Salt Graben near the Guadalupe Mountains to be insufficient for it to be considered part of the Rift (Seager and Morgan, 1979). Three wells were drilled in the mid-Salt Graben near the central section of the Delaware Mountains. Their depths exceeded 747 m (Trentham, personal communication, 2013) so portions of the Graben are deeper than the depth of the most studied portion of the area.

Three additional features between the City of Carlsbad and El Capitan are covered by geomorphic surfaces that some refer to as terraces (Hill, 1998). Like the terraces that flank the Franklin Mountains, these surfaces are believed to be constructional and can be correlated with the glacial and interglacial stages. They formed within the last 600,000 years and have slopes of 0.9%, similar to the slope of the La Mesa Surface west of the Franklin Mountains (Aristarain, 1971; Hawley and others, 1976; Hawley, 1993b). The oldest surface, the Blackdom, was described by Meinzer and others (1926) as a "well-defined...older terrace". This one most nearly correlates with the Camp Rice Formation that forms the terraces around the Franklin Mountains.. The Orchard Park and Lakewood terraces are of similar age to the younger formations of the Mesilla Valley and the Franklin Mountain area (Hall, 1998).

Examination of three USGS 30° by 60° topographic maps gives some indication that the Guadalupe and Delaware Mountains may also have deformed and uplifted similar to the deformation of terraces that flank the Franklin Mountains. The 1000 m contour interval (CI) was compared to the Pecos River which the contour did not follow. The 1200 m and 1400 m contours were checked to determine whether they showed any relation to the 1600 m contour which is near the crest of the Apache and Delaware Mountains. The 1600 CI does not extend to the north end of Carlsbad National Park. The 1400 m CI needs further examination to discover whether it includes the Blackdom surface or if it crosses the Orchard Park or Lakewood terraces.

SAN ANDRES MOUNTAINS

The San Andres Mountains are difficult to study because the San Andres Fault along the east side of the range is on the White Sands Missile Range and access has been limited since the mid-1940s. The two highest peaks within the San Andres Mountains are at either end of the range. San Andres Peak (2510 m) is 770 m above the Tularosa Basin and is of greatest interest for this study as it is stratigraphic in nature. San Andres Peak is composed primarily of PreCambrian and Paleozoic rocks; Salinas Peak on the north end of the range is volcanic with an AFT age of approximately 50 Ma (Kelley, 1997).

The San Andres Fault that bounds the east side of the range can be divided into three segments. Machette's (1996) three studies completed for the USGS describes the southern fault segment as merging on the southern end with the Organ Fault extending into the northern end of the Tularosa Basin. Kelley (1997) was allowed

access to the east side of the range to gather samples with apatite and uranium. She found that the range began uplift and cooling about 21 to 22 Ma; she also found AFT ages of 7 to 8 Ma, or Middle Miocene indicating uplift of the San Andres Mountains is associated with the opening of the Río Grande Rift.

METHODS

Because uplift associated with extension should also correlate with deeper basin subsidence, elevation data along 32° and 33° north were extracted from transects shown in Figures 3.3 and 3.4 . The profile following 32° north (Figure 3.5) extends from the Pecos River where it crosses from New Mexico into Texas at -104° W and west past the Chiracahua Mountains in Arizona. This profile includes both the Guadalupe and Franklin Mountains associated with this study. The transect along 33° north (Figure 3.5) also begins at -104° W in the Great Plains of New Mexico, crosses the Sacramento, the southern end of the San Andres Mountains, and the southern transition zone between the Basin and Range and the Colorado Plateau extending into Arizona where the Santa Teresa Mountains protrude above the smoothed surface.

In order to evaluate whether the digital elevation model (DEM) showing the topography of the region illustrates the uplifts, the DEM data were combined with gravity data for an area bounded by parallels 31° and 35° N and Longitude -104 to -110° W. One third arc-second DEMs were obtained from the U.S. Geological Survey National Map, were merged and reprojected to UTM Zone 13. The area includes the Pecos Valley and high plains of eastern New Mexico on the east and extends beyond the Chiricahua Mountains to the west.

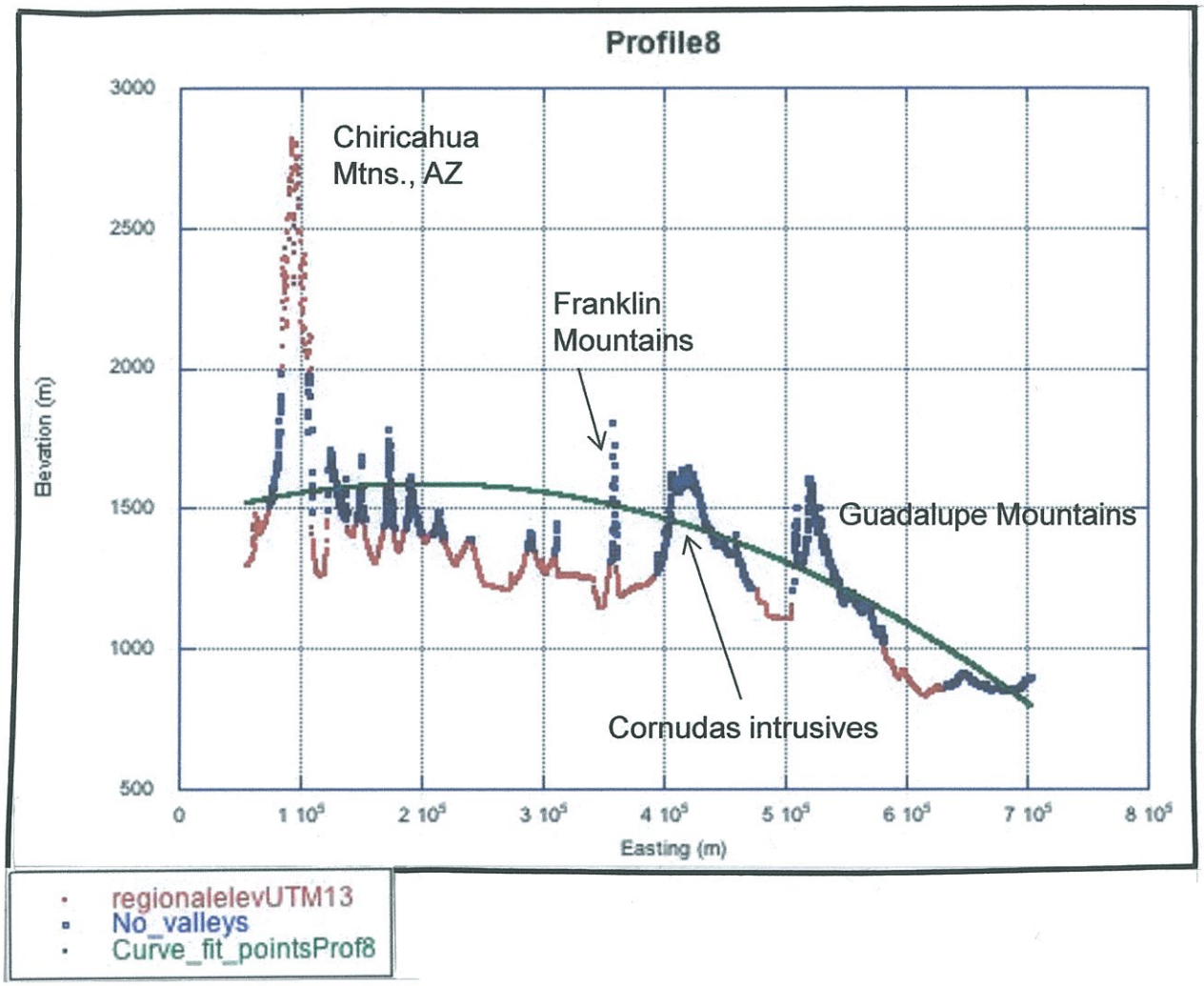

Figure 3.3 Topographic profile along 32° N including both Guadalupe Mountains, the most eastern peak, and Franklin Mountains, the third peak from the east.

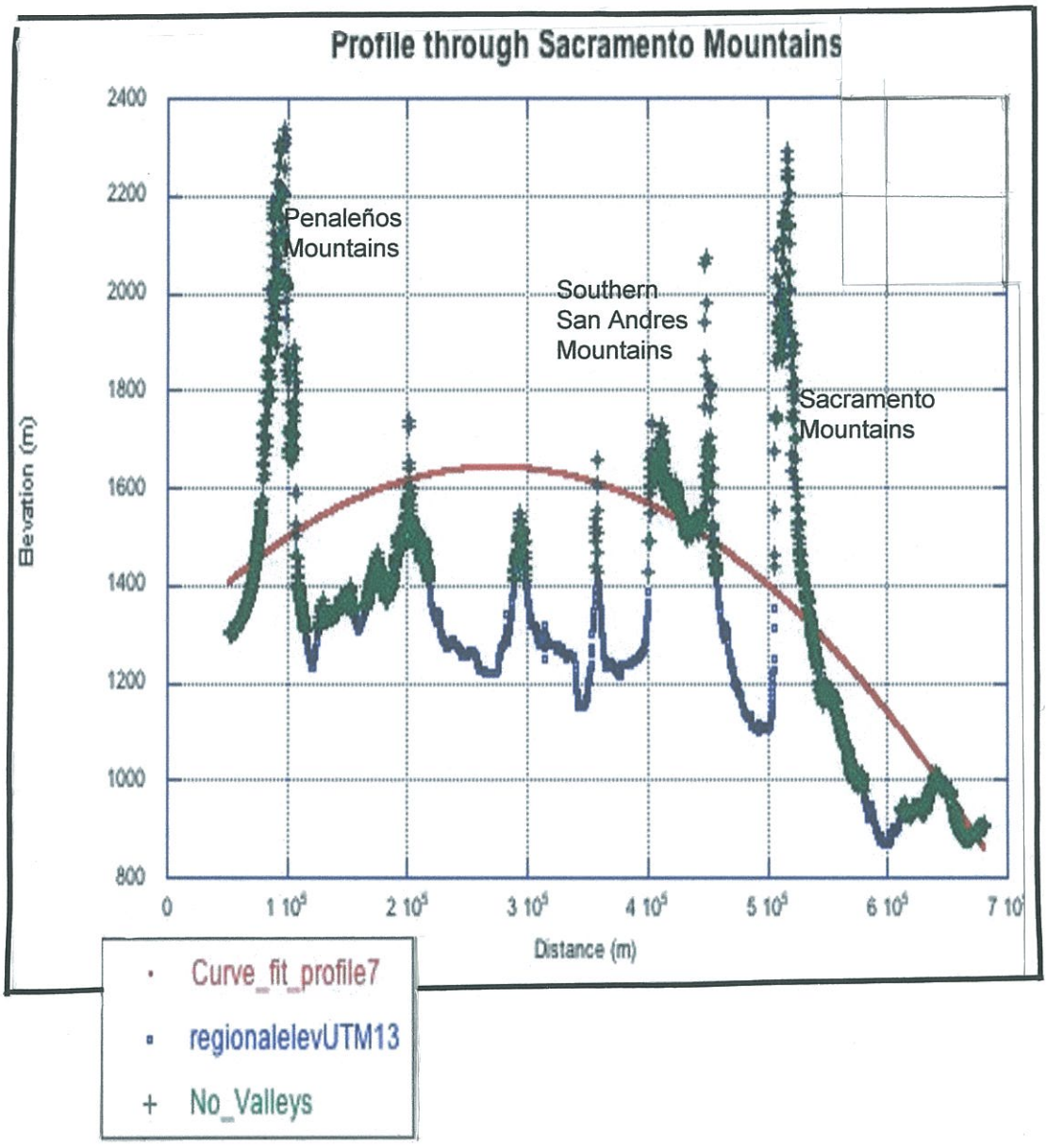

Figure 3.4 Topographic profile across Latitude 33˚ N with second-order polynomial curve. Sacramento, southern San Andres, and Penaleño Mountains extend well above curve.

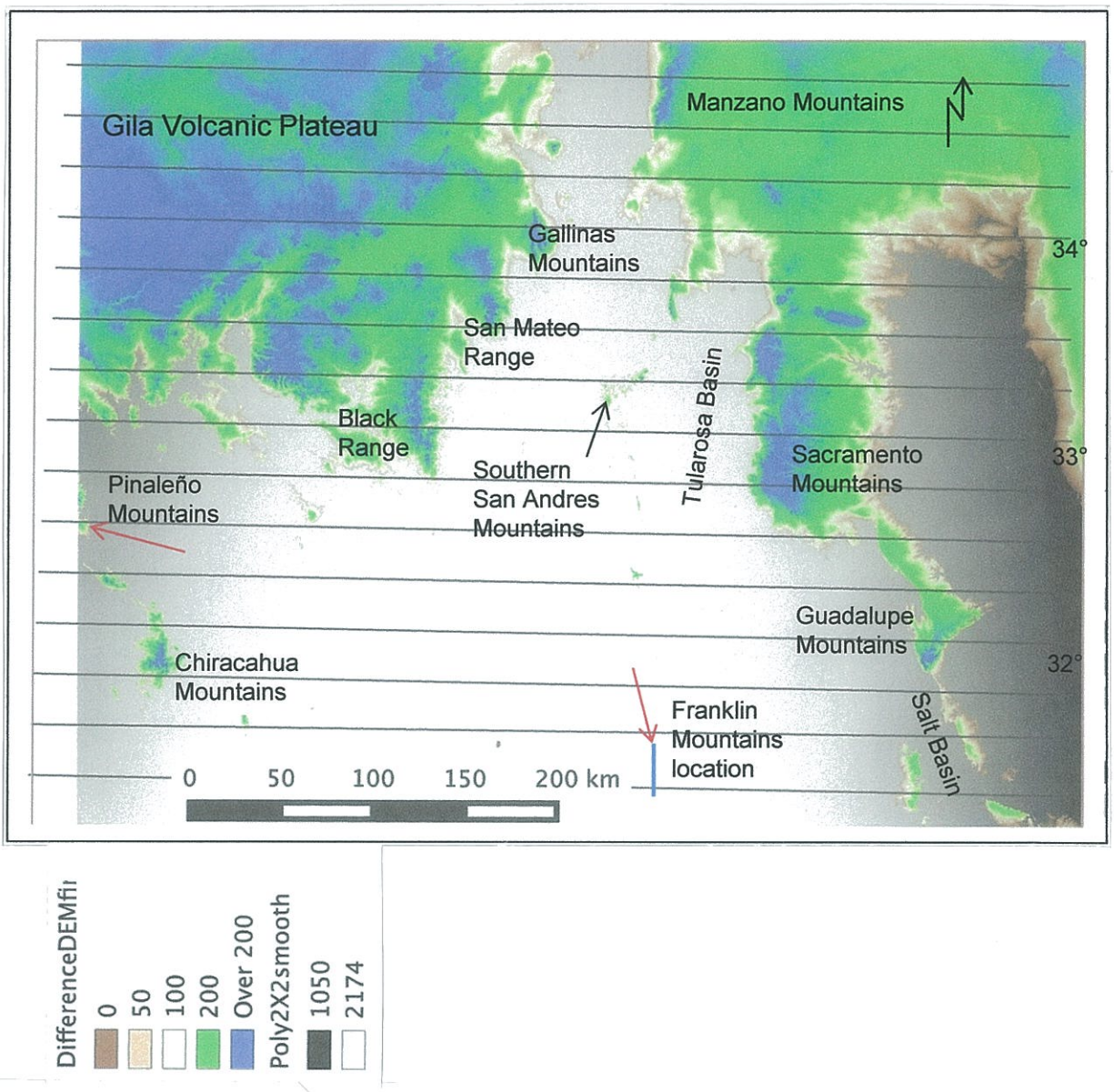

Figure 3.5 Map constructed on polynomial fit surface shown in Figures 3.3 and 3.4. Guadalupe Mountains on the right with Delaware Mountains extending to the bottom of the map; Sacramento Mountains are near top center. Franklin Mountains are too narrow to see at this scale though they stand 250 m above the surface.

Several smoothing equations were tested including least squares, several polynomial surfaces, cubic spline, and logarithmic fits. Of these, the polynomial surface provided the best fit to the data. Polynomial surfaces of order 2 in the X direction and 2 in the Y direction were compared to higher order polynomials up to 4^{th} order in the X and 4^{th} order in the Y directions. No significant differences among these surfaces were found, and the 2^{nd} order by 2^{nd} order polynomial surface provided the best fit with an R^2 value of 0.94. Therefore, the long wave-length topography in the southern Río Grande Rift is best modeled by a three-dimensional parabolic surface. The transects provide profiles similar to the observations by Roy and others (1999) and Brown and Phillips (1999) in their observations of the Alvarado Ridge and thermal buoyancy affects in this area.

TOPOGRAPHIC RESULTS

The results show several important features. The Río Grande Rift sits within a long wavelength topographic high that has been discussed by many authors (Eaton, 1987; Brown and Phillips, 1999; Roy and others, 1999). The Guadalupe, Sacramento, San Andres, and Franklin Mountains lie well above the long wavelength surface. Real uplift as hypothesized in the second paper of this dissertation is tectonic in origin (Figure 3.4, Figure 3.5). These results support the similar studies of uplift of the Sacramento Mountains. by Roy and others, (1999) and Brown and Phillips (1999).

These results contrast with those of Eaton, (1987), who described an Oligocene to Miocene uplift, the Alvarado Ridge, a Neogene uplift which is presumed to include the study area. He predicts heat induced buoyancy may be responsible for the regional

uplift of the mountains and high basins of the southern Río Grande Rift and surrounding area. A slightly later proposal involves the Alvarado Rridge uplift and fragmentation resulting from the development of the Río Grande. The Alvarado Ridge is also an extensional feature, similar in profile to the ocean ridges. The projections shown in Eaton's (1987) Figure 8c shows the Río Grade Rift as the center of the ridge. Pertinent to this study is the topographic profile across 33° N latitude that is similar to the profile of Brown and Phillips (1999).

A map was constructed (Figure 3.3) on the polynomial fit surfaces shown as cross-sections in Figures 3.4 and 3.5. The Franklin, San Andres, Sacramento and Guadalupe Mountains are uplifted by 200 m to 1 km above the regional surface. The Franklin Mountains are located by the arrow as they are difficult to see at this scale. The Franklin Mountains protrude approximately 250 m above the polynomial surface; the Guadalupe Mountains extend approximately 235 m; the Sacramento Mountains reach nearly one km, and the southern end of the San Andres Mountains extend about 600 m above the smoothed surface.

Most of the topography lies below the smoothed surface except in the northern part of the map where almost all of the terrain lies above the smoothed surface (Figure 3.3). This north-south lack of fit results from the origin of the smoothed surface modeled from east-west transects. Many smaller scale topographic features are also evident. In addition to the Guadalupes, Franklins, southern San Andres, and Sacramentos, the Chiracahuas and Pinaleños show up as block uplifts.

The Gila Volcanic Plateau forms a broad upland in the northwest corner of the map. The Black Range, San Mateo and Gallinas ranges, parts of the Plateau, for

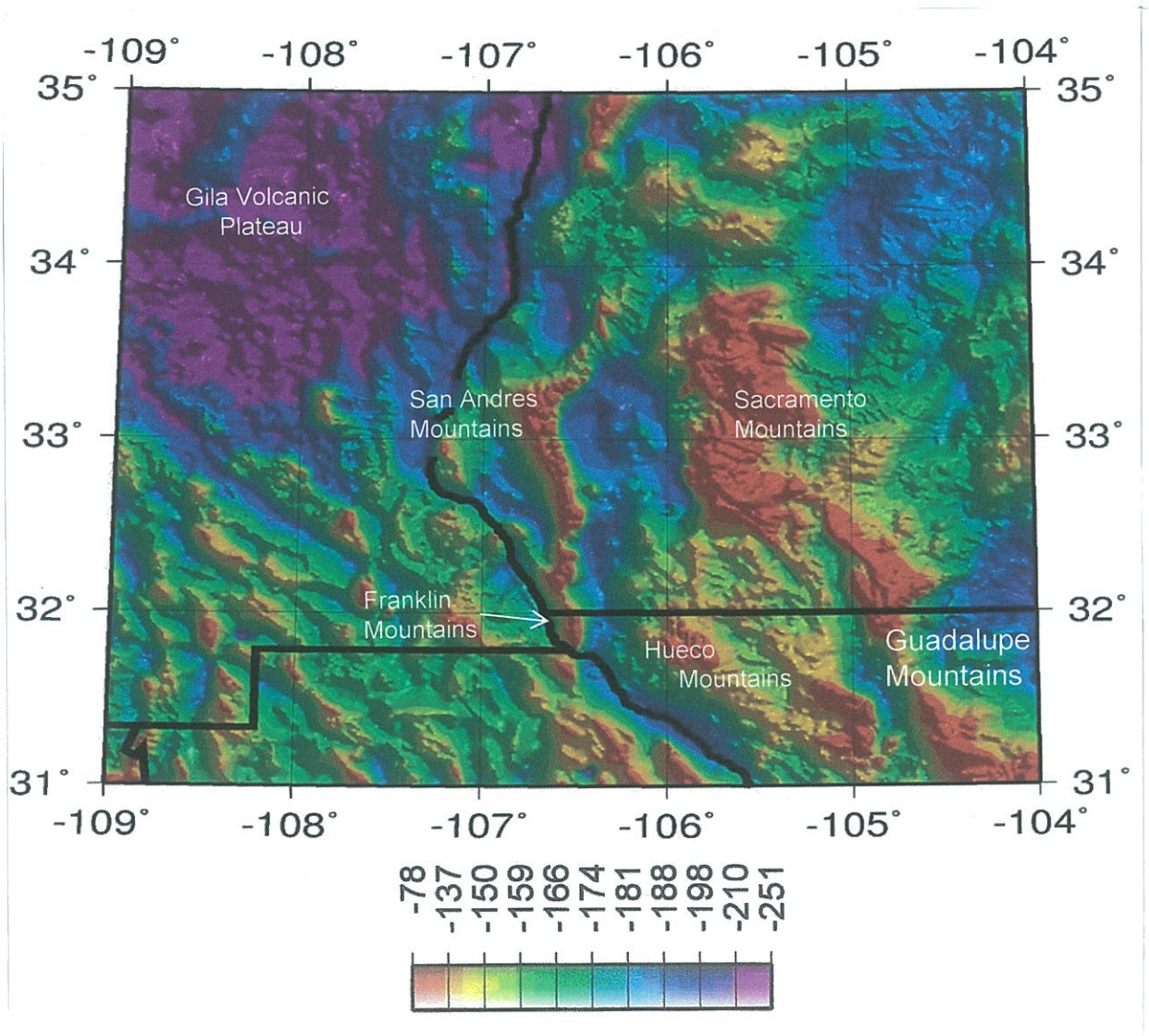

Figure 3.6 Bouguer anomaly map normalized to topography from New Mexico/Arizona border on the west to the Pecos River on the east. (Montana, 2014)

topographic highs that extend southward off the Gila Plateau and the Manzano Mountains. They mark the eastern high that would be expected. They also represent broad topographic uplift to the north of edge of a well-defined rift valley along the north end of the smoothed map surface. All of these lie at least 200 meters above the smoothed surface. Some of the uplifts, especially the Gila are volcanic highlands composed of Oligocene tuffs. The other ranges appear to be flexural uplifts similar to the Franklins as discussed in Chapter 2. The uplfits are all elongate north-south, symmetrical anticlines gently plunging north and south similar to the Franklins and are 30 to 50 km long.

GRAVITY RESULTS

Figure 3.4 shows a map compiled from The University of Texas at El Paso's PACES database. Generic Mapping Tools (GMT) was used with high-resolution free-air anomaly to filter and model a combination gravity / topographic map of the area between 31° N, -104° W to 35° N, -109° W. The resulting map by Montana (2014) shows known topography. For Figure 3.6, the gravity was re-scaled from zero, the highest gravity value and one for lowest gravity value. The topography was scaled so the topographic high is one and low is zero. The scaled results were multiplied together to produce a gravity / topographic composite (Montana, personal communication, 2014). This map emphasizes locations where topographic lows and gravity lows coincide such as in structural basins.

On the gravity map, the Gila Volcanic Plateau forms a prominent low (Figure 3.2). This probably results from low density intrusives in the crust beneath the plateau.

This map does not extend westward far enough to image the prominent highs of the Chiracahuas and Pinaleños. However, most of the other uplifts visible above the smoothed topographic surface exhibit prominent gravity lows suggesting deep basin fills adjacent to these mountains. Blue shaded gravity lows can be seen adjacent to the Sacramentos, Guadalupes, Franklins, and San Andres Mountains (Figure 3.6).

Gravity lows also coincide with deep basins as resistivity and well logs. This compares to basins outside of the rift that are generally more shallow than 1000 m. (Seager and Morgan, 1979, their Figure 3). Goetz (1980) used resistivity and well records to determine a depth of approximately 900 m for the Salt Graben which agrees with Trentham (2013). The western part of the Tularosa half graben holds approximately 2000 m of Neogene sediments (Zohdy, 1969; Doty and Cooper, 1970). Lake sediments were detected to 1585 m of astratigraphic test well that reached 1833 m near the White Sands Missile Range Headquarters (McLean, 1975). The trough along the western side of the Hueco Basin is filled with about 2700 m of sediments according to Mattick (1967) and Gates and others, (1978).

TIMING OF BASIN AND RANGE DEFORMATION

Deformation recorded in the Franklin Mountains (Chapter 2) and evidence from the topography (Figure 3.2) and the gravity (Figure 3.6) data suggest that the southern Río Grande Rift represents deformation of a low relief surface. Data from the Guadalupe and Sacramento Mountains provide the timing of this deformation.

The uplift of the Guadalupe Mountains has been determined by dating caves in the mountains. Approximately 300 caves are found along the Guadalupe Mountains

(DuChene and others, 1999). A hydrologic connection between the Capitan Limestone and the Pecos River aquifer that had developed within the reef. Its level was controlled by the regional base-level of the Pecos River (Hill, 1987). Acidic water dissolves the carbonate formations as it follows the joints within the formations (Jagnow, 1977, 1979; Hinds and Cunningham, 1970). Of key importance is that acidification and cave dissolution occurred at the water table, and therefore, caves in the Guadalupe Mountains record paleo-water tables.

The highest cave along the Guadalupe Mountain trend is Virgin Cave (Figure 3.7). The surface elevation is 2001 m, the deepest accessible point of the cave is 1892 m. Carlsbad Cavern is the lowest of the known major caves of the Guadalupe Mountain escarpment. Carlsbad Cavern is dated at 4 Ma using uranium alunite method (Mosch and Polyak, 1996; Polyak and Güven, 1996). Uranium series dating of cave spar indicates an age of 879,000 ± 124,000 years but probably formed above the water table. Uplift began from a low relief surface about 12 Ma.

Similar results are obtained from the Sacramento Mountains. Apatite Fission-Track (AFT) analysis has been analyzed by Kelley and Chapin (1997) for several mountain ranges within southern New Mexico and far western Texas. AFT cooling ages for the Franklin, Sacramento, and San Andres Mountains were calculated from samples taken near the crests of the mountains. Samples from the crests of the Sacramento and Franklin Mountains exhibit fission track ages of 112 Ma and 51 partial annealing zone (PAZ) results for both of these ranges. This implies relatively shallow burial during the late Cretaceous and little erosion at the range crests. Kelley and Chapen (1997) suggest an episode of uplift at about 35 Ma and a much more

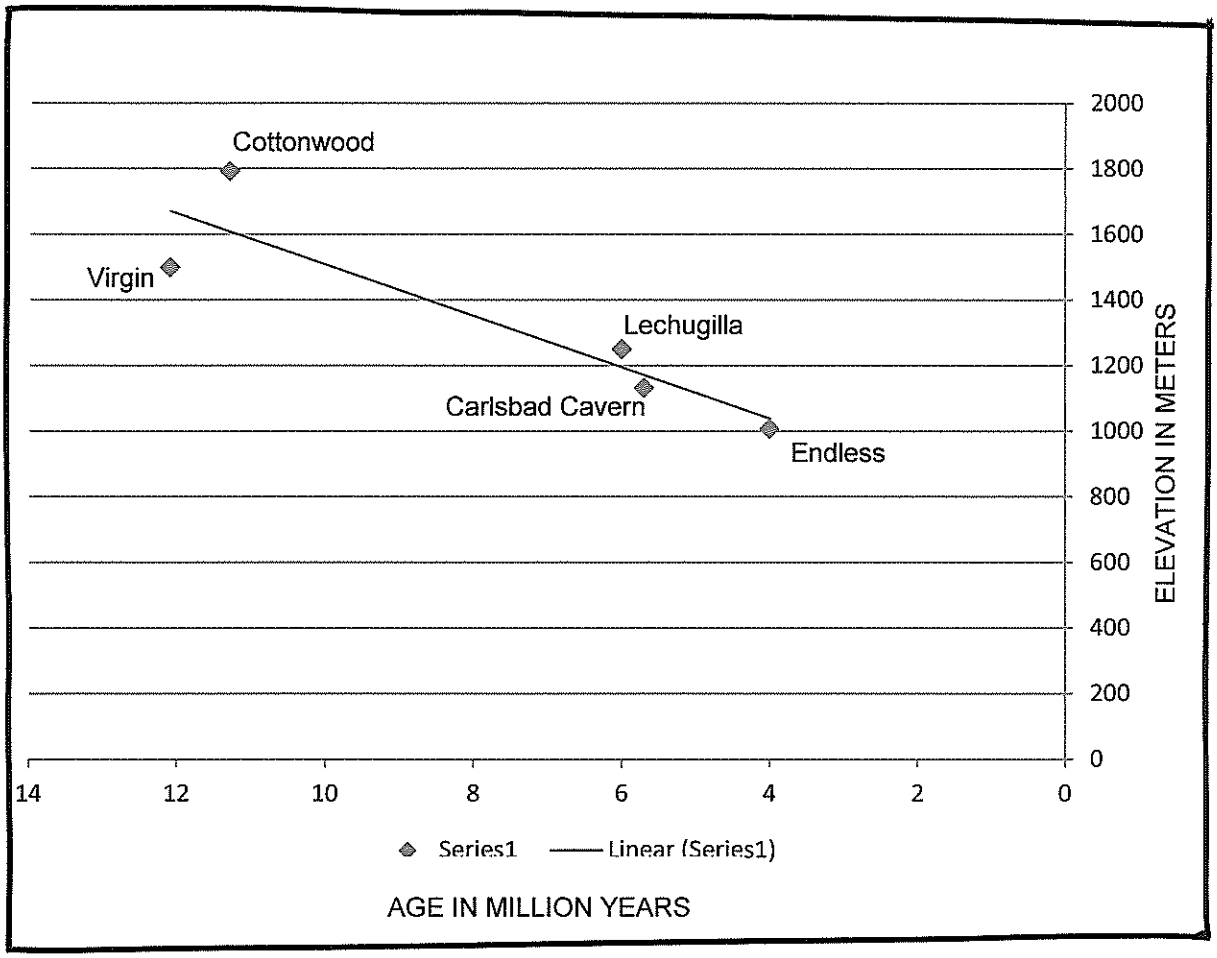

Figure 3.7 Elevation of five caves in Guadalupe Mountains plotted against U-Pb age in million years.

significant uplift and unroofing during the last 20 Ma. Ages that fall within the 7 to 8 Ma range indicate middle Miocene cooling associated with uplift during extension. Similar young ages are observed in the major flank uplifts of the Río Grande rift (Kelley and Chapin, 1997). House and others (2003) conducted a detailed examination of Sandia Mountains. They concluded that there were 3.1 km of uplift along with 2.4 km of flexural, fault-related uplift in the Sandias. Furthermore, similar to this paper, they inferred that the local topography was associated with flexure on the rift-flank fault. And finally, they concluded that almost all of this occurred within the last 15 Ma. It therefore appears that the inferences from the Franklins, Sacramentos, San Andres, and Guadalupes are broadly applicable across the region.

DISCUSSION

Coincident with the theory that topography reflects Basin and Range tectonics, is that these ranges all have long been thought to have been low features if not peneplained during the Laramide (King, 1948; Pray, 1961; Hall, 1987). The Franklin Mountains, as seen today, are the result of Precambrian uplifting and granitic intrusions; early Paleozoic quiescence culminated in Permian folding; Mesozoic compression and tension; and finally Neogene tension and faulting raising the previously deposited and deformed formations obvious today. The uplifted terraces shown in Figure 3.2 lead to the belief that the area surrounding the Franklin Mountains was of low relief.

Peneplanation of the Sacramento Mountains is revealed by the thin Triassic strata exposed north of the Sacramento Mountains in the Sierra Blanca area (Pray,

1961). Only pockets of the Triassic strata survive in the Sacramento Mountains though the formations extend at least 225 km east (Pray, 1961). The Tertiary brought dikes and sills probably associated with Sierra Blanca intruded along joints (Pray, 1961). Quaternary age deposits occur in the Tularosa Basin to the west and within the mountain block itself. Most of the Quaternary deposits are Santa Fe Group (Pray, 1961).

Lindsay and others (1992) proposed that the Alvarado Ridge was the recharge area for the Artesia Group that supplied Permian Basin aquifers east of the Ridge. Freshwater brought microbes to the formations within the Artesia Group thus producing H_2S. Oxygen from meteoric sources was introduced into the system (DuChene, 2013). The oxygen combined with the H_2S and produced the sulfuric acid.

The timing of uplift of the Guadalupe, San Andres, Sacramento and Franklin Mountains suggests that most of the denudation is tectonic as indicated by the flexure of surfaces, topography and gravity data in this report. This deformation can be dated to the last 20 Ma, and probably to the last 15 Ma based on the cave dates in the Guadalupe Mountains.

CONCLUSIONS

The comparison of uplift of the Franklin, Guadalupe, Sacramento, and San Andres Mountains shows that tectonism largely shaped the topography of the ranges. The three mountain ranges protrude between 325 and 1000 m above the long wavelength topographic high.

Uplift of the terraces that flank the Franklin Mountains showed a tectonic

connection between the topography and regional uplift believed to have occurred in the last 5 Ma. (Armour, 2014; Chapter 2 of this dissertation). Uplift of the Guadalupe Mountains is shown through the progression of cave development and uplift. The oldest cave is dated by K-Ar dating of alunite at about 11 Ma. AFT dates also suggest that burial of the range crests was not below the patial anealing zone of the fission tracks and that uplift has occurred in the last 20 Ma (Kelley and Chapin, 1997).

This study supports the concept that mountain uplift largely created the topography of the southern Rio Grande Rift. Roy and others (1999) and Brown & Phillips (1999) have suggested similar topographic highs from flexural uplift of the Sacramento Mountains.

The concept that erosion is relatively minor in shaping local topography has been proposed by House and others (2003). The implications of this study, in conjunction with Roy and others (1999), and Brown & Phillips (1999), Kelley and Chapin (1997), and House and others (2003) is that the local topography of the Rio Grande Rift reflects Neogene Tectonism and not differential erosion of the rift flank mountains.

REFERENCES

Albritton, C. C.,Jr., and Smith J. F., Jr., 1968, Geology of the Sierra Blanca area, Hudspeth County, Texas, U.S. Geological Survey Professional Paper 479, p. 131

Armour, L. K.., 2014, Long-term Deformation in the Southern Río Grande Rift as Inferred from Topography and Uplifted Terraces, [PhD thesis], The University of Texas at El Paso

Armstrong, C., Dutrow, B. L., Henry, D. J., and Thompson, R. A., 2013, Provenance of volcanic clasts from the Santa Fe Group, Culebra graben of the San Luis Basin, Colorado: a guide to tectonic evolution, *in* Hudson, M. R., and Grauch, V.G. S., eds., New Perspectives on Río Grande Rift Basins From Tectonics to Groundwater, Geological Society of America Special Paper 494, p. 463-474, doi10.1130/2013.2494(02)

Aristarian, L. F., 1971, Clay minerals in caliche deposits of eastern New Mexico, Journal of Geology, v. 79, p.75-90

Averill, M. G., and Miller, K. C., 2013, Upper crustal structure of the southern Río Grande rift: a composite record of rift and pre-rift tectonics, *in* Hudson, M. R., and Grauch, V.G. S., eds., New Perspectives on Río Grande Rift Basins From Tectonics to Groundwater, Geological Society of America Special Paper 494, p. 463-474, doi: 10.1130/2013.2494(17)

Axen, G. J., Bartley, J. M., and Selverstone, J., 1995, Structural expression of a rolling hinge in the footwall of the Brenner Line normal fault, eastern Alps, Tectonics, v 14, no. 5, p. 1380-1392

Bachman, G. O., and Mehnert, H. H., 1978, New K-Ar dates and the late Pliocene to Holocene geomorphic history of the central Río Grande region, New Mexico; Bulletin Geological Society of America, v. 89, p. 283-292

Brown, G. and Phillips, R. J., 1999, Flexural rift flank uplift at the Rio Grande rift, New Mexico, Tectonics, v. 18 no. 6, p 1975 - 1291

Buck, W. R., 1988, Flexural rotation of normal faults, Tectonics, v. 7 no. 5 p. 959-973

Cather, S. M., Chamberlin, R. M., Chapin, C. E., and McIntosh, W. C., 1994, Stratigraphic consequences of episodic extension in the Lemiter Mountains, central Río Grande rift, *in* Keller, G. R., and Cather, S. M., eds., Río Grande rift: Structure, stratigraphy, and tectonic setting, Geological Society of America Special paper 291, p. 157-170

Chapin, C. E., 1971, The Río Grande rift, Part 1: Modifications and additions: *in* New Mexico Geological Society, Guidebook 22, p. 191-201

Chapin, C. E., 1979, Evolution of the Rio Grande rifta summary; *in* Riecker, R. E. (ed.), Rio Grande rift: tectonics and magmatism: American Geophysical Union, Washington, D.C., p. 1-5

Chapin, C. E. and Cather. S.M., 1994, Tectonic setting of the axial basins of the northern and central Río Grande rift, *in* Keller, G. R., and Cather, S. M., eds., Río Grande rift: Structure, stratigraphy, and tectonic setting, Geological Society of America Special paper 291, p. 5-25

Chapin, C. E. and Seager, W. R., 1975, Evolution of the Río Grande rift in the Socorro and Las Cruces areas, 1975, *in* Seager, W. R., Clemons, R. E., and Callender, J. F., eds., Las Cruces country: New Mexico Geological Society Guidebook, 26th Annual Field Conference Guidebook, p. 297-321

Collins, E. W., 1996, Geologic map of the Canutillo quandrangle, Texas,, The University of Texas at Austin Bureau of Economic Geology, Open-File Map, 1:24,000

Collins, E. W., 1996, Geologic map of the Smeltertown quadrangle, Texas, The University of Texas at Austin Bureau of Economic Geology, Open-File map, 1:24000

Collins, E. W. and Raney, J. A., 1991, Tertiary and Quaternary Structure and paleotectonics of the Hueco Basin, Trans-Pecos and Chihuahua, Mexico, The University of Texas at Austin Bureau of Economic Geology, p. 44

Collins, E. W. and Raney, J. A., 1994, Geologic map of the El Paso quadrangle, Texas, The University of Texas at Austin Bureau of Economic Geology, Open-File map, 1:24000

Collins, E. W. and Raney, J. A., 1994, Geologic map of the North Franklin quadrangle, Texas, The University of Texas at Austin Bureau of Economic Geology, Open-File map, 1:24000

Collins, E. W. and Raney, J. A., 1997, Quaternary faults within intermountaine basins of Northwest Trans-Pecos Texas and Chihuahua, Mexico, The University of Texas at Austin Bureau of Economic Geology, p. 59

Collins, E. W. and Raney, J. A., 2000, Geologic map of West Hueco Bolson, El Paso Region, Texas, Bureau of Economic Geology, The University of Texas at Austin , Miscellaneous Map No. 40, 1:100,000, p. 24

Doty, G. C., and Cooper, J. B., 1970, Stratigraphic test well T-14, post area, White

Sands Missile Range; U.S. Geological Survey, Open-file Report, p. 34

DuChene, H. R., 2013

Eaton, G. P., 1982, The Basin and Range Province, origin and tectonic significance, Annual Reviews Earth Planetary Science, v 10, p.409-440, doi:0084-6597/82/0409$02.00

Eaton, G. P., 1987, Topography and origin of the southern Rocky Mountains and Alvarado Ridge, *in* Continental Extensional Tectonics, Coward, M. P., Dewey, J. F., and Hancock, P. L., eds. Geological Society of America Special Publication No. 28., p. 355-369

Fenneman, N. M., 1928, Physiographic divisions of the United States, Annals of the Association of American Geographers, 3rd ed. v. 8 p. 261-353

Fenneman, N. M., 1931, Physiography of the western United States, McGraw-Hill, p. 393-395

Gates, J. S., White, D. E., Stanley, W. D., and Ackermann, H. D., 1978, Availability of fresh and slightly saline groundwater in the basins of westernmost Texas, United States Geological Survey, Open-file Report 78-663, p. 115

Gile, L. H., Hawley, J. W., and Grossman, R. B., 1981, Chapter 2, Geology and geomorphology *in*: Soils and geomorphology in the Basin and Range area of the southern New Mexico - guide to the Desert Project, New Mexico Bureau of Mines and Mineral Resources, Memoir 39, 1981 p. 22-51

Gile, L. H., Hawley, J. W., Grossman, R. B., Aherns, R. J., Monger, H. C., Peterson, F.F., Gibbens, R. P., Lenz, J. M., Bestelmeyer, B. T., and Nolan, B. A., 2007, A 50th anniversary guidebook for the desert project, United States Department of Agriculture, p. 279

Goetz, L. K., 1980, Quaternary fault in Salt Basin Graben, West Texas *in* New Mexico Geological Society Guidebook, 31st Field Conference, Trans-Pecos Region, p 83-92

Goetz, L. K., 1985, Salt Basin Graben: A Basin and Range right-lateral transtensional fault zone - some speculations, *in* Structure and Tectonics of Trans-Pecos Texas, Dickerson, P. W., and Muehlberger, W. R., eds, West Texas Geological Society Field Conference Pub. 85-81, p. 165-168

Goteti, R., Mitra, G., Becene, A., Sussman, A., and Lewis, C., 2013, Three-dimensional finite-element modeling of fault interactions in rift-scale normal fault systems: Implications for the late Cenozoic Río Grande rift of north-central New Mexico,

in Hudson, M. R., and Grauch, V. J. S. eds. Geological Society of America Special Paper 494, p. 157-184

Gustavson, T. C., 1991, Arid basin depositional systems and paleosols: Fort Hancock and Camp Rice Formations (Pliocene-Pleistocene) Hueco Bolson, West Texas and adjacent Mexico, The University of Texas at Austin Bureau of Economic Geology Report of Investigations no. 198, p. 49

Harbour, R. L., 1972, Geology of the northern Franklin Mountains, Texas and New Mexico, Geological Survey Bulletin 1298, p. 129

Hawley, J. W., 1975, Quaternary history of Doña Ana County region, south-central New Mexico, in Seager, W. R., Clemons, R. E., Callender, J. F. eds., Las Cruces country: New Mexico Geological Society, 26th Annual field Conference guidebook, p. 139-140

Hawley, J. W., 1986, Physiographic provinces [and] landforms of New Mexico *in* New Mexico in Maps. University of New Mexico Press, Albuquerque, NM (1986): 28-31

Hawley, J. W., 1993, The Ogallala and Gatuña formations in the southeastern New Mexico region, a progress report, *in* New Mexico Geological Society Guidebook, 44th Field Conference, Carlsbad Region, New Mexico and West Texas, p. 261 - 269

Hawley, J. W., 1993b, Overview of the geomorphic history of the Carlsbad area; *in* Love, D. W., Hawley, J. W., Kues, B. S., Adams, J. W., Austin, G. S., and Baker, J. M. eds., Carlsbad region, New Mexico and West Texas: New Mexico Geological Society Guidebook, 44th Annual Field Conference, p . 2-3

Hawley, J. W., and Kottlowski, F. E., 1969, Quaternary geology of the south-central New Mexico border region, Border Stratigraphy Symposium, Kottlowski, F. E., and LeMone, D. V., eds., State Bureau of Mines and Mineral Resources New Mexico Institute of Mining and Technology Campus Station, Socorro, New Mexico, Circular 104, p 89-115

Hawley, J. W., and Lozinsky, R. P., 1992, Hydrogeologic framework of the Mesilla Basin in New Mexico and western Texas, New Mexico Bureau of Mines and Mineral Resources New Mexico Institute of Mining and Technology, Socorro, New Mexico, open-File Report 323, p. 13-20

Hawley, J. W., Kottlowski, F. E., Seager, W. R., King, W. E., Strain, W., S., and LeMone, D. V., 1969, The Santa Fe Group in the south-central New Mexico border region, *in* Border Stratigraphy Symposium, Kottlowski, F. E., and LeMone, D. V., eds., State Bureau of Mines and Mineral Resources New Mexico

Institute of Mining and Technology Campus Station, Socorro, New Mexico, Circular 104, p. 52-76

Hayes, P. T., 1964, Geology of the Guadalupe Mountains, New Mexico, US Geological Survey Professional Paper 446, p.65

Hill, C. A., 1987, Geology of Carlsbad Caverns and other caves in the Guadalupe Mountains, New Mexico and Texas, Bulletin 117, New Mexico Bureau of Mines and Mineral Resources p. 150

Hill, C.A., 1996, Geology of the Delaware Basin, Guadalupe, Apache, and Glass Mountains New Mexico and West Texas *in* Lindsay, R. F., and Garber, R. A., Permian Basin Section - SEPM, No. 96-39, p. 480

Hinds, J. S., and Cunningham, R. R., 1970, Elemental sulfur in Eddy County, New Mexico: U.S. Geological Survey, Circular 628, p 1-12

House, M. A., Kelley, S. A., and Roy, M., 2003, Refining the footwall cooling history of a rift flank uplift, Río Grande rift, New Mexcio, Tectonics V 22, No 5, p. 1-18, doi:10.1029/2002TC001418

Imana, E. C., 2003, The Mesilla bolson: an integrated geophysical hydrological and structural analysis using free-air anomalies, [PhD thesis], The University of Texas at El Paso

Izlett, G. A., and Wilcox R. E., 1982, Map showing localities and inferred distributions of the Huckleberry Ridge, Mesa Falls, and Lava Creek ash beds (Pearlette family ash beds) of Pliocene and Pleistocene age in the western United States and southern Canada. US Geological Survey, Miscellaneous Investigations Series Map I-1325, 1:4,000,000.

Jagnow, D. H., 1977, Geologic factors influencing speleogenesis in the Capitan Reef complex, New Mexico and Texas: Unpublished M. S. Thesis, University of New Mexico, p. 197

Jagnow, D. H., 1979, Cavern development in the Guadalupe Mountains, Cave Research Foundation, Columbus, Ohio, p. 55

Janecke, S. U., Vandenburg, C. J., and Blakenau, J. J., 1998, Geometry, mechanisms and significance of extensional folds from examples in the Rocky Mountain Basin and Range province, U.S.A., Journal of structural Geology, v. 20 no. 2, p. 831-856, doi: PH S0191-8141(98)00016-9

Keller, G. R., and Peeples, W. J., 1985, Regional Gravity and aeromagnetic anomalies in west Texas *in* Structure and Tectonics of Trans-Pecos Texas, Dickerson, P.

W., and Muehlberger, W. R., eds, West Texas Geological Society Field Conference Pub. 85-81 , p. 101-105

Keller, G. R., Morgan, P., and Seager, W. R., 1990, Crustal structure, gravity anomalies and heat flow in the southern Río Grande rift and their relationship to extensional tectonics, Tectonophysics v. 174, no. 1-2, p. 21-37

Keller, G. R., and Cather, S. M., eds., 1994, Río Grande rift: structure, stratigraphy, and tectonic setting: Geological Society of America Special Paper 291, p. 304

Kelley, S. A., and Chapin, C. E., 1997, Cooling histories of mountain ranges in the southern Río Grande rift based on apatite fission-track analysis-a reconnaissance survey, New Mexico Geology, v 19, p. 14

Kelley, S A., Kempter, K. A., McIntosh, W. C., Maldonado, F., Smith, G. A., Connell, S. D., Koning, D. J., and Whiteis, J., 2013, Syndepositional deformation and provenance of Oligocene to Lower Miocene sedimetary rock along the western margin of the Río Grande rift, Jemez Mountains, New Mexico, *in* Hudson, M. R., and Grauch, V. J. S. eds. Geological Society of America Special Paper 494, p. 101-124

King, P. B., 1948, Geology of the southern Guadalupe Mountains, Texas, U. S. Geological Survey, Professional Paper 215, p. 183

King, P. B., Beikman, H. M., 1974, Geologic map of the United States, U. S. Geological survey, Scale 1:2,500,000

Knight, C. L., 1988, The southern Guadalupe Mountains, Texas; Permian stratigraphy and Great Plains/Basin and Range structural transition *in* Geological Society of America Centennial Field Guide, 4, p. 395

Koning, D.J., and Pazzaglia, F. J., 2002, Paleoseismicity of the Alamogordo fault along the Sacramento Mountains, southern Río Grande Rift, New Mexico, *in* Geology of White Sands, Lueth, V. W., Giles, K. A., Lucas, s. G., Kues, B. S., Myers, R., and Ulmer-Scholle, D. S. eds. New Mexico Geological Society fifty-third annual field Conference, p. 107-119

Kottlowski, F. E., 1958, Geologic History of the Río Grande near El Paso in West Texas Geological Society Guide Book, 1958 Field Trip, Franklin and Hueco Mountains, Texas, p. 46-54

Kottlowski, F. E., 1963, Paleozoic and Mesozoic strata of southwestern and south-central New Mexico; New Mexico Bureau of Mines and Mineral Resources, Bulletin 79, p. 100

Kottlowski, F. E., and Seager, W. R., 1998, Robledo Mountains, key outcrops *in* south-central New Mexico, *in* Mack, G. H., Austin, G. S., and Barker, J. M., eds., Las Cruces Country II, New Mexico Geological Society 49th Annual Field Conference, p. 3-4

Lachenbruch, A. H., and Sass, J. H., 1977, Heat flow in the United States and the thermal regime of the crust *in* The Earth's Crust, J. G. Heacock, ed., American Geophysical Union Monograph 20, p. 626-75

Lawton, T. F., and Giles, K. A., 2003, Origin of the Orogrande basin by strike-slip faulting: evidence from subsidence patterns and facies distribution, *in* Late Paleozoic tectonics and hydrocarbon systems of western North America, AAPG Hedberg Conference, p. 292

Lindsay, R. F., Jones, R. H., Keefer, C. M., and Hendrix, D. L, 1992, Role of sequence stratigraphy in reservoir characterization and solving waterflood production problems, Grayburg Formation (Permian Guadalupian), Eunice Monument South unit, Lea County, NM, American Association of Petroleum Geologists, v 76:4, p 133-136

Lovejoy, E. M. P., 1971, Tectonic implication of high-level surfaces bordering Franklin Mountains, Texas, Geological Society of America Bulletin, v. 82, p. 433-445

Lovejoy, E. M. P., 1975, An interpretation of the structural geology of the Franklin Mountains, Texas, *in* Seater, W. R., Clemons, R. E., and Callender, J. F., eds., New Mexico Geological Society Guidebook, 26th Field Conference, Las Cruces Country, p. 261-268

Lucas, S. G., Estep, J. W., Anderson, O. J., 1999, Correlation of Jurassic strata from the Colorado Plateau to the High Plains, across the Rio Grande rift, north-central New Mexico, *in:* Albuquerque Country, Pazzaglia, F. J.; Lucas, S. G.; Austin, G. S., New Mexico Geological Society, Guidebook, 50th Field Conference, p. 317-326

Machette, M. N., compiler, 1996, Fault number 2053a, San Andres Mountains fault, southern section, *in* Quaternary fault and fold database of the United States: USGS website; http://earthquakes.usgs.gov/hazards/qfault

Machette, M. N., compiler, 1996, Complete Report for San Andres Mountains fault, southern section (Class A) No. 2053c, *in* Quaternary fault and fold database of the United States: USGS website; http://earthquakes.usgs.gov/hazards/qfault

Machette, M.N., and Kelson, K.I., compilers, 1996, Fault number 2054b, Alamogordo fault Sacramento Mountains section, in quaternary fault and fold database of the

United States: U.S. Geological Survey website.

Mack, G. H. and Seager, W. R., 1990, Tectonic control on facies distribution of the Camp Rice and Palomas Formations (Pliocene-Pleistocene) in the southern Río Grande rift, Geological Society of America Bulletin, v. 102, p. 45-53

Mack, G. H., Salyards, S. L., James, W. C., 1993a, Magnetostratigraphy of the Plio-Pleistocene Camp Rice and Palomas Formations in the Río Grande rift of the southern New Mexico, American Journal of Science 293, p. 49-77

Mack, G. H., Love, D. W., and Seager, W. R., 1997, Spillover models for axial rivers in regions of continental extension: the Río Mimbres and Río Grande in the southern Río Grande rift, USA, Sedimentology, v. 44, p 637-652

Mack, G. H., Kottlowski, F. E., and Seager, W. R., 1998, The stratigraphy of south-central New Mexico, *in* Las Cruces country II, New Mexico Geological Society, p. 135-154

Mack, G. H., Salyards, S. L., McIntosh, W. C., and Leeder, M. R., 1998, Reversal magnetostratigraphy and radioisotopic geochronology of the Plio-Pleistocene Camp Rica and Palomas Formations, southern Río Grande Rift, *in* 49th Field Conference Las Cruces Country II, p. 229-236

Mack, G. H., Seager, W. R., Leeder, M. R., Perez-Arlucea, M., Salyards, S. L., 2006, Pliocene and quaternary history of the Río Grande, the axial river of the southern Río Grande rift, New Mexico, USA, Earth-Science Reviews 79, p. 141-162

Manning, A. H. and Bartley, J. M., 1994, Postmylonitic deformation in the Raft River metamorphic core complex northwestern Utah: evidence of a rolling hinge, Tectonics, v. 13, no. 2, p 596-612

Marrufo, S. S., 2011, An Integrated geological and geophysical study of the fresh and brackish water boundary in the Hueco Bulson, West Texas, [M.S. thesis] The University of Texas at El Paso, p. 122

Mattick, R. E., 1967, A seismic and gravity profile across the Hueco Bolson, Texas, United States Geological Survey Professional Paper, p. D85-D91

May, S. J., Kelley, S. A., and Russell, L. R., 1994, Footwall unloading and rift shoulder uplifts in the Albuquerque basin: their relation to syn-rift fanglomerates and apatite fission-track ages; *in* Keller, G. R. and Cather, S. M, eds., Basins of the Rio Grande rift; Structure, stratigraphy, and tectonic setting: Geological Society of America, Special Paper 291, p. 125-134

McCalpin, J. P., 2006, Quaternary faulting and seismic source characterization in the El

Paso-Juarez metropolitan area: collaborative research with the University of Texas at El Paso, Final Technical Report Contract 03HQR0056 National Earthquake Hazards Reduction Program U. S. Geological Survey, p. 61

McLean, J. S., 1975, Saline ground water of the Tularosa Basin, New Mexico, New Mexico Geological Society, Guidebook 26, p. 237-238

McLemore, V. T., Leuth, V. W., Pease, T. C., and Guilinger, J. R., 1996, Petrology and mineral resources of the Wind Mountain laccolith, Cornudas Mountains, New Mexico and Texas, The Canadian Mineralogist, v. 34 p. 335-347

Meinzer, O. E., Renick, B. C., and Bryan, K., 1926, Geology of Number 3 reservoir site of the Carlsbad irrigation project, New Mexico, with respect to water tightness, U. S., Geological Survey, Water Supply Paper 580-A 39 p.

Melosh, H. J., 1990, Mechanical basis for low-angle normal faulting in the Basin and Range province, Nature, v. 343, no. 6256, p. 331-335

Melosh, H. J. and Williams, C. A., Jr., 1989, Mechanics of graben formation in crustal rocks: a finite element analysis, Journal of Geophysical Research, v. 94. no. B10, p. 13,961-13,973; doi: 0148-0227/89/79JB-1119

Metcalf, A. L., 1967, Late Quaternary mollusks of the Río Grande Valley, Caballo Dam, New Mexico, to El Paso, Texas: The University of Texas at El Paso Science Series. v. 1, p. 1-62

Metcalf, A. L., 1969, Quaternary surfaces, sediments and mollusks: southern Mesilla Valley, New Mexico and Texas, New Mexico Geological society Guide book of the Border Region, p. 158-164

Meyer, R. F., 1966, Geology of Pennsylvanian and Wolfcampian rocks in southeast New Mexico, New Mexico Bureau of Mines and Mineral Resources, Memoir 17, p.123

Monger, H. C., Gile, L. H., Hawley, J. W., and Grossman, R. E., 2009, The Desert Project - an analysis of arid land soil-geomorphic processes, Bulletin 798, New Mexico State University, College of Agricultural, Consumer and Environmental Sciences, p. 76

Montana, C., 2014, Gravity map, Gravity PACES Data Base, UTEP

Morgan, P., Seager, W.R., and Golombek, LM. P., 1986, Cenozoic thermal, mechanical, and tectonic evolution of the Río Grande rift, Journal of Geophysical Research, B, v. 91, no. 6, p. 6263-6278

Motts, W. S., 1959, Geomorphology of the east side of the Sacramento Mountains, New Mexico, Roswell Geological Society and Permian Basin Section-Society of Economic Paleontologists and Mineralogists, Guidebook of the Sacramento Mountains, 59-5, p. 223-233

Polyak, V. J., Provencio, P. O., 2000, Summary of the timing of sulfuric-acid speleogenesis for Guadalupe Caves based on ages of alunite, Journal of Cave and Karst Studies, 62(2), p. 72-74

Polyak, V. J., McIntosh, W. C., Güsven, N., and Provencio, P. P., 1998, age and origin at Carlsbad Cavern and related caves from $^{40}Ar/^{39}Ar$ of alunite, Science 279, no. 5358, p. 1919-1922 doi: 10.1126/science.279.5358.1919

Pray, L. C., 1961, Geology of the Sacramento Mountains Escarpment, Otero County, New Mexico, State Bureau of Mines and Mineral Resources New Mexico Institute of Mining and Technology, Bulletin 35, p. 144

Pray, L. C. and Allen, J. E., 1956, Outlier of Dakota(?) strata, southeastern New Mexico, American Association of Petroleum Geologists Bulletin, v. 40 p. 2735-2740

Raatz, W. D., 2002, A stratigraphic history of the Tularosa Basin area, south-central New Mexico, *in* Lueth, V. W., Giles, K. A., Lucas, S. G., Kues, B. S., Myers, R., and Ulmer-Scholle, D. S. eds., New Mexico Geological Society Guidebook, 53rd Field Conference, Geology of the White Sands, p. 141-157

Ramberg, O. B., Cook, F. A., Smithson, S. B., 1978, Structure of the Río Grande rift in southern New Mexico and West Texas based on gravity interpretation, Geological Society of America Bulletin, v. 89, p. 107-123

Roy, M., Karlstrom, K., Kelley, S., and Cather, S., 1999, Topographic setting of the Río Grande rift, New Mexico: assessing the roll of flexural "rift-flank uplift" in the Sandia Mountains; *in* New Mexico Geological Society Guidebook, 50th Field Conference, Albuquerque Geology, p. 167-174

Scharman, M. R., 2006, Structural constraints on Laramide shortening and Río Grande Rift extension in the central Franklin Mountains, El Paso County, Texas, [Masters Thesis], The University of Texas at El Paso, p. 59

Seager, W. R., 1980, Quaternary fault system in the Tularosa and Hueco basins, southern New Mexico and West Texas, *in* New Mexico Geological Society Guidebook, 31st Field Conference, Trans Pecos Region, p. 131-135

Seager, W. R., 1983, Possible relations between Quaternary fault system mode of extension, and listric range boundary faults in the tularosa and Hueco Basins,

New Mexico and Texas. *In* Meader-Roberts, ed. Geology of the Sierra Diablo and southern Hueco Mountains West Texas, Field Conference guidebook, Permian Basin Section Society of Economic Paleontologists and Mineralogists, p. 141-150

Seager, W. R., and Morgan, P., 1979, Río Grande rift in southern New Mexico, West Texas, and northern Chihuahua, *in* Río Grande Rift: Tectonics and Magmatism, Riecker, R. E., ed.: American Geophysical Union, p. 87-106

Seager, W. R., Shafiqulío, M., Hawley, J. W., and Marvin, R., 1984, New K-Ar dates from basalts and evolution of the southern Río Grande rift, Bulletin of the Geological Society of America, v. 95, p. 87-99

Seager, W. R., and Mack, G. H., 2003, Geology of the Caballo Mountains, New Mexico, New Mexico Bureau of Mines and Mineral Resources, Report 49, p. 122

Stewart, J. H., 1971, Basin and Range Structure: A system of Horsts and Grabens Produced by Deep-Seated Extension: *in* Bulletin of the Geological Society of America, Bulletin, V. 82, p. 1019-1044

Strain, W. S., 1966, Blancan mammalian fauna and Pleistocene formations, Hudspeth County, Texas: The University of Texas (Austin), Texas Memorial Museum, Bull 10, p. 55

Strain, W. S., 1969a, Late Cenozoic strata of the El Paso area, *in* border stratigraphy symposium: New Mexico Bureau of Mines and Mineral Resources, Circ. 104, p. 122-123

Strain, W. S., 1969b, Late Cenozoic strata of the El Paso-Juarez area: *in* New Mexico Geological Society, Guidebook 20th field conference, p. 155-157

Strain, W. S., 1969, Late Cenozoic strata of the El Paso area, *in* Border Stratigraphy Symposium, eds., Kottlowski, F. E. and LeMone, D. V., State Bureau of Mines and Mineral Resources New Mexico Institute of Mining and Technology Campus Station, Socorro, New Mexico, Circular 104, p. 122-123

Strain, W. S., 1980, Pleistocene rocks in El Paso and Hudspeth Counties, Texas adjacent to interstate highway 10, *in* New Mexico Geological Society Guidebook, 31st Field Conference, Trans-Pecos Region p. 179-181

Trentham, R. C., 2013, The ancestral Salt Flat Graben. Alternative Paleozoic history of the Sierra Diablo and Apache Mountains, Trans Pecos, West Texas, Docstochttp://www.docstoc.com/docs/158317482/The-Ancestral-Salt-Flat-Graben-Alternative-Paleozoic----CEED Confirmed by personal communication, 2014

Vanderhill, J. B., 1986, Lithostratigraphy, vertebrate paleontology, and magnetostratigraphy of the Plio-Pleistocene sediments in the Mesilla Basin, New Mexico. [Ph.D thesis] Austin, The University of Texas, p. 305

Weissel, J. K. and Karner, G. D., 1989, Flexural uplift of rift flanks due to mechanical unloading of the lithosphere during extension, Journal of Geophysical research, v. 94, No. B10, p. 13,919-13,950

Wernicke, B. and Axen, G. J., 1988, On the role of isostasy in the evolution of normal fault systems, Geology, v. 16, p. 848-851

Zandt, G. and Owens, T. J.; 1980, Crustal flexure associated with normal faulting and implications for seismicity along the Wasatch Front, Utah, bulletin of the Seismological Society of America, v. 70, no 5, p. 1501-1520

Zohdy, A. A. R., 1969, Geophysical survery for ground water at White Sands Missile Range, New Mexico: U. S. Geological Survey open-file report, p. 144

APPENDIX
Raw GPS Data

Data were gathered in UTM, Zone 13.

Data for the La Mesa Surface in New Mexico is best plotted north to south. This is the control because there is little deformation along that side of the river.

The Robledo Mountains also plot north-south.

The remaining readings are best plotted easting against elevation. The data have been arranged from the southern end of the Franklin Mountains to Fillmore Gap on the north end of the mountains. Data from adjacent terraces have a single space between them. Data from opposite sides of the mountain have double spaces between them.

See Figure 3.2 for an index to the locations of Scenic Drive/Point, McKelligon Canyon, Vinton Canyon, NM 404 is Anthony Gap, and Fillmore Gap/Ft. Bliss gate are the most northerly points associated with the Franklin Mountains.

ID	Easting	Northing	Elevation	Comment
	Data for La Mesa Surface best plotted elevation against northing - this is control data			
1	334839.429	3534006.046	1252.023	La Mesa Surface, NM
2	333721.003	3532855.310	1256.874	La Mesa Surface, NM
3	334488.923	3531719.267	1250.886	La Mesa Surface, NM
4	335528.091	3530565.970	1252.028	La Mesa Surface, NM
5	336590.722	3529365.816	1251.684	La Mesa Surface, NM
6	337659.815	3528234.606	1250.453	La Mesa Surface, NM
7	338724.466	3527078.077	1252.294	La Mesa Surface, NM
8	339815.916	3525892.821	1250.673	La Mesa Surface, NM
9	340612.884	3526222.849	1242.787	La Mesa Surface, NM
10	340584.799	3524600.676	1244.303	La Mesa Surface, NM
11	340544.097	3523048.804	1250.396	La Mesa Surface, NM
12	340505.174	3521474.290	1253.293	La Mesa Surface, NM
13	340514.506	3519827.730	1254.226	La Mesa Surface, NM
14	340591.037	3522101.496	1253.759	La Mesa Surface, NM
15	342049.061	3522275.490	1247.156	La Mesa Surface, NM
16	343648.713	3522395.575	1250.481	La Mesa Surface, NM
17	344523.812	3522175.512	1243.084	La Mesa Surface, NM
18	340894.664	3527291.862	1242.386	La Mesa Surface, NM
19	338642.848	3536540.938	1248.714	La Mesa Surface, NM
20	337237.607	3535815.978	1251.196	La Mesa Surface, NM
21	335936.168	3535153.888	1255.759	La Mesa Surface, NM
22	340079.717	3536998.941	1246.608	La Mesa Surface

The east-west component is the important direction for the Franklin and Robledo Mountain data.

ID	Northing	Easting	Elevation	Comment
				Southern end of Franklin Mountains
23	3518119.759	360672.735	1206.082	Scenic Point
24	3518112.389	360668.147	1205.634	Scenic Point
25	3518103.593	360662.658	1205.606	Scenic Point
26	3518099.380	360655.623	1209.994	Scenic Point
27	3518092.582	360646.906	1214.170	Scenic Point
28	3517288.229	359880.547	1284.476	little south of Idalia St.
29	3517651.777	359297.845	1257.167	Scenic Point
30	3517624.028	359292.483	1255.295	Scenic Point
31	3519427.851	360767.991	1329.193	end of flat
32	3519456.010	360702.296	1330.405	edge Falt
33	3519201.630	360642.235	1316.099	little lower than Idalia St)
34	3519456.033	360702.326	1330.463	faulted dn to S (above Idalia)
35	3519456.027	360702.341	1330.471	faulted dn to S
36	3519456.024	360702.350	1330.451	faulted dn to S
37	3519456.026	360702.314	1330.460	faulted dn to S
38	3519456.026	360702.316	1330.477	faulted dn to S
39	3519454.801	360703.557	1330.551	faulted dn to S
40	3519452.291	360709.312	1330.601	faulted dn to S
41	3519451.169	360713.374	1330.591	faulted dn to S
42	3519448.389	360717.335	1330.681	faulted dn to S
43	3519445.676	360720.832	1330.584	faulted dn to S
44	3519444.975	360725.010	1330.712	faulted dn to S

ID	Northing	Easting	Elevation	Comment
45	3519443.798	360729.399	1330.540	faulted dn to S
46	3519440.233	360734.009	1330.697	faulted dn to S
47	3519438.253	360737.735	1330.888	faulted dn to S
48	3519435.867	360741.876	1330.881	faulted dn to S
49	3519435.561	360746.938	1330.696	faulted dn to S
50	3519433.081	360751.268	1330.414	faulted dn to S
51	3519431.440	360756.226	1330.060	faulted dn to S
52	3519431.472	360761.778	1329.708	faulted dn to S
53	3519429.504	360765.196	1329.503	faulted dn to S
54	3519427.914	360768.045	1329.291	faulted dn to S
55	3519427.843	360767.982	1329.190	Scarp w of Idalia St
56	3519427.794	360767.974	1329.207	Scarp w of Idalia St
57	3519428.125	360768.972	1329.111	Scarp w of Idalia St
58	3519426.748	360772.609	1328.823	Scarp w of Idalia St
59	3519424.693	360777.092	1328.252	Scarp w of Idalia St
60	3519423.379	360781.117	1327.849	Scarp w of Idalia St
61	3519423.351	360785.968	1327.215	Scarp w of Idalia St
62	3519421.919	360789.731	1326.804	Scarp w of Idalia St
63	3519420.529	360792.494	1326.319	Scarp w of Idalia St
64	3519419.698	360797.573	1325.681	Scarp w of Idalia St
65	3519418.199	360799.702	1325.364	Scarp w of Idalia St
66	3519417.680	360801.152	1325.111	Scarp w of Idalia St
67	3519417.966	360804.897	1324.809	Scarp w of Idalia St
68	3519418.588	360809.495	1324.273	Scarp w of Idalia St
69	3518154.368	359223.975	1277.318	at mountain next to crazy cat
70	3518332.099	358210.661	1245.862	by ghost house

ID	Northing	Easting	Elevation	Comment
71	3519597.280	360764.920	1329.328	minimum ht on granite abov mobil
72	3520057.211	358113.617	1341.945	top of Stanton St
73	3520066.054	358126.946	1342.472	above west side water tank
74	3520073.192	358144.466	1343.954	above west side water tank
75	3520080.106	358161.939	1347.110	above west side water tank
76	3520087.004	358178.311	1350.085	above west side water tank
77	3520092.765	358195.843	1353.403	above west side water tank
78	3520101.310	358212.230	1356.349	above west side water tank
79	3520107.398	358230.648	1359.205	above west side water tank
80	3520103.731	358252.072	1361.390	above west side water tank
81	3520099.602	358274.457	1362.603	above west side water tank
82	3520095.097	358294.350	1364.482	above west side water tank
83	3520095.157	358315.808	1366.336	above west side water tank
84	3520098.871	358335.995	1368.129	above west side water tank
85	3520101.053	358357.471	1370.181	above west side water tank
86	3520104.587	358378.833	1371.842	above west side water tank
87	3520109.175	358399.586	1373.870	above west side water tank
88	3520116.441	358420.515	1376.137	above west side water tank
89	3520135.486	358426.187	1378.966	above west side water tank
90	3520151.411	358438.868	1381.371	above west side water tank
91	3520168.496	358449.517	1384.250	above west side water tank
92	3520187.477	358455.250	1387.779	above west side water tank
93	3520203.329	358468.665	1390.978	above west side water tank
94	3520195.970	358453.168	1388.189	above west side water tank
95	3520186.292	358436.727	1387.207	above west side water tank
96	3520175.730	358423.418	1382.374	above west side water tank
97	3520164.216	358408.333	1379.212	above west side water tank
98	3520152.083	358394.446	1378.570	above west side water tank
99	3520141.532	358379.296	1375.396	above west side water tank

ID	Northing	Easting	Elevation	Comment
100	3520134.612	358359.496	1373.497	above west side water tank
101	3520125.748	358343.188	1369.856	above west side water tank
102	3520116.880	358325.667	1367.132	above west side water tank
103	3520106.993	358310.316	1366.607	above west side water tank
104	3520099.334	358291.287	1364.322	above west side water tank
105	3520096.726	358286.497	1363.804	above west side water tank
106	3520284.394	360290.152	1393.602	below aeriel tram
107	3520279.192	360263.010	1396.206	below Tram station
108	3520283.175	360237.758	1398.543	below Tram station
109	3520283.159	360237.728	1398.877	below Tram station
110	3520443.254	358371.343	1399.688	between tank & gray house
111	3520440.015	358355.754	1397.051	between tank & gray house
112	3520441.140	358337.302	1394.427	between tank & gray house
113	3520435.304	358321.187	1391.736	between tank & gray house
114	3520427.193	358305.080	1389.100	between tank & gray house
115	3520418.450	358289.551	1386.556	between tank & gray house
116	3520408.124	358275.316	1384.168	between tank & gray house
117	3520397.509	358261.285	1381.520	between tank & gray house
118	3520386.780	358247.801	1379.061	between tank & gray house
119	3520375.617	358234.126	1376.373	between tank & gray house
120	3520365.346	358220.614	1373.747	between tank & gray house
121	3520355.609	358208.276	1371.011	between tank & gray house
122	3520345.402	358195.417	1367.624	between tank & gray house
123	3520335.519	358181.811	1366.572	between tank & gray house
124	3520324.803	358169.191	1362.414	between tank & gray house
125	3520314.197	358156.639	1359.492	between tank & gray house
126	3520302.115	358144.483	1356.935	between tank & gray house
127	3520288.769	358132.389	1354.641	between tank & gray house

ID	Northing	Easting	Elevation	Comment
128	3520274.639	358119.215	1352.599	between tank & gray house
129	3520260.500	358105.196	1351.293	between tank & gray house
130	3520246.442	358090.956	1349.038	between tank & gray house
131	3520238.025	358077.322	1346.172	between tank & gray house
132	3520192.040	357550.605	1327.019	street w/ gray house (N of tank, w side)
133	3520208.635	357563.693	1327.997	street w/ gray house (N of tank, w side)
134	3520224.411	357579.382	1328.852	street w/ gray house (N of tank, w side)
135	3520239.338	357594.642	1329.665	street w/ gray house (N of tank, w side)
136	3520255.166	357609.294	1330.481	street w/ gray house (N of tank, w side)
137	3520271.008	357624.643	1331.385	street w/ gray house (N of tank, w side)
138	3520286.832	357639.709	1332.628	street w/ gray house (N of tank, w side)
139	3520302.973	357655.320	1333.965	street w/ gray house (N of tank, w side)
140	3520326.743	357662.955	1335.428	street w/ gray house (N of tank, w side)
141	3520345.512	357686.979	1337.046	street w/ gray house (N of tank, w side)
142	3520357.193	357705.628	1338.139	street w/ gray house (N of tank, w side)
143	3520367.980	357724.554	1339.177	street w/ gray house (N of tank, w side)
144	3520377.243	357744.617	1340.379	street w/ gray house (N of tank, w side)
145	3520386.405	357764.235	1341.570	street w/ gray house (N of tank, w side)
146	3520394.650	357783.860	1342.848	street w/ gray house (N of tank, w side)
147	3520404.036	357803.673	1344.143	street w/ gray house (N of tank, w side)
148	3520413.237	357824.868	1345.530	street w/ gray house (N of tank, w side)
149	3520421.874	357844.786	1346.823	street w/ gray house (N of tank, w side)
150	3520431.427	357865.022	1348.160	street w/ gray house (N of tank, w side)
151	3520440.379	357886.197	1349.640	street w/ gray house (N of tank, w side)
152	3520449.901	357905.846	1350.793	street w/ gray house (N of tank, w side)
153	3520462.910	357923.488	1351.503	street w/ gray house (N of tank, w side)
154	3520477.923	357939.104	1352.225	street w/ gray house (N of tank, w side)
155	3520492.534	357954.724	1353.066	street w/ gray house (N of tank, w side)
156	3520508.369	357971.213	1353.848	street w/ gray house (N of tank, w side)
157	3520523.163	357987.058	1354.666	street w/ gray house (N of tank, w side)

ID	Northing	Easting	Elevation	Comment
158	3520539.383	358002.662	1355.443	street w/ gray house (N of tank, w side)
159	3520556.317	358018.528	1355.648	street w/ gray house (N of tank, w side)
160	3520954.832	357470.760	1341.478	Kings hill
161	3521002.408	357555.734	1348.233	above King's Hill Apts
162	3521001.028	357534.264	1347.455	above King's Hill Apts
163	3520996.674	357515.048	1346.289	above King's Hill Apts
164	3520991.605	357495.668	1345.312	above King's Hill Apts
165	3520987.516	357476.591	1342.421	above King's Hill Apts
166	3520985.668	357456.861	1341.200	above King's Hill Apts
167	3520993.949	357436.558	1341.597	above King's Hill Apts
168	3520997.006	357418.222	1339.565	above King's Hill Apts
169	3520992.626	357398.858	1338.101	above King's Hill Apts
170	3520990.340	357380.790	1337.042	above King's Hill Apts
171	3521551.267	357512.111	1356.287	top of Festival St
172	3522528.018	357495.104	1389.146	north of Festival
173	3522035.357	360194.364	1391.946	start of terrace McKelligon
174	3522891.329	357621.159	1417.301	Agave Canyon St
175	3522889.294	357605.378	1414.143	Agave Canyon St
176	3522879.446	357590.369	1411.717	Agave Canyon St

ID	Northing	Easting	Elevation	Comment
177	3522870.556	357572.464	1408.971	north of Agave Canyon St
178	3522039.480	360179.935	1390.367	mouth of mckelligon
179	3522035.343	360194.346	1392.002	entrance McKelligon Canyon
180	3522035.859	360190.922	1392.243	entrance McKelligon Canyon
181	3522035.005	360185.714	1393.179	entrance McKelligon Canyon
182	3522037.153	360180.967	1393.510	entrance McKelligon Canyon
183	3522039.667	360175.190	1393.872	entrance McKelligon Canyon
184	3522041.114	360169.164	1394.253	entrance McKelligon Canyon
185	3522041.590	360165.427	1394.794	entrance McKelligon Canyon
186	3522041.683	360165.382	1394.841	entrance McKelligon Canyon
187	3522041.677	360165.393	1394.811	entrance McKelligon Canyon
188	3522041.051	360162.671	1395.082	w side McKelligon Canyon
189	3522040.832	360160.454	1395.096	w side McKelligon Canyon
190	3522041.306	360154.844	1396.045	w side McKelligon Canyon
191	3522041.321	360149.213	1396.775	w side McKelligon Canyon
192	3522042.506	360143.830	1397.337	w side McKelligon Canyon
193	3522043.960	360138.217	1397.958	w side McKelligon Canyon
194	3522044.409	360137.296	1398.134	w side McKelligon Canyon
195	3522044.278	360134.543	1398.323	w side McKelligon Canyon
196	3522046.064	360128.676	1398.996	w side McKelligon Canyon
197	3522048.052	360123.442	1399.830	w side McKelligon Canyon
198	3522049.694	360118.883	1400.397	w side McKelligon Canyon
199	3522050.865	360115.812	1400.886	w side McKelligon Canyon
200	3522051.397	360114.900	1400.887	w side McKelligon Canyon
201	3522053.207	360109.606	1401.906	w side McKelligon Canyon
202	3522056.071	360104.683	1402.628	w side McKelligon Canyon
203	3522057.370	360101.989	1403.216	w side McKelligon Canyon

ID	Northing	Easting	Elevation	Comment
204	3522057.400	360101.994	1403.231	w side McKelligon Canyon
205	3522057.430	360101.911	1403.191	w side McKelligon Canyon
206	3523169.067	361612.766	1324.360	N of Shrine Temple
207	3523173.291	361629.852	1322.995	N of Shrine Temple
208	3523174.417	361647.047	1321.122	N of Shrine Temple
209	3523174.663	361664.289	1319.074	N of Shrine Temple
210	3523175.604	361681.053	1317.141	N of Shrine Temple
211	3523177.138	361700.045	1315.479	N of Shrine Temple
212	3523177.669	361717.658	1313.930	N of Shrine Temple
213	3523178.441	361735.519	1312.355	N of Shrine Temple
214	3523179.363	361771.150	1310.126	N of Shrine Temple
215	3523179.548	361790.077	1309.914	N of Shrine Temple
216	3523180.772	361809.025	1309.385	N of Shrine Temple
217	3523182.267	361828.051	1308.803	N of Shrine Temple
218	3523177.144	361844.246	1306.819	N of Shrine Temple
219	3524750.294	361188.515	1366.842	top zion
220	3524750.299	361188.631	1366.742	top zion
221	3524750.293	361188.303	1367.025	top zion
222	3524750.437	361188.524	1366.963	top zion
223	3524750.394	361188.490	1366.594	top zion
224	3524750.365	361188.615	1366.945	top zion
225	3524750.427	361188.578	1367.050	top zion
226	3524750.294	361188.515	1366.842	top zion
227	3524750.193	361188.374	1367.187	top of zion
228	3524750.169	361188.354	1367.160	top of zion

ID	Northing	Easting	Elevation	Comment
229	3524750.283	361188.419	1367.233	top of zion
230	3524750.202	361188.249	1366.757	top of zion
231	3524750.208	361188.321	1367.183	top of zion
232	3524750.175	361188.441	1367.035	top of zion
233	3524750.268	361188.245	1366.958	top of zion
234	3524750.425	361187.452	1365.284	top of zion
235	3524750.289	361187.925	1367.163	top of zion
236	3524750.960	361187.208	1367.415	top of zion
237	3524751.891	361186.849	1365.698	top of zion
238	3524755.004	361184.621	1366.874	top of zion
239	3524753.704	361184.372	1367.105	top of zion
240	3524753.902	361184.160	1367.060	top of zion
241	3524753.606	361183.585	1366.352	top of zion
242	3524753.865	361183.755	1365.823	top of zion
243	3524753.868	361183.944	1366.072	top of zion
244	3524753.730	361183.981	1366.099	top of zion
245	3524750.193	361188.374	1367.187	top of zion
246	3526247.947	356475.786	1378.967	Country Club
247	3525748.138	360985.043	1407.889	above Edgar Park
248	3526830.862	361869.263	1354.824	by Hondo Pass
249	3526856.866	362099.995	1297.760	North end Hondo Pass
250	3526858.005	362108.052	1295.627	North end Hondo Pass
251	3526860.585	362116.914	1292.258	North end Hondo Pass
252	3526864.205	362126.162	1289.469	North end Hondo Pass
253	3526872.116	362144.635	1284.866	North end Hondo Pass

ID	Northing	Easting	Elevation	Comment
254	3526831.237	361771.792	1370.286	high path above Hondo St
255	3526830.381	361769.318	1370.392	high path above Hondo St
256	3526829.027	361764.733	1371.137	high path above Hondo St
257	3526826.803	361760.601	1371.464	high path above Hondo St
258	3526824.661	361756.925	1371.769	high path above Hondo St
259	3526820.108	361754.097	1371.949	high path above Hondo St
260	3526816.727	361749.364	1372.183	high path above Hondo St
261	3526814.479	361744.392	1372.696	high path above Hondo St
262	3526812.142	361740.578	1372.988	high path above Hondo St
263	3526809.923	361736.088	1373.603	high path above Hondo St
264	3526810.501	361730.121	1374.326	high path above Hondo St
265	3526811.801	361724.091	1375.321	high path above Hondo St
266	3526813.417	361718.550	1376.055	high path above Hondo St
267	3526813.708	361718.174	1376.148	high path above Hondo St
268	3526833.342	361779.879	1369.462	above hondo
269	3526835.490	361782.219	1369.144	above hondo
270	3526837.416	361784.846	1368.701	above hondo
271	3526835.907	361789.247	1368.383	above hondo
272	3526836.050	361790.771	1368.091	above hondo
273	3526836.046	361790.751	1368.149	above hondo
274	3526834.492	361793.194	1367.741	above hondo
275	3526834.438	361799.712	1366.706	above hondo
276	3526837.068	361805.989	1366.345	above hondo
277	3526838.864	361810.931	1365.914	above hondo
278	3526839.647	361815.496	1365.163	above hondo
279	3526840.467	361819.689	1364.567	above hondo
280	3526840.722	361823.105	1364.102	above hondo
281	3526840.343	361827.353	1363.432	above hondo
282	3526840.324	361830.372	1362.673	above hondo
283	3526839.962	361834.687	1362.295	above hondo

ID	Northing	Easting	Elevation	Comment
284	3526841.254	361837.432	1362.141	above hondo
285	3526831.240	361771.843	1370.394	above Hondo Pass Rd
286	3527853.665	355255.891	1345.671	between Country Club & TransMountain
287	3529562.834	361541.369	1396.108	Trans Mtn fan on terr?
288	3529796.977	362268.408	1343.273	east side of Trans Mnt at con
289	3530186.827	356517.224	1488.405	Trans Mnt
290	3531126.396	352923.543	1289.027	N TransMountain
291	3531911.327	356597.023	1455.213	Tom Mayes Park - picnic area
292	3531910.544	356591.626	1455.222	Tom Mayes Park
293	3531921.223	356517.654	1450.399	Tom Mayes Park
294	3531921.264	356517.604	1450.531	Tom Mayes Park - trail
295	3531921.716	356496.540	1449.470	Tom Mayes Park - trail
296	3531921.725	356496.516	1449.485	Tom Mayes Park - trail
297	3531924.605	356474.935	1448.364	Tom Mayes Park - trail
298	3531924.608	356474.974	1448.314	Tom Mayes Park - trail
299	3531928.089	356453.238	1447.396	Tom Mayes Park - trail
300	3531928.120	356453.250	1447.425	Tom Mayes Park - trail
301	3531929.871	356432.036	1446.433	Tom Mayes Park - trail
302	3531932.154	356410.988	1445.322	Tom Mayes Park - trail
303	3531935.231	356389.652	1444.260	Tom Mayes Park - trail
304	3531940.498	356368.762	1443.337	Tom Mayes Park - trail
305	3531944.256	356347.236	1442.268	Tom Mayes Park - trail
306	3531947.314	356325.639	1440.988	Tom Mayes Park - trail

ID	Northing	Easting	Elevation	Comment
307	3531949.778	356196.905	1433.091	Tom Mayes Park - trail
308	3531954.623	356176.628	1431.890	Tom Mayes Park - trail
309	3531961.616	356157.548	1430.904	Tom Mayes Park - trail
310	3531967.999	356137.835	1429.777	Tom Mayes Park - trail
311	3531975.389	356118.124	1428.851	Tom Mayes Park - trail
312	3531997.478	356059.231	1426.118	Tom Mayes Park - trail
313	3532002.417	356038.536	1425.036	Tom Mayes Park
314	3532007.043	356018.235	1424.174	Tom Mayes Park
315	3532013.683	355998.168	1423.547	Tom Mayes Park
316	3532019.667	355978.619	1422.837	Tom Mayes Park
317	3532029.987	355959.849	1422.133	Tom Mayes Park
318	3532039.267	355940.324	1421.392	Tom Mayes Park
319	3532044.519	355919.467	1420.864	Tom Mayes Park
320	3532043.373	355878.050	1419.378	Tom Mayes Park
321	3532540.959	353014.609	1289.984	upper terrace n of TransMountain
322	3532565.621	352806.383	1270.410	north of Transmountain
323	3532724.163	353820.142	1321.188	top end of upper terrace
324	3534118.424	362502.554	1298.404	Terrace above NW corner housing development
325	3534127.841	362505.792	1296.242	Terrace above NW corner housing development
326	3534136.237	362510.145	1294.586	Terrace above NW corner housing development
327	3534145.683	362512.818	1295.268	Terrace above NW corner housing development
328	3534163.716	362518.361	1294.768	Terrace above NW corner housing development
329	3534249.433	352738.694	1292.416	may be low eros s of quarry

ID	Northing	Easting	Elevation	Comment
330	3535134.456	353046.801	1305.082	n of quarry
331	3535797.271	353059.661	1298.777	s ov vinton
332	3535878.798	352366.238	1258.208	vinton canyon
333	3536805.910	362013.459	1305.877	Vinton canyon
334	3536804.358	362022.881	1303.901	Vinton canyon
335	3536805.933	362032.695	1302.159	Vinton canyon
336	3536806.396	362042.500	1302.036	Vinton canyon
337	3536806.942	362052.329	1301.408	Vinton canyon
338	3537312.122	354687.532	1339.174	Vinton canyon
339	3537530.348	353524.383	1304.219	vinton cnyn area
340	3537533.430	353522.782	1304.240	Toe of Vinton fan
341	3535782.505	352367.192	1258.990	along Pipeline Rd, just N of Westway
342	3539668.495	363700.016	1256.208	east side by Jobe quarry
343	3539669.495	363708.756	1256.085	east side by Jobe quarry
344	3539670.519	363718.713	1255.121	east side by Jobe quarry
345	3539670.860	363729.094	1253.480	east side by Jobe quarry
346	3539672.336	363737.975	1252.576	east side by Jobe quarry
347	3539731.451	361104.025	1352.857	Bowen Ranch by gas tank
348	3539739.791	361128.858	1351.681	Bowen Ranch by gas tank
349	3539744.042	361148.461	1350.588	Bowen Ranch by gas tank

ID	Northing	Easting	Elevation	Comment
350	3539743.580	361166.993	1349.744	Bowen Ranch by gas tank
351	3539830.954	353709.916	1298.181	maybe high on thick fan
352	3539873.839	362193.145	1314.969	Bowen Ranch -probably on fan
353	3539786.773	361230.238	1344.600	W of Jobe N quarry
354	3539786.599	361248.434	1343.671	W of Jobe N quarry
355	3539797.349	361290.572	1341.893	W of Jobe N quarry
356	3539797.480	361333.199	1341.653	W of Jobe N quarry
357	3539805.998	361373.667	1340.636	W of Jobe N quarry
358	3539807.880	361394.407	1339.902	W of Jobe N quarry
359	3539814.286	361429.165	1338.597	W of Jobe N quarry
360	3539821.497	361444.626	1338.063	W of Jobe N quarry
361	3539829.543	361462.656	1337.412	W of Jobe N quarry
362	3539845.777	361521.354	1335.377	W of Jobe N quarry
363	3539876.316	361715.009	1328.755	W of Jobe N quarry
364	3541951.307	353265.213	1291.406	n of gun range
365	3541975.471	353469.454	1303.708	north of EP Gun Club Range
366	3541952.817	353241.199	1288.886	south of NM 404 near crest
367	3541995.844	353507.777	1306.332	south of NM 404 near crest
368	3541959.348	353390.331	1295.957	south of NM 404 near crest
369	3541959.204	353369.478	1294.576	south of NM 404 near crest
370	3541961.578	353348.811	1293.510	south of NM 404 near crest
371	3541961.658	353326.967	1292.670	south of NM 404 near crest
372	3541958.373	353305.560	1292.097	south of NM 404 near crest
373	3541955.731	353283.939	1291.202	south of NM 404 near crest

ID	Northing	Easting	Elevation	Comment
374	3541953.413	353261.740	1290.594	south of NM 404 near crest
375	3541964.264	353430.045	1300.112	near Pipeline Rd, S of NM 404
376	3541978.334	356591.793	1384.727	south side NM 404, next to road
377	3541997.241	356593.074	1383.403	south side NM 404, next to road
378	3541997.226	356593.080	1383.315	south side NM 404, next to road
379	3542003.389	353528.670	1307.196	1st stop south of NM 404
380	3542048.982	356599.482	1379.012	north side NM 404, next to road
381	3542066.947	356598.090	1377.608	north side NM 404, next to road
382	3542085.906	356594.758	1376.159	north side NM 404, next to road
383	3542104.269	356593.337	1374.331	north side NM 404, next to road
384	3542121.732	356593.434	1372.485	north side NM 404, next to road
385	3542250.289	356503.362	1366.140	decided was fan rather than terrace
386	3542232.002	356512.233	1366.416	decided was fan rather than terrace
387	3542212.038	356516.605	1366.216	decided was fan rather than terrace
388	3542192.385	356522.134	1367.590	decided was fan rather than terrace
389	3542192.485	356522.078	1367.488	decided was fan rather than terrace
390	3542176.818	356526.605	1368.432	decided was fan rather than terrace
391	3542159.144	356531.797	1368.570	decided was fan rather than terrace
392	3542146.216	356546.362	1369.638	decided was fan rather than terrace
393	3542129.022	356553.853	1370.509	decided was fan rather than terrace
394	3542112.027	356561.929	1372.658	decided was fan rather than terrace
395	3542094.026	356570.778	1374.562	decided was fan rather than terrace
396	3542077.341	356580.109	1376.513	decided was fan rather than terrace

ID	Northing	Easting	Elevation	Comment
397	3542057.467	356584.032	1378.004	decided was fan rather than terrace
398	3542041.547	356592.534	1379.703	decided was fan rather than terrace
399	3542572.414	354838.744	1310.141	Anthony Gap west
400	3542580.250	360381.015	1320.270	s of pipeline E side
401	3542594.302	355190.008	1300.284	along service rd N of NM404
402	3542640.171	355354.261	1314.989	along service rd N of NM404
403	3542654.942	355442.391	1325.043	along service rd N of NM404
404	3542642.960	355431.820	1322.863	along service rd N of NM404
405	3542633.321	355416.580	1319.740	along service rd N of NM404
406	3542752.309	355525.456	1330.988	along stream S of NM 404
407	3542737.697	355508.295	1330.327	along stream S of NM 404
408	3542721.459	355494.490	1329.569	along stream S of NM 404
409	3542708.266	355477.227	1329.009	along stream S of NM 404
410	3542692.452	355462.449	1328.048	along stream S of NM 404
411	3542816.452	355715.336	1355.628	south of power line
412	3542835.307	355705.906	1355.550	south of power line
413	3542855.300	355695.178	1354.640	south of power line
414	3542867.690	355676.649	1354.053	south of power line
415	3542876.078	355657.320	1353.451	south of power line
416	3542816.118	355579.657	1337.205	south of power line
417	3542785.816	355551.998	1333.868	south of power line
418	3542853.818	355685.690	1354.645	North side NM 404 w/ Stephanie
419	3542858.931	355679.694	1354.631	North side NM 404 w/ Stephanie

ID	Northing	Easting	Elevation	Comment
420	3542875.374	355654.542	1353.236	North side NM 404 w/ Stephanie
421	3542874.959	355632.537	1352.306	North side NM 404 w/ Stephanie
422	3542887.236	355623.790	1349.697	North side NM 404 w/ Stephanie
423	3542879.650	355609.670	1346.574	North side NM 404 w/ Stephanie
424	3542866.046	355597.132	1344.166	North side NM 404 w/ Stephanie
425	3542853.871	355584.058	1342.215	North side NM 404 w/ Stephanie
426	3542841.183	355570.883	1340.230	North side NM 404 w/ Stephanie
427	3542823.358	355568.035	1338.977	North side NM 404 w/ Stephanie
428	3542806.030	355562.478	1336.602	North side NM 404 w/ Stephanie
429	3542791.546	355552.490	1334.896	North side NM 404 w/ Stephanie
430	3542775.336	355542.219	1332.517	North side NM 404 w/ Stephanie
431	3542757.859	355530.275	1330.852	North side NM 404 w/ Stephanie
432	3542742.939	355514.940	1330.629	North side NM 404 w/ Stephanie
433	3542727.352	355501.032	1329.885	North side NM 404 w/ Stephanie
434	3542715.454	355482.241	1329.354	North side NM 404 w/ Stephanie
435	3542702.203	355467.300	1328.521	North side NM 404 w/ Stephanie
436	3542687.088	355453.790	1327.348	North side NM 404 w/ Stephanie
437	3542674.970	355439.639	1325.270	North side NM 404 w/ Stephanie
438	3542663.148	355426.027	1322.054	North side NM 404 w/ Stephanie
439	3543044.784	354579.250	1314.043	near trip w\steph
440	3543106.133	354486.407	1309.485	anthony gap
441	3543511.814	359988.158	1314.472	anthony gap east
442	3544068.400	356622.973	1331.078	car was her3 no terrace
443	3544346.391	353941.074	1291.400	top of Basin fl seds

ID	Northing	Easting	Elevation	Comment
444	3544361.274	353980.231	1300.959	top of terr
445	3544569.014	353708.011	1295.411	near 404 west
446	3544569.604	353708.931	1295.240	2nd tryb n o ant gaap
447	3545509.684	356317.546	1345.056	on fan
448	3545897.599	353728.016	1309.038	top of terrace
449	3545897.523	353728.038	1309.015	top of terrace
450	3545897.543	353728.048	1309.062	top of terrace
451	3545897.522	353728.052	1309.036	top of terrace
452	3545897.519	353728.037	1309.031	top of terrace
453	3545895.776	353728.257	1308.835	top of terrace
454	3545892.378	353729.974	1309.008	top of terrace
455	3545889.345	353728.108	1309.048	top of terrace
456	3545886.761	353725.323	1308.942	top of terrace
457	3545883.741	353724.433	1308.788	top of terrace
458	3545879.991	353723.696	1308.726	top of terrace
459	3545876.683	353721.114	1308.573	top of terrace
460	3545874.077	353717.824	1308.457	top of terrace
461	3545873.781	353714.737	1308.322	top of terrace
462	3545873.694	353711.029	1308.074	top of terrace
463	3545873.880	353704.579	1307.506	top of terrace
464	3545873.271	353700.783	1307.388	top of terrace
465	3545873.122	353696.986	1307.248	top of terrace
466	3545873.390	353693.484	1306.905	top of terrace
467	3545875.906	353690.205	1307.036	top of terrace
468	3545879.001	353688.391	1307.032	top of terrace
469	3545882.713	353680.313	1306.612	top of terrace

ID	Northing	Easting	Elevation	Comment
470	3545883.527	353676.190	1306.503	top of terrace
471	3545883.367	353672.352	1306.565	top of terrace
472	3545882.393	353670.489	1306.476	top of terrace
473	3545883.639	353661.973	1306.336	top of terrace
474	3545882.674	353657.318	1306.150	top of terrace
475	3545882.698	353653.788	1306.239	top of terrace
476	3545881.577	353649.355	1306.024	top of terrace
477	3545881.140	353644.552	1305.893	top of terrace
478	3545879.939	353639.966	1305.707	top of terrace
479	3545878.638	353635.943	1305.620	top of terrace
480	3545876.562	353631.756	1305.450	top of terrace
481	3545875.647	353627.910	1305.399	top of terrace
482	3545875.301	353625.120	1305.360	top of terrace
483	3545873.965	353622.340	1305.185	top of terrace
484	3545874.227	353618.131	1304.932	top of terrace
485	3545872.688	353613.661	1304.902	top of terrace
486	3545871.912	353609.875	1304.740	top of terrace
487	3545871.223	353606.425	1304.662	top of terrace
488	3545870.046	353601.939	1304.546	top of terrace
489	3545870.757	353598.298	1304.465	top of terrace
490	3545872.572	353594.387	1304.307	top of terrace
491	3545871.577	353590.193	1304.227	top of terrace
492	3545871.529	353586.067	1304.066	top of terrace
493	3545873.261	353582.679	1303.831	top of terrace
494	3545876.191	353579.188	1303.745	top of terrace
495	3545879.283	353576.175	1303.588	top of terrace
496	3545885.595	353570.329	1303.396	top of terrace
497	3545889.455	353569.505	1303.458	top of terrace
498	3545893.603	353567.362	1303.421	top of terrace
499	3545897.357	353564.586	1303.264	top of terrace
500	3545900.721	353561.699	1303.269	top of terrace

ID	Northing	Easting	Elevation	Comment
501	3545902.329	353558.063	1303.102	top of terrace
502	3545902.643	353553.461	1302.874	top of terrace
503	3545904.801	353548.877	1302.767	top of terrace
504	3545906.717	353544.650	1302.613	top of terrace
505	3545904.791	353540.806	1302.680	top of terrace
506	3545903.637	353537.383	1302.468	top of terrace
507	3545906.197	353535.096	1302.161	top of terrace
508	3545908.046	353530.658	1302.008	top of terrace
509	3545909.932	353526.081	1301.741	top of terrace
510	3545912.287	353521.939	1301.741	top of terrace
511	3545912.920	353517.557	1301.712	top of terrace
512	3545914.673	353512.988	1301.537	top of terrace
513	3545916.093	353508.726	1301.441	top of terrace
514	3545918.176	353500.106	1301.015	top of terrace
515	3545917.910	353495.534	1300.776	top of terrace
516	3545920.116	353491.556	1300.677	top of terrace
517	3545919.780	353486.923	1300.542	top of terrace
518	3545920.115	353482.618	1300.331	top of terrace
519	3545918.554	353478.425	1300.004	top of terrace
520	3545917.531	353473.973	1299.678	top of terrace
521	3545918.139	353469.985	1299.546	top of terrace
522	3545916.822	353466.323	1299.383	top of terrace
523	3545914.862	353463.720	1299.115	top of terrace
524	3545913.392	353460.028	1298.814	top of terrace
525	3545912.174	353455.751	1298.780	top of terrace
526	3545912.405	353451.793	1298.757	top of terrace
527	3545911.741	353447.636	1298.513	top of terrace
528	3545909.298	353443.616	1298.299	top of terrace
529	3545909.026	353439.123	1298.405	top of terrace
530	3545907.974	353435.237	1298.303	top of terrace
531	3545907.589	353431.585	1298.217	top of terrace

ID	Northing	Easting	Elevation	Comment
532	3545906.920	353428.237	1298.130	top of terrace
533	3545907.287	353424.388	1298.001	top of terrace
534	3545905.960	353421.029	1297.814	top of terrace
535	3545905.578	353419.516	1297.879	top of terrace
536	3545956.273	353920.124	1322.470	along Pipeline Rd between Anthony & Webb Gap
537	3545956.956	353919.669	1322.364	along Pipeline Rd between Anthony & Webb Gap
538	3545957.491	353916.426	1322.236	along Pipeline Rd between Anthony & Webb Gap
539	3545958.435	353913.773	1322.150	along Pipeline Rd between Anthony & Webb Gap
540	3545956.142	353912.220	1321.936	along Pipeline Rd between Anthony & Webb Gap
541	3545952.946	353910.220	1321.754	along Pipeline Rd between Anthony & Webb Gap
542	3545949.322	353909.113	1321.688	along Pipeline Rd between Anthony & Webb Gap
543	3545946.623	353906.773	1321.417	along Pipeline Rd between Anthony & Webb Gap
544	3545944.171	353904.976	1321.274	along Pipeline Rd between Anthony & Webb Gap
545	3545941.562	353901.944	1320.980	along Pipeline Rd between Anthony & Webb Gap
546	3545940.997	353898.535	1320.845	along Pipeline Rd between Anthony & Webb Gap
547	3545941.755	353895.824	1320.637	along Pipeline Rd between Anthony & Webb Gap
548	3545939.279	353892.773	1320.445	along Pipeline Rd between Anthony & Webb Gap
549	3545937.405	353888.575	1320.071	along Pipeline Rd between Anthony & Webb Gap
550	3545935.723	353884.103	1319.874	along Pipeline Rd between Anthony & Webb Gap
551	3545934.385	353880.273	1319.568	along Pipeline Rd between Anthony & Webb Gap
552	3545932.927	353876.391	1319.394	along Pipeline Rd between Anthony & Webb Gap
553	3545931.319	353872.761	1319.115	along Pipeline Rd between Anthony & Webb Gap
554	3545930.032	353869.987	1318.987	along Pipeline Rd between Anthony & Webb Gap
555	3545928.593	353866.987	1318.663	along Pipeline Rd between Anthony & Webb Gap
556	3545926.520	353864.699	1318.403	along Pipeline Rd between Anthony & Webb Gap
557	3545925.260	353863.167	1318.306	along Pipeline Rd between Anthony & Webb Gap
558	3545924.166	353861.621	1318.158	along Pipeline Rd between Anthony & Webb Gap
559	3545924.186	353858.673	1317.953	along Pipeline Rd between Anthony & Webb Gap
560	3545921.638	353856.848	1317.762	along Pipeline Rd between Anthony & Webb Gap
561	3545920.069	353853.898	1317.584	along Pipeline Rd between Anthony & Webb Gap

ID	Northing	Easting	Elevation	Comment
562	3545919.943	353850.393	1317.349	along Pipeline Rd between Anthony & Webb Gap
563	3545922.170	353847.294	1317.002	along Pipeline Rd between Anthony & Webb Gap
564	3545922.060	353844.174	1316.823	along Pipeline Rd between Anthony & Webb Gap
565	3545920.259	353842.097	1316.781	along Pipeline Rd between Anthony & Webb Gap
566	3545919.312	353841.100	1316.563	along Pipeline Rd between Anthony & Webb Gap
567	3545919.720	353837.979	1316.287	along Pipeline Rd between Anthony & Webb Gap
568	3545919.219	353835.781	1316.093	along Pipeline Rd between Anthony & Webb Gap
569	3545919.893	353832.671	1315.779	along Pipeline Rd between Anthony & Webb Gap
570	3545918.323	353830.086	1315.775	along Pipeline Rd between Anthony & Webb Gap
571	3545915.740	353827.036	1315.389	along Pipeline Rd between Anthony & Webb Gap
572	3545915.744	353823.104	1315.203	along Pipeline Rd between Anthony & Webb Gap
573	3545915.227	353819.656	1315.014	along Pipeline Rd between Anthony & Webb Gap
574	3545914.721	353816.201	1314.650	along Pipeline Rd between Anthony & Webb Gap
575	3545915.023	353813.196	1314.493	along Pipeline Rd between Anthony & Webb Gap
576	3545914.634	353809.248	1314.129	along Pipeline Rd between Anthony & Webb Gap
577	3545915.088	353805.224	1313.899	along Pipeline Rd between Anthony & Webb Gap
578	3545916.489	353802.403	1313.879	along Pipeline Rd between Anthony & Webb Gap
579	3545917.228	353799.717	1313.617	along Pipeline Rd between Anthony & Webb Gap
580	3545916.636	353796.260	1313.346	along Pipeline Rd between Anthony & Webb Gap
581	3545915.028	353794.254	1313.184	along Pipeline Rd between Anthony & Webb Gap
582	3545912.034	353792.296	1312.939	along Pipeline Rd between Anthony & Webb Gap
583	3545909.403	353789.671	1312.922	along Pipeline Rd between Anthony & Webb Gap
584	3545910.426	353786.256	1312.512	along Pipeline Rd between Anthony & Webb Gap
585	3545911.074	353782.736	1312.300	along Pipeline Rd between Anthony & Webb Gap
586	3545911.474	353779.223	1312.029	along Pipeline Rd between Anthony & Webb Gap
587	3545910.944	353776.697	1311.835	along Pipeline Rd between Anthony & Webb Gap
588	3545908.739	353775.149	1311.958	along Pipeline Rd between Anthony & Webb Gap
589	3545910.547	353772.076	1311.733	along Pipeline Rd between Anthony & Webb Gap
590	3545911.088	353769.016	1311.755	along Pipeline Rd between Anthony & Webb Gap
591	3545910.703	353765.434	1311.428	along Pipeline Rd between Anthony & Webb Gap
592	3545910.200	353761.805	1311.193	along Pipeline Rd between Anthony & Webb Gap

ID	Northing	Easting	Elevation	Comment
593	3545911.135	353757.834	1311.042	along Pipeline Rd between Anthony & Webb Gap
594	3545909.453	353754.025	1310.851	along Pipeline Rd between Anthony & Webb Gap
595	3545909.031	353749.987	1310.533	along Pipeline Rd between Anthony & Webb Gap
596	3545910.534	353746.909	1310.326	along Pipeline Rd between Anthony & Webb Gap
597	3545909.115	353743.961	1310.112	along Pipeline Rd between Anthony & Webb Gap
598	3545908.462	353741.201	1309.940	along Pipeline Rd between Anthony & Webb Gap
599	3545906.211	353740.188	1309.916	along Pipeline Rd between Anthony & Webb Gap
600	3545904.234	353737.691	1309.727	along Pipeline Rd between Anthony & Webb Gap
601	3545901.195	353736.691	1309.684	along Pipeline Rd between Anthony & Webb Gap
602	3545897.746	353736.478	1309.656	along Pipeline Rd between Anthony & Webb Gap
603	3545898.397	353735.125	1309.560	along Pipeline Rd between Anthony & Webb Gap
604	3545898.406	353735.122	1309.587	along Pipeline Rd between Anthony & Webb Gap
605	3545901.051	353733.092	1309.386	along Pipeline Rd between Anthony & Webb Gap
606	3545900.402	353730.171	1309.234	along Pipeline Rd between Anthony & Webb Gap
607	3545897.743	353728.195	1308.901	along Pipeline Rd between Anthony & Webb Gap
608	3545897.667	353728.088	1308.934	along Pipeline Rd between Anthony & Webb Gap
609	3545897.617	353728.021	1309.032	along Pipeline Rd between Anthony & Webb Gap
610	3546005.132	353105.835	1288.433	terrace above qry n of 404
611	3546004.977	353105.589	1288.407	terrace above qry n of 404
612	3546005.108	353108.472	1288.369	terrace above qry n of 404
613	3546007.016	353114.083	1288.493	terrace above qry n of 404
614	3546007.146	353120.027	1288.689	terrace above qry n of 404
615	3546008.084	353125.772	1288.766	terrace above qry n of 404
616	3546009.435	353131.562	1288.933	terrace above qry n of 404
617	3546010.377	353137.854	1289.141	terrace above qry n of 404
618	3546011.726	353143.326	1289.260	terrace above qry n of 404
619	3546013.445	353148.787	1289.384	terrace above qry n of 404
620	3546015.321	353153.936	1289.431	terrace above qry n of 404
621	3546017.141	353159.035	1289.541	terrace above qry n of 404

ID	Northing	Easting	Elevation	Comment
622	3546018.983	353164.907	1289.891	terrace above qry n of 404
623	3546020.948	353170.966	1290.015	terrace above qry n of 404
624	3546023.078	353176.937	1290.120	terrace above qry n of 404
625	3546025.118	353182.815	1290.177	terrace above qry n of 404
626	3546026.380	353187.343	1290.307	terrace above qry n of 404
627	3546028.393	353191.141	1290.327	terrace above qry n of 404
628	3546028.873	353193.281	1290.376	terrace above qry n of 404
629	3546030.664	353195.272	1290.410	terrace above qry n of 404
630	3546033.082	353201.044	1290.437	terrace above qry n of 404
631	3546033.855	353204.418	1290.548	terrace above qry n of 404
632	3546033.904	353204.466	1290.535	terrace above qry n of 404
633	3546142.361	353573.374	1305.733	terr e of qry
634	3546142.939	353573.595	1305.683	terr e of qry
635	3546143.022	353573.658	1305.762	terr e of qry
636	3546143.035	353573.665	1305.750	terr e of qry
637	3546143.608	353573.816	1305.640	terr e of qry
638	3546149.978	353576.352	1305.818	terr e of qry
639	3546156.231	353579.771	1305.856	terr e of qry
640	3546162.183	353583.815	1306.090	terr e of qry
641	3546166.283	353589.522	1306.540	terr e of qry
642	3546167.896	353596.652	1307.018	terr e of qry
643	3546169.542	353604.310	1307.298	terr e of qry
644	3546172.245	353612.024	1307.600	terr e of qry
645	3546174.801	353619.582	1307.855	terr e of qry
646	3546177.525	353627.243	1308.281	terr e of qry
647	3546179.875	353634.862	1308.666	terr e of qry
648	3546183.179	353642.482	1308.941	terr e of qry
649	3546186.945	353649.655	1309.312	terr e of qry
650	3546190.318	353657.007	1309.648	terr e of qry
651	3546192.974	353664.772	1310.027	terr e of qry

ID	Northing	Easting	Elevation	Comment
652	3546195.471	353672.217	1310.309	terr e of qry
653	3546199.081	353679.144	1310.597	terr e of qry
654	3546202.390	353685.787	1310.920	terr e of qry
655	3546208.310	353691.261	1310.988	terr e of qry
656	3546212.613	353697.957	1311.076	terr e of qry
657	3546217.466	353704.120	1311.412	terr e of qry
658	3546221.328	353711.212	1311.473	terr e of qry
659	3546222.060	353719.269	1311.638	terr e of qry
660	3546221.993	353727.328	1311.962	terr e of qry
661	3546224.085	353735.168	1312.232	terr e of qry
662	3546228.048	353742.386	1312.596	terr e of qry
663	3546231.988	353749.243	1312.832	terr e of qry
664	3546234.973	353756.555	1313.164	terr e of qry
665	3546237.737	353763.452	1313.426	terr e of qry
666	3546241.086	353770.725	1313.795	terr e of qry
667	3546244.133	353777.489	1314.237	terr e of qry
668	3546246.514	353781.521	1314.448	terr e of qry
669	3546248.768	353785.829	1314.697	terr e of qry
670	3546249.875	353788.408	1314.921	terr e of qry
671	3546250.384	353793.221	1315.262	terr e of qry
672	3546250.843	353798.034	1315.215	terr e of qry
673	3546250.892	353798.936	1315.313	terr e of qry
674	3546251.014	353800.799	1315.412	terr e of qry
675	3546252.307	353805.002	1315.652	terr e of qry
676	3546254.340	353810.415	1315.881	terr e of qry
677	3546255.562	353816.376	1316.191	terr e of qry
678	3546256.395	353822.220	1316.504	terr e of qry
679	3546257.097	353828.356	1316.708	terr e of qry
680	3546258.062	353834.062	1316.914	terr e of qry
681	3546257.694	353834.059	1316.880	terr e of qry
682	3546257.586	353835.009	1316.921	terr e of qry

ID	Northing	Easting	Elevation	Comment
683	3546258.516	353838.654	1317.039	terr e of qry
684	3546259.499	353844.714	1317.375	terr e of qry
685	3546247.973	353861.491	1318.147	terr e of qry
686	3546249.322	353868.446	1318.597	terr e of qry
687	3546247.362	353873.493	1318.979	terr e of qry
688	3546246.745	353874.876	1318.913	terr e of qry
689	3546245.607	353880.788	1319.328	terr e of qry
690	3546235.715	353897.525	1320.178	terr e of qry
691	3546233.556	353915.402	1321.327	terr e of qry
692	3546231.123	353925.575	1321.749	terr e of qry
693	3546231.155	353926.101	1322.366	terr e of qry
694	3546231.354	353926.350	1322.324	terr e of qry
695	3546231.269	353926.246	1322.329	terr e of qry
696	3546231.311	353926.214	1322.227	terr e of qry
697	3546231.315	353926.224	1322.249	terr e of qry
700	3546231.320	353925.783	1322.169	cont of line
701	3546231.301	353925.719	1322.146	cont of line
702	3546231.960	353927.109	1322.213	cont of line
703	3546231.287	353931.537	1322.534	cont of line
704	3546231.427	353934.549	1322.702	cont of line
705	3546230.034	353937.241	1322.929	cont of line
706	3546228.066	353941.887	1323.246	cont of line
707	3546225.955	353946.311	1323.598	cont of line
708	3546224.646	353948.569	1323.759	cont of line
709	3546223.669	353952.337	1324.084	cont of line
710	3546223.355	353953.282	1324.183	cont of line
711	3546222.758	353958.641	1324.502	cont of line
712	3546220.077	353963.401	1324.993	cont of line
713	3546216.908	353966.932	1325.252	cont of line
714	3546215.160	353968.397	1325.516	cont of line

ID	Northing	Easting	Elevation	Comment
715	3546213.523	353972.595	1325.654	cont of line
716	3546213.966	353977.379	1326.077	cont of line
717	3546209.598	353981.660	1326.507	cont of line
718	3546209.286	353982.163	1326.481	cont of line
719	3546209.773	353987.279	1326.980	cont of line
720	3546211.227	353992.890	1327.421	cont of line
721	3546210.836	353998.819	1327.853	cont of line
722	3546205.168	354008.337	1328.838	cont of line
723	3546192.941	354029.777	1330.355	cont of line
724	3546189.774	354035.430	1330.886	cont of line
725	3546187.859	354040.637	1331.398	cont of line
726	3546183.128	354043.477	1332.017	cont of line
727	3546179.028	354047.703	1332.453	cont of line
728	3546170.989	354056.338	1333.363	cont of line
729	3546168.251	354061.477	1333.801	cont of line
730	3546165.571	354067.209	1334.278	cont of line
731	3546162.523	354071.951	1334.811	cont of line
732	3546160.037	354082.706	1335.986	cont of line
733	3546163.055	354088.493	1336.240	cont of line
734	3546161.624	354094.267	1336.728	cont of line
735	3546157.555	354098.029	1337.215	cont of line
736	3546155.770	354103.546	1337.786	cont of line
737	3546156.190	354108.441	1338.226	cont of line
738	3546158.384	354114.501	1338.585	cont of line
739	3546161.960	354119.852	1338.865	cont of line
740	3546162.947	354126.034	1339.369	cont of line
741	3546160.242	354130.820	1339.898	cont of line
742	3546158.452	354136.504	1340.193	cont of line
743	3546157.620	354142.959	1340.889	cont of line
744	3546156.379	354148.737	1341.402	cont of line
745	3546154.681	354154.575	1341.994	cont of line

ID	Northing	Easting	Elevation	Comment
746	3546155.276	354160.742	1342.470	cont of line
747	3546155.708	354166.865	1343.006	cont of line
748	3546153.903	354172.376	1343.553	cont of line
749	3546154.402	354174.981	1343.399	cont of line
750	3546152.132	354180.864	1344.059	cont of line
751	3546152.944	354187.282	1344.611	cont of line
752	3546152.566	354193.955	1345.049	cont of line
753	3546150.945	354200.287	1345.875	cont of line
754	3546148.339	354205.806	1346.311	cont of line
755	3546147.842	354212.293	1346.918	cont of line
756	3546145.828	354218.468	1347.571	cont of line
757	3546143.758	354224.568	1348.289	cont of line
758	3546141.706	354229.560	1348.852	cont of line
759	3546137.606	354234.006	1349.377	cont of line
760	3546136.063	354240.026	1350.377	cont of line
761	3546135.739	354242.431	1350.895	cont of line
762	3548589.009	355689.091	1285.542	terrace
763	3545914.862	353463.720	1299.115	top of terrace
764	3546834.245	353078.285	1291.167	2 m grv on basin flr good
765	3547898.608	355127.655	1308.206	bicycle
766	3547898.953	355127.686	1308.556	bicycle
767	3550846.285	350737.195	1274.031	Terr on basin floor
768	3550846.265	350737.197	1273.996	Terr on basin floor
769	3550846.287	350737.174	1273.976	Terr on basin floor

ID	Northing	Easting	Elevation	Comment
770	3550846.285	350737.166	1273.977	Terr on basin floor
771	3550846.285	350737.195	1274.031	Terr on basin floor
772	3550846.295	350737.185	1273.975	Terr on basin floor
773	3550846.297	350737.227	1274.038	Terr on basin floor
774	3550846.229	350737.177	1273.904	terr bs flr calcrete
775	3550846.247	350737.175	1273.898	terr bs flr calcrete
776	3550846.251	350737.196	1273.856	terr bs flr calcrete
777	3550846.213	350737.216	1273.891	terr bs flr calcrete
778	3550846.232	350737.208	1273.887	terr bs flr calcrete
779	3550846.718	350736.834	1273.894	terr bs flr calcrete
780	3550853.169	350737.463	1273.931	terr bs flr calcrete
781	3550858.778	350740.418	1274.102	terr bs flr calcrete
782	3550864.564	350744.845	1274.054	terr bs flr calcrete
783	3550870.027	350750.112	1274.102	terr bs flr calcrete
784	3550873.072	350756.615	1274.129	terr bs flr calcrete
785	3550876.167	350760.095	1274.114	terr bs flr calcrete
786	3550883.329	350759.639	1274.099	terr bs flr calcrete
787	3550890.642	350759.225	1274.045	terr bs flr calcrete
788	3550897.697	350759.227	1274.055	terr bs flr calcrete
789	3550905.729	350759.067	1273.941	terr bs flr calcrete
790	3550912.885	350758.421	1273.793	terr bs flr calcrete
791	3550919.795	350761.975	1273.790	terr bs flr calcrete
792	3550926.499	350764.792	1273.746	terr bs flr calcrete
793	3550932.454	350768.780	1273.807	terr bs flr calcrete
794	3550937.585	350773.743	1273.808	terr bs flr calcrete
795	3550942.612	350776.638	1273.820	terr bs flr calcrete
796	3550945.009	350778.778	1274.050	terr bs flr calcrete

ID	Northing	Easting	Elevation	Comment
797	3556158.106	348557.052	1278.213	5 terrace
798	3557645.796	349752.154	1279.950	Fillmore Gap
799	3557936.020	350855.354	1282.213	Ft Bliss Gate
				Northern end of Franklin Mountains
800	3592611.040	320126.964	1315.211	Robledo, area around end of canyon
801	3592611.034	320126.932	1315.286	Robledo, northern area around end of canyon
802	3592617.498	320118.739	1316.881	Robledo, northern area around end of canyon
803	3592611.007	320086.503	1314.744	Robledo, northern area around end of canyon
804	3592584.084	320045.093	1315.634	Robledo, northern area around end of canyon
805	3592677.083	319982.694	1324.085	Robledo, northern area around end of canyon
806	3592670.235	320007.560	1328.428	Robledo, northern area around end of canyon
807	3592651.548	320047.216	1338.618	Robledo, northern area around end of canyon
808	3592619.226	320001.907	1341.245	Robledo, northern area around end of canyon
809	3592757.030	319839.426	1330.171	north of original Robledo terrace
810	3593054.750	319784.353	1331.462	north of original Robledo terrace
811	3591986.118	320148.872	1330.175	Robledo, @ 1 km S of original
812	3591657.963	320385.341	1334.860	Robledo, @ 1 km S of original

VITA

Linda Kay Armour was graduated from a central Kansas high school then earned a BA in geography at the University of Oklahoma in 1967. She taught grade school in San Antonio from 1970 – 1973. The family moved to New York where she pursued additional teacher certifications in geography and in earth science. Upon return to Texas in 1981, she taught junior high prior to moving to Midland to work as draftsman for Gulf Oil Company.

She completed her BS in geology at The University of Texas of the Permian Basin (UTPB) in 1988. She promised her daughters she'd not begin her MS in geology until they graduated from high school. The MS was completed in 2001 from UTPB.

After completing her MS in geology, she served as research geologist for a Department of Energy geothermal study with Dr. Richard Erdlac, Jr. She developed the database and oversaw student help. Several publications developed from the geothermal project.

Dr. Armour is retired. She decided to return to school for a PhD in the branch of geology that enticed her into the discipline for the pleasure of attending school and challenge of obtaining the degree. She expects to return to the petroleum industry as a consultant after her return to Midland. She holds Texas Professional Geology License #490.

In addition to teaching and work as a draftsman, Dr. Armour has worked as geological technician, environmental technician, and assistant geologist for Chevron, Phillips, Conoco, Mobil, Pure, a few independent and small petroleum companies, and the Center for Energy and Economic Diversification, the community service branch of

UTPB. All of these positions have been in Midland, TX or Hobbs, NM. She claims three discoveries. Additional publications include poster sessions at Geological Society of America meetings.

Permanent address:

205 East County Road 127

Midland, Texas 79706

This dissertation was typed by Linda Kay Armour.